GEOMAR REPORT

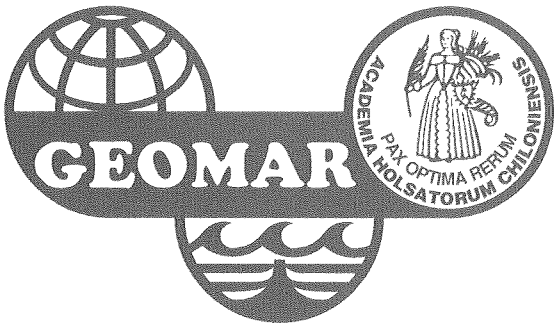

CHARLOTTE M. KRAWCZYK

DETACHMENT TECTONICS DURING CONTINENTAL RIFTING OFF THE WEST IBERIA MARGIN: SEISMIC REFLECTION AND DRILLING CONSTRAINTS

37

GEOMAR REPORT

CHARLOTTE M. KRAWCZYK

DETACHMENT TECTONICS DURING CONTINENTAL RIFTING OFF THE WEST IBERIA MARGIN: SEISMIC REFLECTION AND DRILLING CONSTRAINTS

GEOMAR
Forschungszentrum
für marine Geowissenschaften
der Christian-Albrechts-Universität
zu Kiel

Kiel 1995

GEOMAR REPORT 37

GEOMAR
Research Center
for Marine Geosciences
Christian Albrechts University
in Kiel

Dissertation
zur Erlangung des Doktorgrades
der mathematisch-naturwissenschaftlichen Fakultät
der Christian-Albrechts-Universität zu Kiel
Zum Druck genehmigt am 21.2.1995

Redaktion der Serie: Gerhard Haass
Umschlag: Kerstin Kreis, Harald Gross, GEOMAR Technologie GmbH

Managing Editor: Gerhard Haass
Cover: Kerstin Kreis, Harald Gross, GEOMAR Technologie GmbH

GEOMAR REPORT
ISSN 0936 - 5788

GEOMAR REPORT
ISSN 0936 - 5788

GEOMAR
Forschungszentrum
für marine Geowissenschaften
D-24148 Kiel
Wischhofstr. 1-3
Telefon (0431) 7202-0
Telefax (0431) 72 53 91, 7 20 22 93, 72 56 50

GEOMAR
Research Center
for Marine Geosciences
D-24148 Kiel / Germany
Wischhofstr. 1-3
Telephone (49) 431 / 7202-0
Telefax (49) 431 / 72 53 91, 7 20 22 93, 72 56 50

Vorwort

Die hier vorliegende Arbeit wurde von 1991-1995 am GEOMAR-Forschungszentrum für marine Geowissenschaften in Kiel erstellt. Sie zeigt zum einen neue Tiefenabbildungen der Krustenstrukturen des passiven, nicht-vulkanischen Kontinentalrandes westlich von Galizien. Zum anderen wurden bis dahin noch nicht gekannte Extensionsstrukturen in der unmittelbar südlich anschließenden Iberischen Tiefsee-Ebene aufgedeckt. So entstand schließlich ein Modell für die Rekonstruktion der Extensionsereignisse, die zum kontinentalen Aufbrechen zwischen Nordamerikanischer und Iberischer Platte geführt haben.

Demzufolge ist diese Schrift so angelegt, daß sie zunächst die verwendeten Methoden beschreibt, dann die dadurch erzielten Ergebnisse für die untersuchten Teilgebiete anspricht und schließlich deren Interpretation in einem integrierenden Modell verarbeitet. Die Bedeutung der einzelnen Ergebnisse wie auch ihre Grenzen und die daraus resultierenden weiteren Forschungsziele werden im Rahmen der einzelnen Kapitel diskutiert. Einen zusätzlichen Beitrag im Hintergrund dieser Arbeit stellen die Ergebnisse einzelner DSDP-/ODP-Bohrkampagnen dar, deren Lokationen teilweise mit den hier gezeigten, neu bearbeiteten Profilen überdeckt werden.

Im Verlauf der Untersuchungen erteilte der Dekan der Mathematisch-Naturwissenschaftlichen Fakultät der Christian-Albrechts-Universität zu Kiel die Genehmigung zur Abfassung dieser Arbeit in englischer Sprache sowie die Erlaubnis, vorab einzelne Ergebnisse veröffentlichen zu dürfen. Bis zu dem Zeitpunkt der Vorlage dieser Schrift als Dissertationsarbeit sind die Ergebnisse der nachfolgend aufgeführten Abschnitte in verschiedenen Beiträgen zur Veröffentlichung angenommen, vorbereitet oder eingereicht worden:

Kapitel 3:
Krawczyk, C.M. & Reston, T.J., *in press*, Detachment Faulting and Continental Break-up: the S Reflector offshore Galicia. - In E. Banda, M. Talwani & M. Torne, eds, Rifted Ocean-Continent Boundaries, Kluwer.

Kapitel 4:
Krawczyk, C.M., Reston, T.J. & Boillot, G., *in prep.*, Analyses and Comparison of bright Crustal Reflections on the West Galicia Continental Margin.

Kapitel 5:
Krawczyk, C.M., Reston, T.J., Beslier, M.-O. & Boillot, G., *in review*, Evidence for Detachment Tectonics on the Iberia Abyssal Plain Rifted Margin. - In D. Sawyer, R. Whitmarsh, A. Klaus et al., Proc. ODP, Sci. Results, v. 149, Ocean Drilling Program, College Station, TX.

Danksagung

Diese Arbeit entstand in der Abteilung Ozeanische Geodynamik am GEOMAR-Forschungszentrum unter der Leitung von Prof. Dr. Roland von Huene. Ihm danke ich für die freundliche Aufnahme in die Arbeitsgruppe und die unkomplizierte Unterstützung und Zusammenarbeit.

Mein ganz besonderer Dank gilt Dr. Timothy Reston für seine Anregungen und die fachliche Betreuung dieser Arbeit. Ihm fühle ich mich sehr durch sein persönliches Engagement und die Ermutigung zur "Öffentlichkeitsarbeit" verbunden. Er ließ mich an seinen internationalen Kontakten teilhaben und ermöglichte mir einen steten Austausch an Erfahrung sowie Zugewinn von Kenntnissen.

Neben allen anderen Mitarbeitern und Mitarbeiterinnen der Abteilung bedanke ich mich insbesondere bei Dipl. Geophys. Dirk Klaeschen und Dr. Wilhelm Weinrebe für ihre stetige Diskussions- und Hilfsbereitschaft bei der Lösung von Hard- und Softwareproblemen.

Meinen französischen Projektkollegen Prof. Gilbert Boillot und Dr. Marie-O. Beslier an diese Stelle ein Dankeschön für ihre Kooperation und die fruchtbaren Diskussionen über die Natur des S-Reflektors und des Peridotit Rückens.

Die Datenakquisition übernahmen die technischen Teams vom Ifremer, Brest, Kapitän und Crew der "Le Suroît" und das Institut Français du Pétrole, Paris; hier stellte Dr. Jaques Wannesson die Daten unkompliziert zur Verfügung. Ebenso seien die technischen Teams der DV "Joides Resolution" und stellvertretend für die gesamte wissenschaftliche Arbeitsgruppe von Leg 149 Dr. Bob Whitmarsh und Dr. Dale Sawyer in den Dank einbezogen.

Die großzügige Unterstützung seitens der DFG (Projekte Re 873/1 und 873/3), durch das Procope-Programm zur Finanzierung des deutsch-französischen Austausches sowie das deutsche ODP ermöglichten diese Arbeit.

Bei allen "von unserem Flur" bedanke ich mich nicht zuletzt sehr herzlich für die freundliche und auch freundschaftliche Arbeitsatmosphäre, die die Bewältigung vieler Aufgaben erleichtert hat.

Kiel, im Januar 1995

Charlotte Krawczyk

Contents

Summary

Lithospheric extension and thinning leading to complete continental rupture and the formation of rifted margins are among the most fundamental geological processes. The west Iberia Atlantic margin represents a type-example of a non-volcanic rifted margin, and is an ideal site to study the nature of lithospheric extension. It is relatively sediment-starved and exhibits in the Galicia Bank area landward tilted crustal blocks, which are bound by west-dipping normal faults. Seismic time sections image these faults underlain by an apparently undulating and discontinuous bright reflection, the S reflector, terminating further west near the ocean-continent boundary (OCT). This boundary is marked by a mantle outcrop shown by drilling to consist of serpentinised peridotite. Similar observations in the Iberia Abyssal Plain had not been reported until the beginning of this study, except the hypothesis of mantle material at the OCT proved in 1993 by drilling.

The investigated area is crossed by a number of high-quality MCS reflection lines, and has been investigated by two drilling campaigns, allowing the reflection seismic analyses to be constrained by results from sampling. The objective of the study was to reveal the true geometry and extent of the extensional structures, to clarify the relationship between S and the overlying faults, and finally to better understand their nature. To achieve this, iterative prestack depth migration and waveform and amplitude analyses for an estimation of reflection coefficients were applied in addition to more standard techniques. The results allow detachment models for lithospheric extension on both the Galicia Bank and the Iberia Abyssal Plain segments of the Iberian passive margin to be advanced.

The results presented in this study reveal that the S reflector, instead of undulating or being cut by the overlying normal faults, passes continuously on the depth sections beneath the crustal blocks, and shows either a domal shape or a gentle dip to the west. Furthermore, velocities identify wedge-shaped sequences of syn-rift sediments overlying basement within the tilted blocks. Hence, S is an intra-basement detachment, and was active in the last phase of rifting before continental break-up (c. 105 Ma), as the crustal blocks are bound by syn-rift faults.

The internal structure of S is revealed by complex trace analyses: its waveform is remarkably close to that of the seafloor, positive polarity, and

reflection coefficient estimates deduce a value of c. 0.2 for S. This points to a stepwise increase in acoustic impedance at a first order interface, leading to the interpretation of S as a sharp boundary separating an upper crustal upper plate from a higher velocity and density lower plate.

The depth sections allow the construction of a depth map to S. This shows that S shallows towards the continent, implying that the breakaway lies to the east, and supporting the idea that S accomodated lithospheric extension by top-to-the-west movement synthetic to the overlying normal faults. S cannot be followed further north than 42°20´N, thus it is a structure different to S´ proposed to represent its northern counterpart, and more important it does not crop out at the Peridotite Ridge at the proposed drill location GAL1. S rather appears to be truncated by east-dipping reflections cutting down from the Peridotite Ridge, which may be explained by either an antithetic relationship during simultaneous activity or subsequent events. In summary, the S reflector is an intra-crustal detachment, which might have accomodated extension by top-to-the-west movement, and controlled final continental break-up in this region.

To the south, in the Iberia Abyssal Plain (IAP), new images show for the first time small, landward tilted crustal blocks overlying a bright reflection, also interpreted as detachment. This structure, named H, appears to have been rotated by later faulting and the development of a deeper detachment system (L). These features are similar to the Galicia Bank margin in the sense that H like S is also characterised by a sharp acoustic impedance contrast (R c. 0.15), positive polarity and a waveform close to that of the seafloor.

A detachment model advanced for this margin is further supported by the transect drilled recently across the OCT: extension of the upper lithosphere was accomodated first along a west-dipping detachment (H), which was subsequently dismembered by steeper normal faults separating the tilted crustal blocks. This exposed a cross-section characterised by a shallowing of lithospheric level towards the OCT.

Although both segments of the Iberia Atlantic margin have been controlled by detachment tectonics and show landward tilted blocks, they differ in some respects, as extension was accomodated by detachment faulting in the last phase of rifting on the Galicia Bank, whereas it occured in an earlier phase of rifting in the Iberia Abyssal Plain.

Zusammenfassung

Extension und Ausdünnung der Lithosphäre sind grundlegende geologische Prozesse, da sie schließlich zum Aufbrechen der Kontinente und somit zur Bildung von Kontinentalrändern führen. Der west-Iberische Kontinentalrand stellt ein typisches Beispiel eines nicht-vulkanischen Kontinentalrandes dar und ist ideal, um die Extension der Lithosphäre zu untersuchen. Unter einen dünnen Sedimentdecke zeigen sich an der Galizia Bank landwärts gekippte Krustenblöcke, die durch westwärts geneigte Abschiebungen begrenzt werden. Seismische Zeitsektionen bilden unterhalb dieser Verwerfungen eine scheinbar undulierende und diskontinuierliche, starke Reflexion ab, den S-Reflektor, der nahe der Übergangszone von ozeanischer zu kontinentaler Kruste (OCT) durch einen Rücken serpentinisierten Peridotits begrenzt wird. Bis zu Beginn dieses Projektes gab es keine ähnlichen Beobachtungen in der Iberischen Tiefsee-Ebene (IAP), jedoch wurde analog ein Mantelrücken an der OCT vorgeschlagen und durch anschließende Bohrungen bestätigt.

Das Untersuchungsgebiet wurde mit einer Vielzahl reflexionsseismischer Profile vermessen und während zweier Bohrkampagnen beprobt, sodaß die reflexionsseismischen Analysen durch die Bohrergebnisse unterstützt und ergänzt werden. Um nun die Geometrie und Ausdehnung der Extensionsstrukturen festzustellen, die Beziehung zwischen dem S-Reflektor und den Abschiebungen im Hangenden zu klären und schließlich deren Natur besser zu verstehen, werden neben den Standardmethoden der seismischen Datenbearbeitung die iterative Tiefenmigration vor dem Stapeln sowie Wellenform- und Amplitudenanalysen zur Abschätzung von Reflexionskoeffizienten eingesetzt.

Die Ergebnisse der vorliegenden Arbeit zeigen den S-Reflektor weder unduliert noch durch Abschiebungen im Hangenden gestört. S verläuft vielmehr auf seismischen Tiefensektionen als eine teilweise über mehr als 20 km kontinuierliche Reflexion unterhalb der Krustenblöcke und zeigt eine domartige oder leicht westwärts geneigte Form. Darüber hinaus trennen Intervallgeschwindigkeiten innerhalb der Blöcke keilförmige Sedimentpakete der Synrift-Phase vom Kristallin. S ist also eine Abscherung innerhalb des Kristallins, die in der letzten Phase des Riftgeschehens vor dem kontinentalen Aufbrechen (ca. 105 Ma) aktiv war,

da Synrift-Abschiebungen die Krustenblöcke trennen.

Die interne Struktur des S-Reflektors wird durch komplexe Spuranalysen beschrieben: die Wellenform von S ähnelt sehr stark der des Meeresbodeneinsatzes, ist positiv polarisiert und weist einen Reflexionskoeffizienten von etwa 0.2 auf. Dies deutet auf einen sprunghaften Anstieg der akustischen Impedanz an einer Grenzfläche erster Ordnung hin, sodaß S als scharfe Grenzfläche interpretiert wird, die die obere Kruste von einer unteren Platte höherer Geschwindigkeit und Dichte trennt.

Die Tiefensektionen erlauben die Konstruktion einer Tiefenkarte des S-Reflektors. Diese Karte zeigt, daß S landwärts verflacht, was den möglichen Austrittspunkt von S im Osten vermuten läßt. Ebenso wird dadurch die Vorstellung unterstützt, daß der Ausgleich der Extension entlang S durch die westwärtige Bewegung der oberen Platte erfolgt, also auch synthetisch zu den darüberliegenden Verwerfungen. S kann nördlich von 42°20´N nicht mehr eindeutig beobachtet werden, ist also eine Struktur verschieden zu dem als seine nördliche Verlängerung vorgeschlagenen S´-Reflektor und steigt demnach nicht an der vorgeschlagenen Bohrlokation GAL1 an der Ostflanke des Peridotit Rückens zum Meeresboden auf. Statt dessen wird S dort durch ostwärts einfallende Strukturen geschnitten. Dies kann entweder mit einer gleichzeitigen, antithetischen Bewegung oder zeitlich aufeinanderfolgenden Ereignissen erklärt werden.

In der Iberischen Tiefsee-Ebene (IAP) im Süden der Galizia Bank zeigen neu bearbeitete Daten zum ersten Mal relativ kleine, landwärts geneigte Krustenblöcke oberhalb einer starken Reflexion, ebenfalls als "Detachment Fault" interpretiert. Diese Struktur, H, ist wahrscheinlich durch spätere Verwerfungen und die Ausbildung eines tieferen "Detachment-Systems" (L) rotiert worden. H zeigt ebenso wie S eine mit dem Meeresboden nahezu identische Wellenform, positive Polarität sowie einen starken Impedanzkontrast (R ca. 0,12), ist also eine markante Reflexion.

Ein Bohrprofil über die OCT unterstützt darüber hinaus das "Detachment-Modell" für das IAP-Segment vor Iberien: die Extension der oberen Lithosphäre wurde entlang einer westwärts geneigten Abscherung ausgeglichen, welche nachfolgend durch steilere Abschiebungen der oberen Krustenblöcke zerschnitten wird. So entsteht ein Querschnitt , dessen lithosphärisches Tiefenniveau in Richtung der OCT verflacht.

Obwohl die Galizia Bank und das IAP-Segment des Kontinentalrandes

vor Iberien durch "Detachment Faulting" kontrolliert wurden und beide Gebiete geneigte Krustenblöcke zeigen, sind auch Unterschiede vorhanden. So hat "Detachment Faulting" die Lithosphärenextension an der Galizia Bank erst in der letzten Riftphase vor dem kontinentalen Aufbrechen ausgeglichen, während es in der IAP schon eine frühere Episode des Riftgeschehens prägte.

1 Introduction

Divergent rifted margins are among the most prominent tectonic features as they exhibit structures developed during progression of rifting from intra-cratonic processes to complete lithospheric rupture, leading finally to the opening of a new ocean basin. In general, two types of rifted continental margins are defined: those margins accompanied by an excess volcanism during rifting (volcanic rifted margins - e.g. East Greenland and the NW European Margins - Hinz, 1972; Talwani & Eldholm, 1977), and those characterised by thin crust, multiple rift episodes and little or no volcanic activity (non-volcanic margins - e.g. the west Iberian Margin - de Charpal et al., 1978), the subject of this study (Figure 1.1).

The thinning mechanism of continental lithosphere and the formation of passive rifted margins is one of the fundamental geological processes. A variety of different possible explanations for the evolution of passive margins have been suggested, before extensional models were developed (Emery & Uchupi, 1984). Sheridan (1969) proposed that metamorphosis in the lower crust played a dominant role, also discussed by Falvey and Mutter (1981). Subsequently, horizontal extrusion of hot lithosphere towards the ocean (Bott, 1971), and subaerial erosion following thermal uplift (Sleep, 1971) were proposed, and finally Royden (1980) considered large-scale magmatic intrusion responsible for the evolution of passive continental margins. Although likely important for volcanic margins, this mechanism is unlikely important for non-volcanic rifted margins.

The first application of a lithospheric extensional model (McKenzie, 1978) to rifted margins was made by LePichon and Sibuet (1981), a model which has become accepted since then. In the last decade, the discussion has focussed on the controlling tectonic mechanism, based on pure- and simple-shear models (McKenzie, 1978; Wernicke, 1985), which are explained further below. These mechanisms are difficult to constrain, because rift structures are commonly buried beneath thick sediment sequences in extensional basins, thus hampering the analyses of deep features.

In the light of these difficulties, the west Iberian passive margin appears an ideal site to study the nature of lithospheric extension: it is relatively sediment starved and exhibits at the ocean-continent transition deeper lithospheric levels brought close to the surface by extreme extension.

Furthermore, this area is crossed by a number of high-quality multichannel seismic reflection lines, and has been investigated by two campaigns of the "Ocean Drilling Program" (ODP Legs 103 and 149).

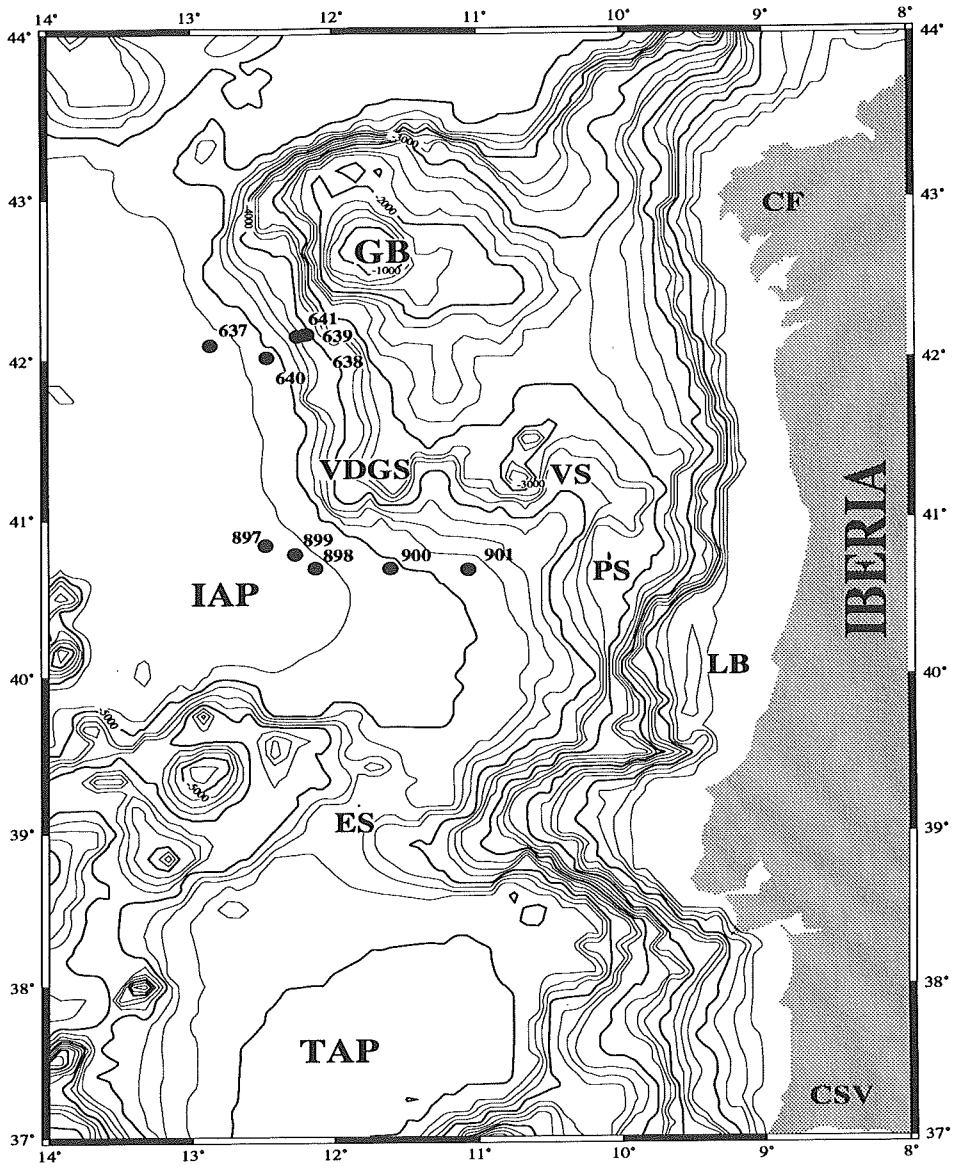

Figure 1.1: Bathymetric map of the west Iberian continental margin and its structural segments: CF-Cape Finisterre; GB-Galicia Bank; VDGS-Vasco da Gama Seamount; VS-Vigo Seamount; IAP-Iberia Abyssal Plain; PS-Porto Seamount; LB-Lusitanian Basin; ES-Estremadura Spur; TAP-Tagus Abyssal Plain; CSV-Cape St. Vincent. DSDP/ODP drill sites are numbered and marked by circles. Contours in 250 m-intervals, 1000 m-contours bold.

The western Iberian continental margin extends between Cape Finisterre in the north to Cape Saint Vincent in the south (Figure 1.1). The bathymetry reveals a narrow shelf area with a steep continental slope, truncated by canyons south of the Lusitanian Basin (Wilson et al., 1989). Further offshore, the west Iberian margin can be considered as three structural segments: the Galicia Bank to the north, the Iberia Abyssal Plain in the centre, and the Tagus Abyssal Plain to the south. The Galicia Bank area is additionally characterised by some seamounts (Vigo, Vasco da Gama and Porto Seamount) to the north and east of the Iberia Abyssal Plain.

With the combination of reflection seismic analyses, determination of detailed velocity models for conversion into depth sections, analyses of physical attributes of the main structural features, and the drilling constraints, this study advances models for lithospheric extension on both the Galicia Bank and the Iberia Abyssal Plain segments of the Iberian passive margin.

1.1 Tectonic history

The North Atlantic rifted margins were formed during different phases of continental separation, and plate kinematics show that plate separation north of the Newfoundland-Azores-Gibraltar Fracture Zone was sequential and progressed from south to north (Srivastava et al., 1990).

During Late Triassic-Early Jurassic divergence between Africa and North America (Tucholke et al., 1989) led to continental break-up and subsequent seafloor spreading south of the Grand Banks, and created rift basins on the Grand Banks (Tankard & Welsink, 1987) and off Iberia (Montenat et al., 1988; Moullade et al., 1988). In the Middle Jurassic final separation between the African and North American Plates took place and rifting between Iberia and Newfoundland continued throughout Jurassic and Early Cretaceous. In the Lusitanian Basin and the south Portuguese Margin these rifting episodes are observed (Mougenot, 1988; Murillas et al., 1990) as well as on Grand Banks and Newfoundland Fracture Zone (Austin et al., 1989). The next phase of motion caused the break-up between Iberia and North America east of the Grand Banks (Srivastava et al., 1990).

On the Iberian margin the rifting occured in three phases: Triassic to Mid-Jurassic, Late Jurassic, and Early Cretaceous. Break-up between Iberia and the Grand Banks appears to have propagated northwards (Figure 1.2),

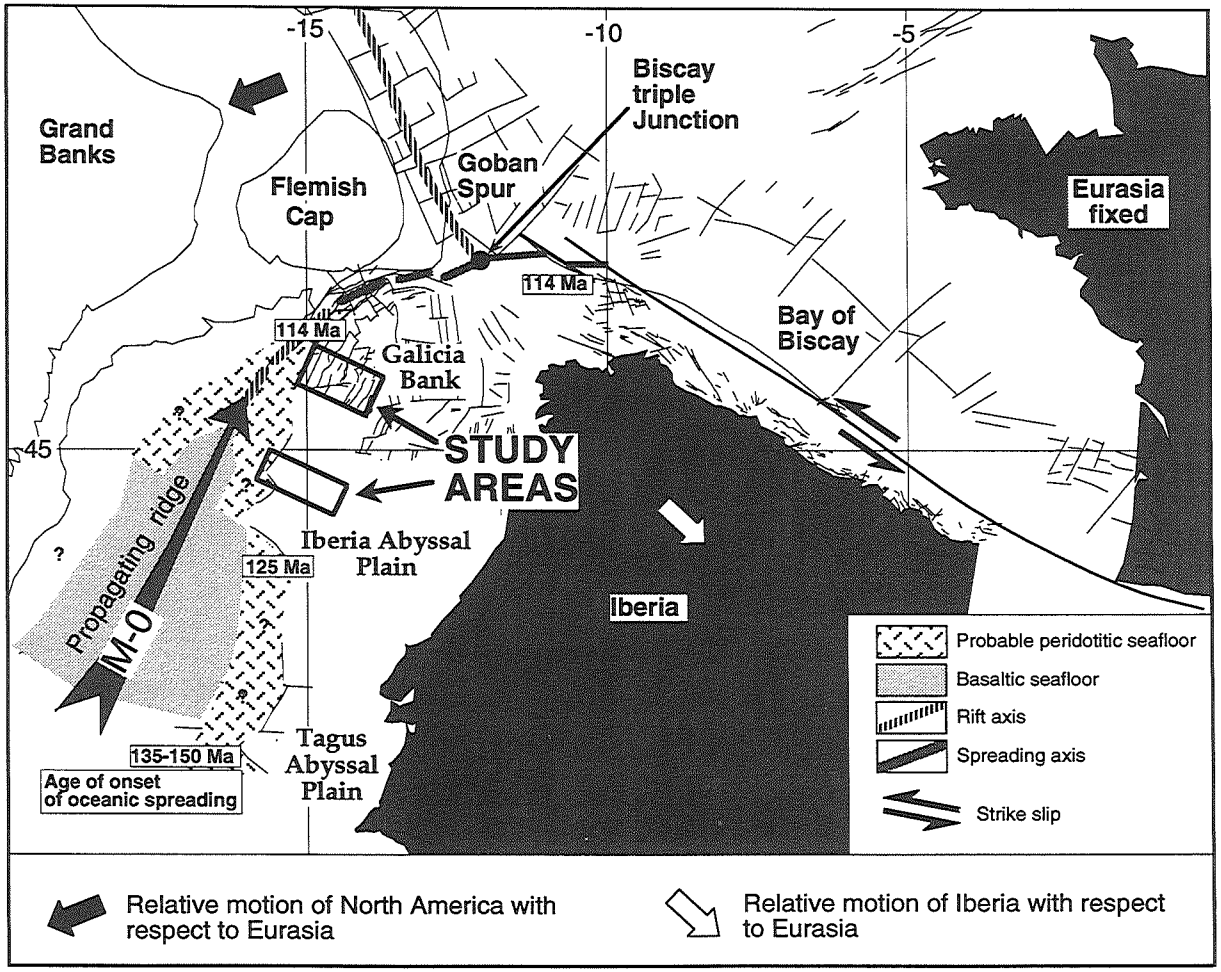

Figure 1.2: Plate reconstruction (after Malod & Mauffret, 1990) at the time of the M0 magnetic anomaly (114 Ma), showing the tectonic setting of the study area when seafloor spreading started off Galicia. The heavy boxes show the investigated areas.

occurring during Early Cretaceous at c. 137 Ma in the Tagus Abyssal Plain (Pinheiro et al., 1992), at c. 130 Ma in the Iberia Abyssal Plain (Whitmarsh et al., 1990a) and finally at c. 114 Ma in the Galicia Bank area (Boillot, Winterer, Meyer et al., 1987; 1988). During the Eocene Pyrenean orogeny and partial subduction of the Bay of Biscay oceanic crust, this region underwent compression, which reactivated some of the rift faults and uplifted basement blocks by perhaps as much as 2500 m to produce the Galicia Banks (Grimaud et al., 1982 - Figure 1.1) and various seamounts (Mougenot et al., 1984). Further compression during the Miocene Rif-Betic orogeny caused a gentle folding of sediments in the Iberia and northern Tagus Abyssal Plains (Mauffret et al., 1989).

Different reconstructions of the positions of the North American, Iberian and European Plates have been suggested (Le Pichon et al., 1977; Klitgord & Schouten, 1986; Masson & Miles, 1994 - e.g. Figure 1.2, reconstruction after Malod & Mauffret, 1990). In general, these reconstructions are poorly constrained: offshore the Galicia Banks and the Flemish Cap the first oceanic crust formed during the Cretaceous constant-polarity interval (Keen & deVoogd, 1988); no large fracture zone occurs within this area; and Iberia was alternatively attached to Africa or Europe (Srivastava et al., 1990), causing intra-plate deformations (Masson et al., 1995).

Despite these complications, the northward propagation of the spreading centre during the early Cretaceous is further evidenced by the sea-floor spreading magnetic anomaly pattern west of the Iberia margin. The large amplitude magnetic J-anomaly is found westward of the presumed ocean-continent transition (OCT) in the Iberia and Tagus Abyssal Plain basins, but not west of the Galicia Banks (Figure 1.2). J is the oldest oceanic magnetic anomaly positively identified west of the Iberia Abyssal Plain (IAP) margin, and is thought to be slightly older than chron M0 as modelled by Whitmarsh and others (1990a). This indicates that sea-floor spreading off the IAP margin started shortly prior to J's formation in Hauterivian-Barremian time, and break-up off Galicia must have occurred later.

1.2 Structural Setting

Following considerable work in the last 15 years, the basic history and structure of the Iberian rifted margin is well understood in the area of the

Galicia Bank (e.g. Mauffret & Montadert, 1987, Boillot, Winterer, Meyer et al., 1987; 1988; Mamet et al., 1991). Numerous seismic reflection profiles image deep structures on this sediment starved margin: the structural style is illustrated by part of the time migrated profile GP12 (Figure 1.3) running normal to the passive margin. This and other profiles image numerous fault blocks, tilted towards the continent by extensional normal faulting (Figure 1.4). The block-bounding normal faults dip consistently to the west (Thommeret et al., 1988) and appear to detach onto a bright crustal reflection, the so-called S reflector (de Charpal et al., 1978), which is the fundamental structure of this margin (Figure 1.4) and shown by samples obtained by drilling and diving (see below) to be an intra-basement feature. It is imaged either as a single, high-amplitude reflection or in places as a narrow band of subordinate reflections. The S reflector occurs about 1-3 seconds TWT beneath the seafloor, and appears to undulate with a wavelength of 10 km and an amplitude of 0.75 seconds on the time sections (Figure 1.3). This may result from strong lateral velocity variations, and represents the effects of velocity pull-up near the tilted blocks and velocity push-down at the sediment-filled half-grabens. The break-up unconformity separates post-rift sediment from syn- and pre-rift sequences and basement (Figure 1.3).

Drilling (Boillot, Winterer, Meyer et al., 1987; 1988) and submersible diving (Boillot et al., 1988b; Mamet et al., 1991) sampled continental granodioritic basement (see also Figure 1.5) overlain by tilted sequences of pre-rift Tithonian carbonates and syn-rift clastic sedimentary units, the Synrift I-sequence of Mauffret and Montadert (1987). In contrast, the sediment fill of the half-grabens thickens towards the faults, and was hence deposited in a later syn-rift phase, corresponding to the Synrift II-sequence (Mauffret & Montadert, 1987). In summary, two rift phases are identified within the sediments on the Galicia Bank: preceding tilting and faulting in early syn-rift (Hauterivian-Valanginian), and accompanying the second phase of faulting in late syn-rift (Aptian-Hauterivian). In the Iberia Abyssal Plain, few extensional structures such as tilted blocks and no possible detachment faults had been reported until this study.

Another important aim in research of non-volcanic rifted margins is the definition of the nature of the basement, thus the location and characterisation of the ocean-continent transition (OCT). Both segments of the Iberian margin exhibit a ridge of mantle material within the transition

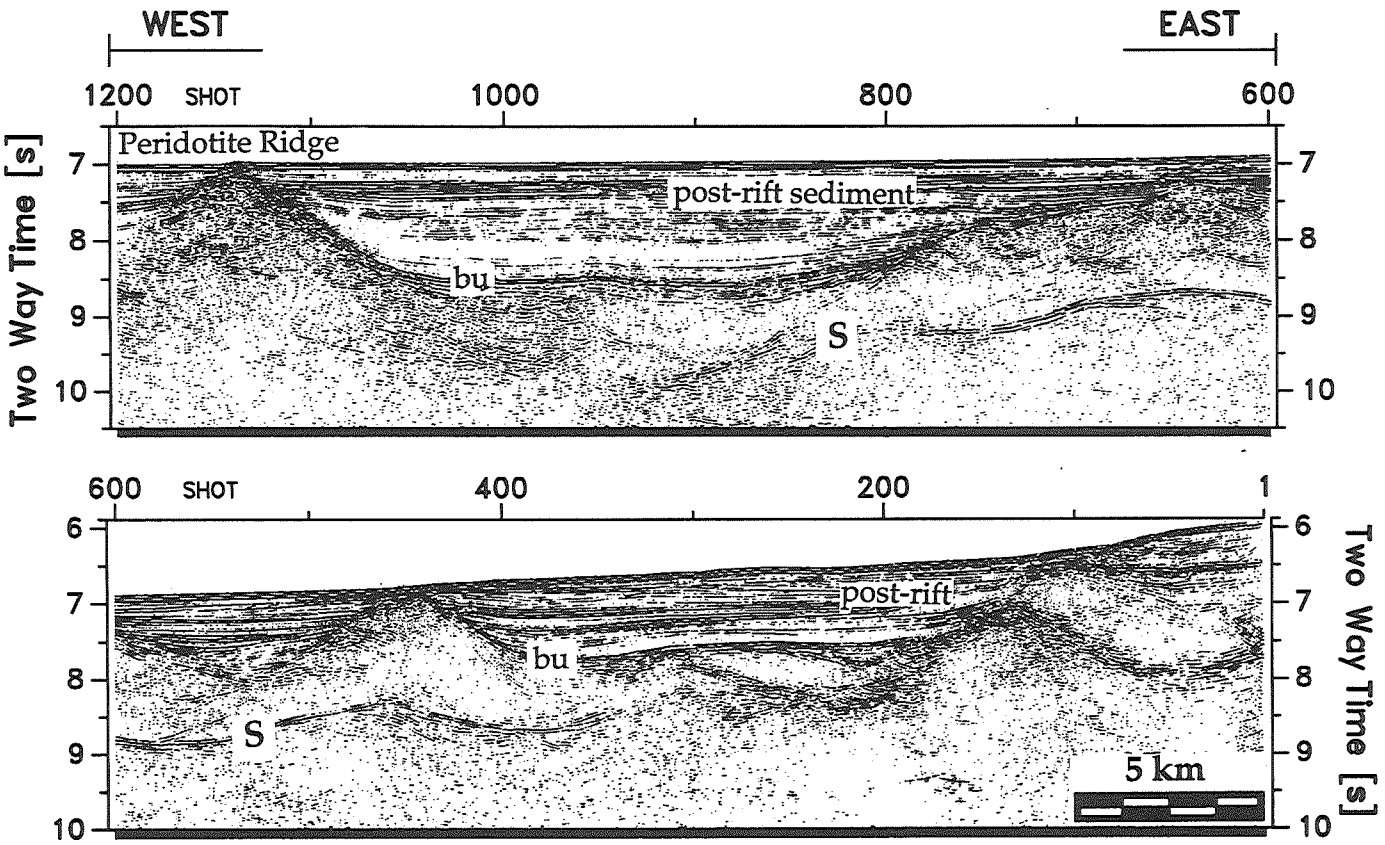

Figure 1.3: Time migrated seismic section of profile GP12, showing the typical extensional structures found off the Iberian Atlantic margin in the Galicia Bank area. The break-up unconformity (bu) separates regularly bedded post-rift sediments from syn-rift sequences and basement. Below the series of continentalward tilted crustal blocks, the S reflector is imaged as a bright crustal, apparently undulating reflection (8-10 sec TWT). To the west, the Peridotite Ridge marks the ocean-continent boundary.

between continental and oceanic crust: the Peridotite Ridge off Galicia is shown in Figure 1.3 to the west of the S reflector. Prior to drilling, seismic data had been used in the first stage of investigations to define the OCT on the basis of a change in seismic character of the top of basement and the mapping of basement highs (Montadert et al., 1979; Mauffret & Montadert, 1987). Subsequently, the hypothesis of a mantle outcrop at the western end of the OCT was confirmed for the northern segment of the Iberian margin (Girardeau et al., 1988; Beslier et al, 1990) from drilling ODP Leg 103 (Boillot, Winterer, Meyer et al., 1987), dredging and submersible diving (e.g. Boillot et al, 1988b; Mamet et al., 1991). The summary of the basement geology of

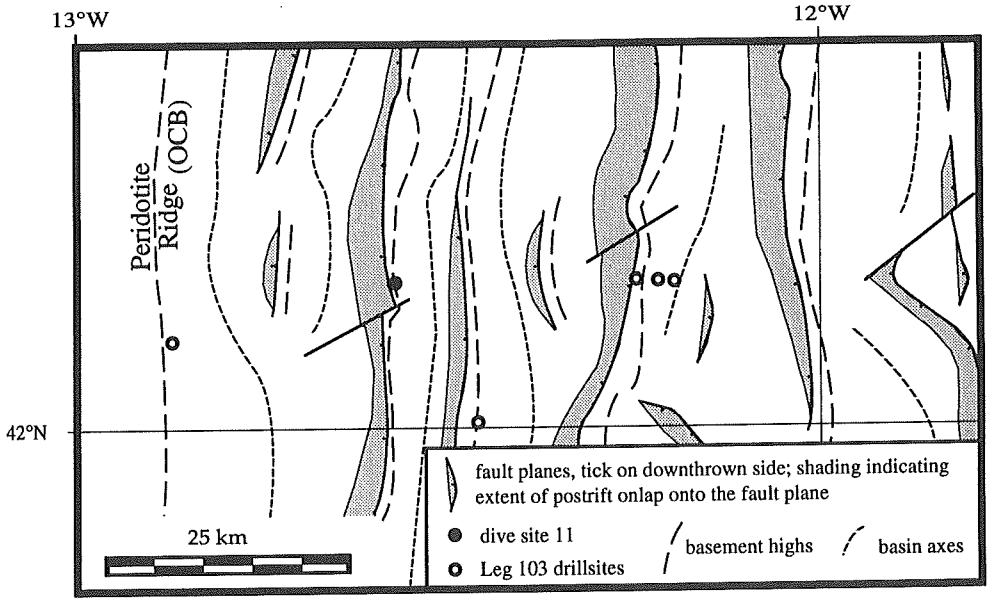

Figure 1.4: Structural map of the west Galicia margin in the region of the S reflector (after Thommeret et al., 1988). The structure of the upper plate to S is dominated by west-dipping faults and clearly defined tilted blocks. Drilling on ODP Leg 103 and diving established the nature of the basement highs across this margin.

the Galicia Bank area (Figure 1.5) constrains the position of the Peridotite Ridge marking the OCT and the nature of the basement.

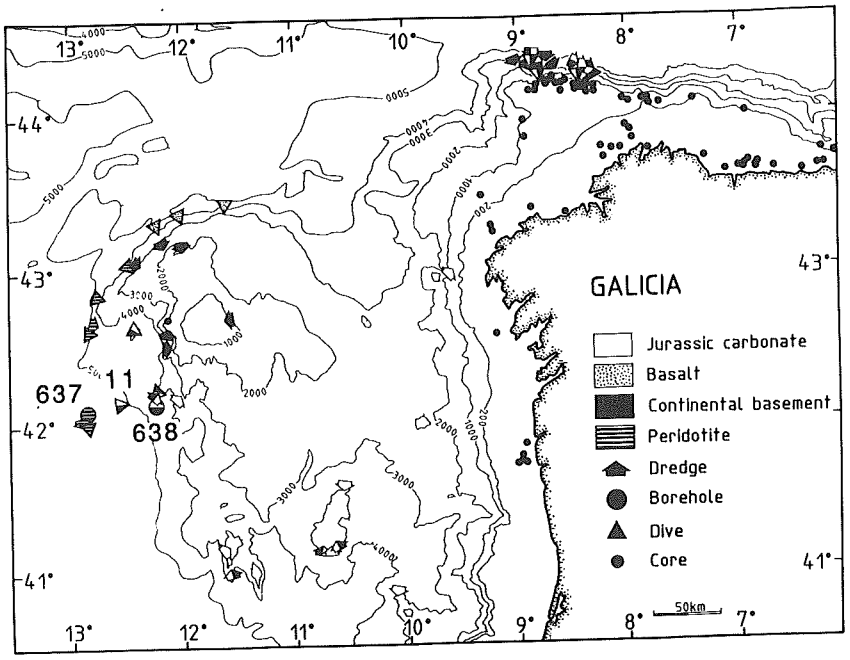

Figure 1.5: Summary of basement geology deduced from drilling, diving and dredging showing nature of basement. Numbers 637 and 638 refer to Leg 103 drill sites, 11 to Galinaute cruise dive site.

In the Iberia Abyssal Plain, first interpretations were also based on seismic records and seismic velocities (Whitmarsh et al., 1990b), resulting in a basement contour map (Figure 1.6). A basement ridge similar to the Peridotite Ridge off Galicia was interpreted by Beslier et al. (1993) to consist of serpentinised peridotite and to mark the ocean-continent transition as the southward counterpart of the mantle outcrop west off Galicia. Simultaneously, the analysis of refraction seismic data was combined with the modelling of a single east-west gravity profile (Whitmarsh et al., 1993), and magnetic modelling (Whitmarsh & Miles, 1994). This led to the identification of a layer of extremely thinned continental crust adjacent to thin oceanic crust, both underlain by partly serpentinised mantle material.

Drilling on ODP Leg 149 (Sawyer, Whitmarsh et al., 1993) confirmed indeed that the basement ridge comprises serpentinised mantle rocks bounding the western end of the OCT (Site 897 - Figure 1.6), and thus partly proved the existing geophysical model.

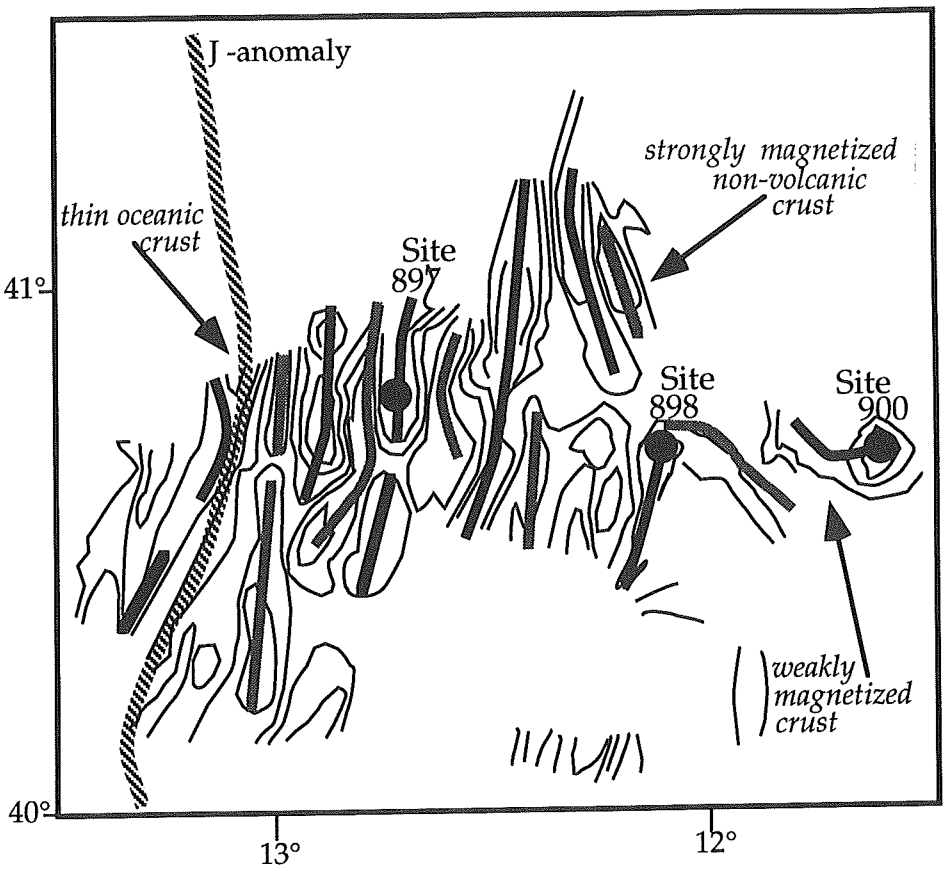

Figure 1.6: Basement contour map of the Iberia Abyssal Plain based on unmigrated MCS and single-channel data (after Sawyer, Whitmarsh, Klaus et al., 1994). Highs and lows are marked as black and gray lines, numbers label Leg 149 drill sites (0.25 s TWT contours).

To resolve the problem of crustal type, no further information or analogy is provided by the existing data across the conjugate passive margin off Newfoundland. There, the basement structure, the nature of the break-up conformity and the quiet magnetic field are invoked by Austin and

others (1989) and Tucholke and others (1989) to suggest thin continental crust within the OCT. However, it is possible that the crust in the transition is oceanic (Mauffret et al., 1989), formed during slow spreading in the Jurassic. A similar line of argument led Sawyer (1994, pers. comm.) to propose that in the Iberia Abyssal Plain the region immediately landward of the Peridotite Ridge is oceanic crust.

Beslier and others (1993) pointed out that the width of the transition zone from oceanic crust through serpentinised mantle to definite continental crust is four to five times wider on the Iberia Abyssal Plain than west of Galicia: in contrast to 40 km west of the Galicia Bank, the transition extends over 150 km width on the the Iberia Abyssal Plain margin. This may mean that a low strain rate and a very long duration of extension would be required, lasting approximately several tens of Ma to form such a margin (Kusznir & Park, 1987) and to produce such a wide region of very extended thin crust. Nevertheless, the basic structure of both margins is similar (Krawczyk et al., 1994). The crustal type landward of the Peridotite Ridge and the crustal thickness are still not completely determined and understood, and are the subject of further investigations and ongoing work.

1.3 Models for Lithospheric Extension

Numerous models have been proposed to describe the mechanics of extreme continental extension resulting in the formation of a passive margin (e.g. Meissner, 1986), but the matter remains controversial.

In general, two classes of models for lithospheric extension have been advanced: pure shear (McKenzie, 1978) and simple shear (Wernicke, 1985; Lister et al., 1986). These two end-member models both imply extension of crustal and subcrustal lithospheric levels by brittle or ductile processes, and in both models upwelling of asthenospheric material occurs in response to lithospheric thinning. However, the models have a number of fundamental differences.

The pure-shear model (Figure 1.7) predicts that all crustal and lithospheric layers should be thinned by the same amount and the centre of subsidence after rifting should be directly above the rift axis (McKenzie, 1978). Assuming symmetric extension and excluding large-scale rotation of crustal blocks, this would result in a sequence of layers with post-rift on top, then syn-rift sediments, upper and lower crustal and mantle material. The

rift zone undergoes two phases of subsidence: the first one is related to faulting and occurs during ongoing extension, and in the second phase thermal subsidence occurs.

The mathematical model of McKenzie based on uniform lithospheric stretching and thinning explained many of the features of sedimentary basins and their thermal evolution. But as he assumed the entire lithosphere to be stretched uniformly, his model did not consider the mechanism of extension at different lithospheric levels.

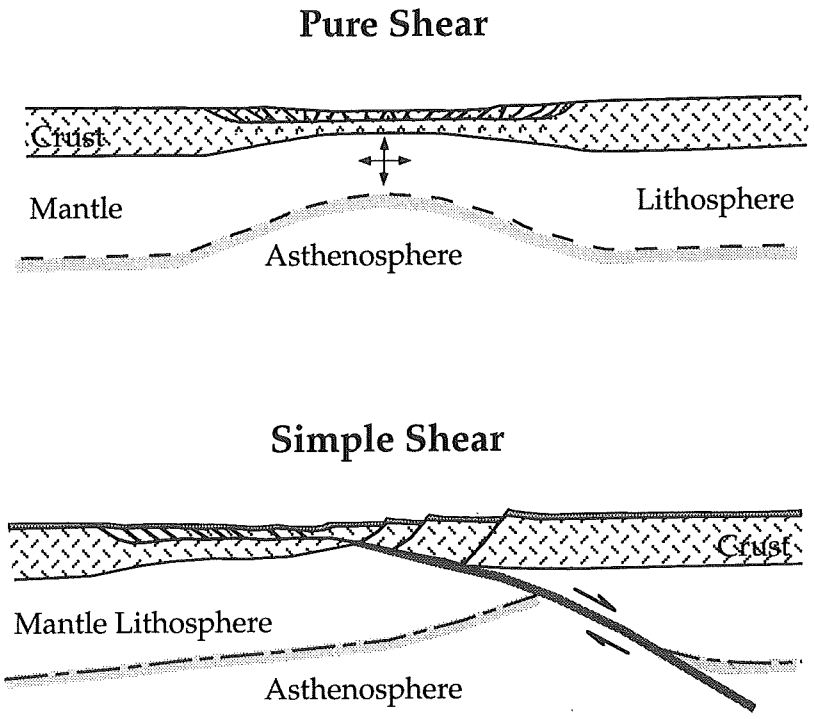

Figure 1.7: The pure-shear model of McKenzie (1978) predicts symmetric extension and uniform thinning of all lithospheric levels, while Wernicke's (1985) simple-shear model accounts for completely asymmetric conditions, putting into contact sediment and deep crustal/mantle material.

In contrast, the simple-shear model (Figure 1.7) is inherently asymmetric, predicting the denudation of large blocks of deep, relatively unthinned lithospheric material along the master shear zone (Wernicke, 1985), the detachment. The locus of extension in the mantle is offset from that in the crust, producing asymmetric subsidence, so that some areas are devoid of syn-rift sediment and that post-rift sediments can be found directly above deep crustal or mantle material. Whereas the pure-shear model allows only subsidence, the simple-shear model predicts both subsidence of the upper crust, and uplift of the area where the shear zone deepens into the mantle, and where hot asthenosperic material upwells away from the crustal rift.

A number of composite models have also been proposed, including features from both pure- and simple-shear models (e.g. Coward, 1986; Mutter et al., 1989) to explain structures in the Basin and Range province of the western United States (Wernicke, 1981), sedimentary basins formed by lithospheric extension, and the structure of passive margins (e.g. Lister et al., 1986; Mutter et al., 1989). Recent workers combined the pure- and simple-shear models temporally and spatially. For instance, Keen and Dehler (1993) applied the pure-shear model on a lithospheric scale to the Newfoundland margin, with localized simple shear in the crust. Sibuet (1992) did likewise for the west Galicia rifted margin. On the other hand, Harry and Sawyer (1992) suggested a temporal succession for the Baltimore Trough, assuming for the whole lithosphere first "simple shear" (driven by offset pre-existing weaknesses in the crust and mantle - Figure 1.8), and "pure shear" in a later rift stage. However, there is still no consensus, and outstanding problems of lithospheric extension still remain, as these models cannot fully explain crustal and tectonic asymmetries and even mantle exposure on non-volcanic rifted margins. On these non-volcanic passive margins, older rift basins are landward of, and sub-parallel to fairly wide, younger, faulted basins floored by thin crust of continental origin. The areas of thin crust flank the line of break-up and show mantle outcrops or subcrops, evidenced partially by drilling (see sections 1.1 and 1.2).

One key question about the mechanics of lithospheric extension is the importance of detachment models and low-angle normal faulting during rifting. The most relevant detachment models for discussing the structures found offshore the Iberian continental margin are those from Buck (1988), Lister and Davis (1989) and Axen (1992) combined with that from Hoffmann

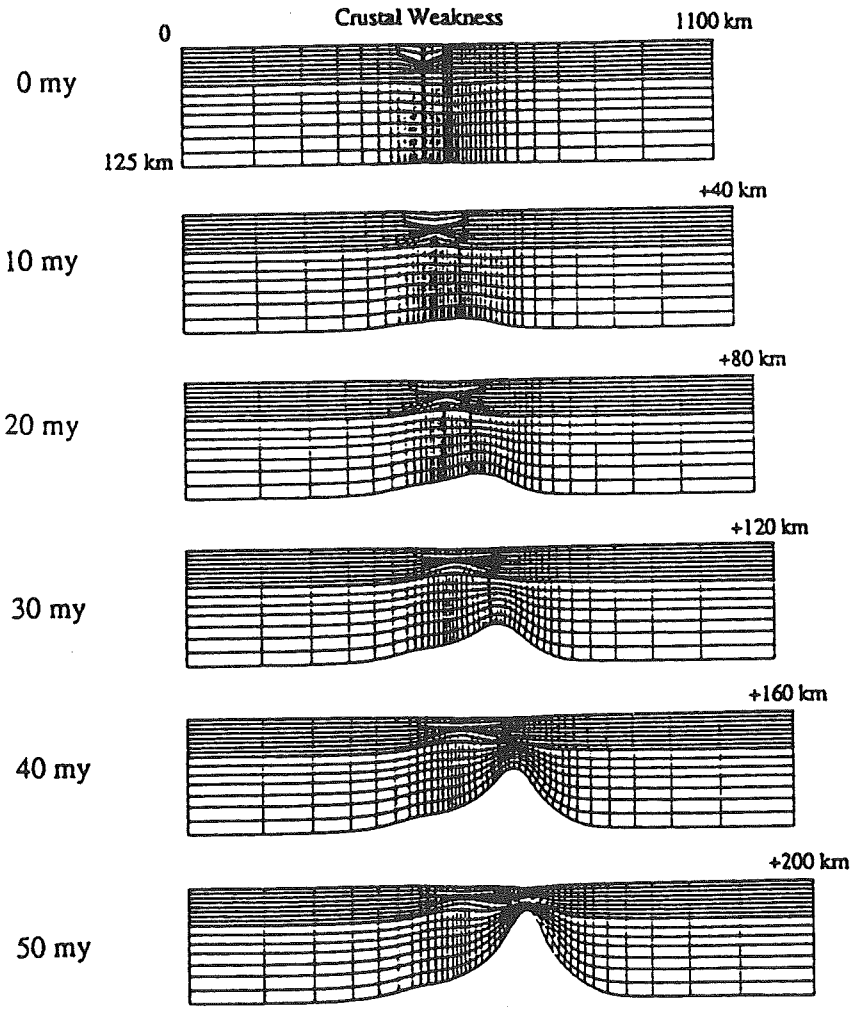

Figure 1.8: Dynamic model of extension (from Harry & Sawyer, 1992), driven by pre-existing crustal and mantle weaknesses. The starting finite element mesh is 1100km wide, with a 40 km thick crust overlying mantle. Whereas the upper mantle weakness is modeled as a 200 km wide region, the midcrustal weakness is modeled in a 100 km wide region, both overlapping with the weakest portion beneath the eastern edge of the midcrustal weakness. Times are measured relative to the start of extension, and total extension is indicated to the right.

and Reston (1992). These models (Figure 1.9) differ mainly in the dip assumed for the detachment when rifting started, in other words whether the detachment was always active at low-angle, or started initially with a steeper dip. The second aspect is the relative timing of rifting in the upper plate to the detachment and of movement along the detachment itself.

Lister and Davis (1989) proposed detachment faults formed at low angle cutting across steeper normal faults (Figure 1.9A). Therefore, the upper plate normal faults (domino style or other) intersect the underlying detachment at a high angle, and are truncated by it. Hence, the key aspect of this model is that the detachment post-dates the upper plate faults, such that the base of the fault blocks is cut by later low-angle normal faulting.

A second model has been suggested (Axen, 1992; Hoffmann & Reston, 1992), which assumes simultaneous motion along the steeply dipping faults in the upper plate and the underlying detachment (Figure 1.9 B). This synchronous movement would require deformation of either the fault blocks or the lower plate to the detachment to solve the space problem arising from this motion. If, for instance, the keels of the blocks in the domino-model were abraded, and subsequently this debris scraped into the adjacent gaps, then the detachment could be active at the same time as the upper plate faults. Although this theory might be difficult to prove in detail without drilling, the analyses from Axen (1992) support this idea.

Axen (1992) argues that low-angle faults can remain active within the brittle crust by maintaining high pore pressure through mineralisation along the detachment and through hydrous alteration in the breccia zone, effectively sealing up fractures in the upper plate. This mechanism allows the detachment to be active at low dips, and is consistent with large volume redistribution and cataclastic deformation, thereby facilitating the abrasion of the fault block keels, as suggested in the model of Hoffmann and Reston (1992).

A third possible model (Buck, 1988) suggests that during progressive extension along initially steeply dipping normal faults, these flatten and become inactive low-angle detachments (Figure 1.9 C). A new normal fault cuts up to the surface when the unloading of the footwall causes the fault to bow up sufficiently to hinder movement along it. This results in a system of fault blocks on top of an inactive detachment, which is hence always older than the immediately overlying faults and which youngs away from the breakaway.

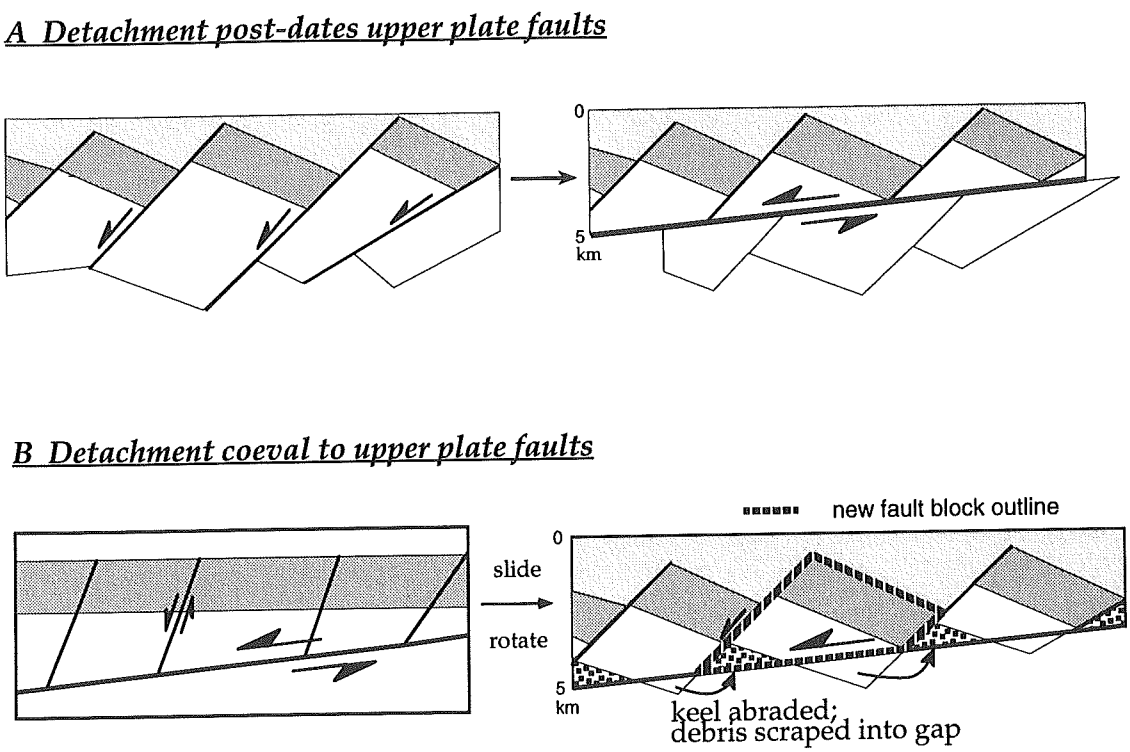

Figure 1.9: Detachment fault models relevant for the structures off Iberia. Key differences are the initial angle of the detachment and the time relation between upper and lower plate faulting. A) Lister and Davis (1989) suggest the detachment post-dating upper plate faulting, whereas B) Axen (1992) and Hoffmann and Reston (1992) favour simultaneous motion. C) Buck (1988) invoked an initially steep detachment pre-dating upper plate faulting.

Whatever the mechanism and timing of steep- and low-angle faulting might be, the final section generated by detachments post-dating or coeval to upper plate faulting would show almost the same geometrical image (compare Figures 1.9 A and B), despite their different age relationships. Thus it is not possible to distinguish between these models from seismic data alone without detailed dating of the succession of events. In the case of rifted margins, such dating requires sampling by drilling. On land, where samples are easier to obtain, no consensus has yet been reached, and different models may be applicable in different places. Although Keener and others (1993) argued recently, that three of six fault segments in the Death Valley, western US, have been rotated from steep to low dips during extension, the Buck (1988) and Wernicke and Axen (1988) models are not always that well constrained by critical field relations. Scott and Lister (1992) and Axen (1992) have presented evidence for the low-angle origin of detachment faults from field investigations in several different core complexes, and have explained how such features can move at low angle. Another possible low-angle mechanism was also advanced by Parsons and Thompson (1993), who investigated detachment structures in the western US cordillera. They attribute the domal or irregular shape of detachment faults not necessarily to rotation during extension, but to an intrusive zone beneath these faults. This magmatism creates the stress regime necessary for low-angle normal fault activity. A feature of this idea is that the detachment is located in the brittle crust and does not represent the elevated brittle-ductile transition.

1.4 Application of Extension Models to the West Iberia Rifted Margin

A variety of composite models with features from both pure- and simple-shear models have been suggested for the west Iberia continental margin (e.g. Whitmarsh et al., 1990a). The simple-shear model (Wernicke, 1985) explains much better than the pure-shear model (McKenzie, 1978) the existence of mantle rocks near the seafloor surface, such as the ridge of serpentinised peridotite near the Galicia Bank (Boillot et al., 1988a), although Winterer et al. (1988) proposed it formed by the diapiric rise of serpentinised mantle material.

In all interpretations of the west Galicia margin the S reflector is the most critical structure (Figure 1.10). It was first described in a pure-shear

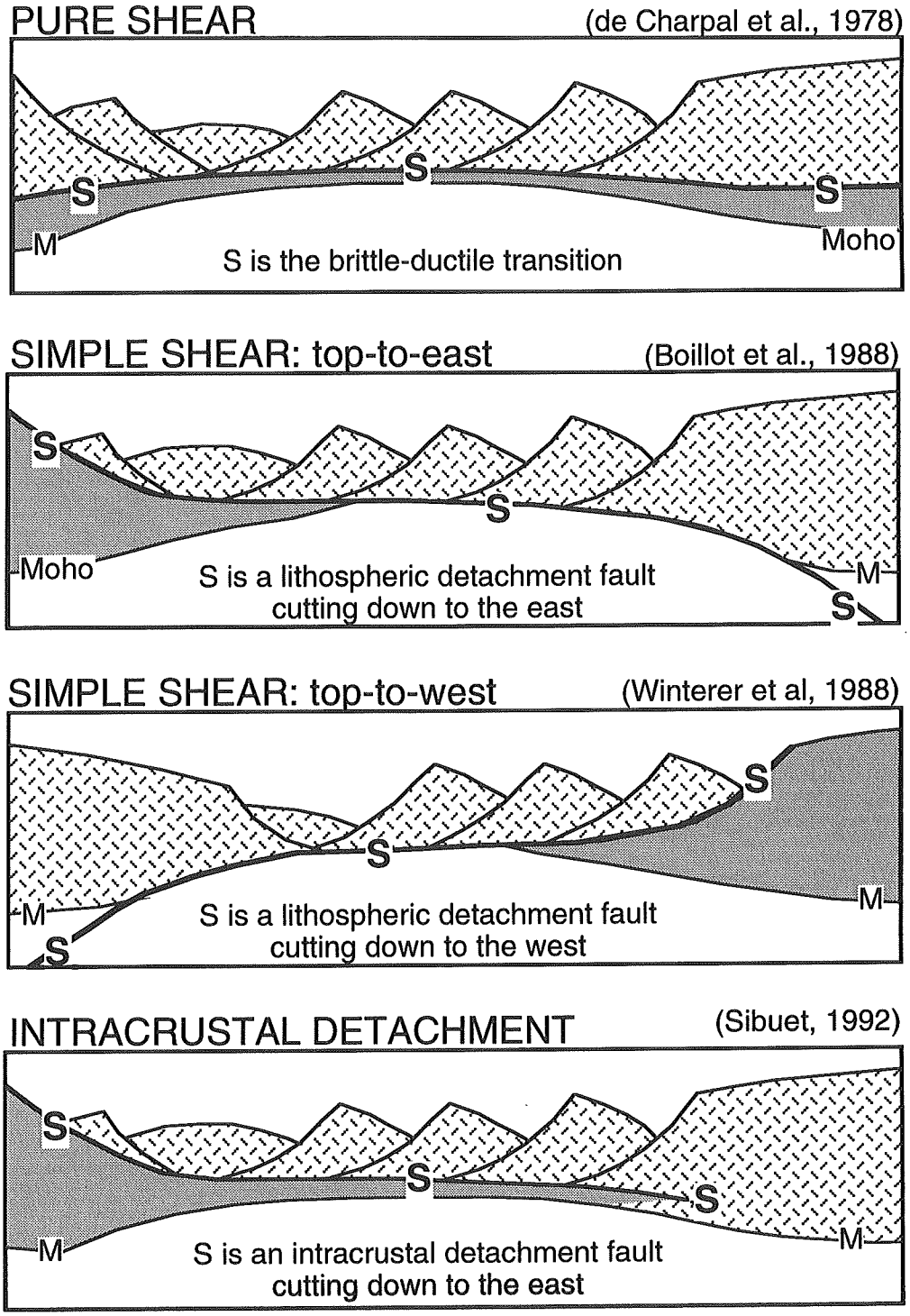

Figure 1.10: Extensional models applied to the Galicia Bank margin. The key structure is the S reflector beneath the tilted blocks, interpreted in the pure-shear model (de Charpal et al., 1978) as brittle-ductile transition, in the subsequent models as either east- or west-dipping detachment.

model by de Charpal et al. (1978) and interpreted as the brittle-ductile transition. In 1982, Wernicke and Burchfiel interpreted S as a lithosphere-penetrating detachment in a simple-shear model. Subsequent workers also interpreted S as such a structure, but dipping either to the west (Winterer et al., 1988) or to the east (Boillot et al., 1988a). S has also been thought to mark the crust-mantle boundary (underlain by serpentinised peridotites) and to be cut by later normal faulting prior to continental break-up (Boillot et al., 1989). In the composite models of LePichon and Barbier (1987) and Sibuet (1992) S is an intracrustal landward-dipping detachment, and recently it was described as the top of a layer of mafic underplate (Horsefield, 1992). Clearly an understanding of S is key to developing a model for the evolution of the west Galicia margin.

1.5 Aims and Approach

The principal aim of this work was to study the processes of continental extension leading to continental break-up on the Galicia Banks and Iberia Abyssal Plain segments of the west Iberia rifted margin through the use of modern state-of-the-art commercial processing techniques on existing high-quality multichannel seismic reflection data (Figure 1.11). For the west Galicia margin, the work set out to determine the nature of the S reflector, a possible detachment fault, and to place this structure within the context of the extensional evolution of this margin. The aim for the second part of the project was to develop an integrated model for the evolution of the Iberia Abyssal Plain margin through analysis of the seismic reflection data and integration of this with other geophysical data and drilling results. Thus, the understanding of the way the lithosphere extends, the importance of detachment tectonics in continental break-up and the nature of the ocean-continent transition were subject of analyses.

To achieve these objectives, secondary aims like analysis of geophysical attributes of the S reflector west of Galicia and other key structures were included, analysing the polarity, reflection coefficient, and internal structure of the main features (see Chapter 2). Such an approach had not previously been applied to the S reflector, although in places it is a bright and continuous reflection, and as such ideal for these analyses (see Chapter 3).

The same techniques were also applied to key structures beneath the Iberia Abyssal Plain, although there the presence of structures similar to S

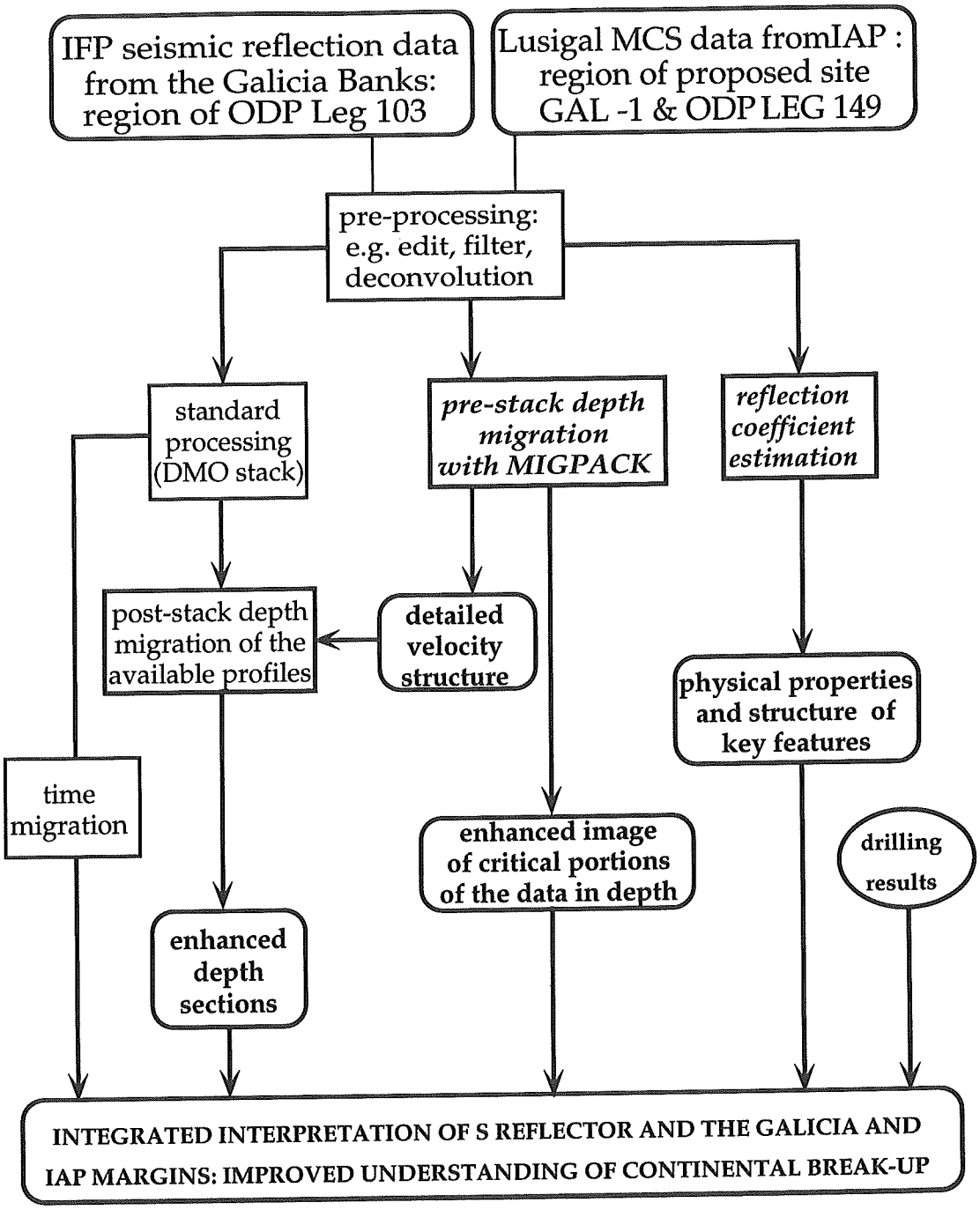

Figure 1.11: Schematic illustration of the structure of processing and analyses carried out in this study, based on MCS reflection data from the Galicia Bank and Iberia Abyssal Plain rifted continental margins.

was unknown prior to this work (see Chapter 5).

Another aim was the resolution of geometry of both the S reflector and major extensional faults of the Galicia margin and investigation of their relationship. Previous interpretations have been based on time migrated sections, with the problems of velocity pull-up and push-down, inaccurate velocity information, inaccurate depth conversion, the degradation of the data through CMP smearing, and the attenuation of steeply dipping events. These are the reasons why numerous interpretations have been advanced in the past, as critical portions of the data were prevented from confident extrapolation of S either to depth or to the surface. These imaging problems arise from the complex upper crustal structure (e.g. sediment-filled half-grabens and tilted blocks - Figure 1.3) where S shows maximum undulation because of the velocity effects and raypath bending (Peddy et al., 1986).

It was considered probable that substantial improvement could be achieved through processing techniques like prestack depth migration, a major part of this work. This technique accounts for raypath bending and refraction, and provides a final section in depth; two major advantages compared to the conventional time migration. Additionally, CMP-smearing is reduced (Sherwood, 1989) and a detailed velocity model may be generated by depth focussing error analyses (see Chapter 2).

A final subject of the study of the west Galicia margin was the investigation of the relationship between the S reflector and the Peridotite Ridge to the west, and to another bright crustal reflection located to the north (S´), suggested as a possible drilling target to ODP (Boillot et al., 1994). Thus, the region between the Peridotite Ridge, S and S´ was investigated to determine the northern and southern limits of S and S´, the nature of the overlying units, and reveal the relationship between the features (Chapter 4).

Prior to this work, the structure of the Iberia Abyssal Plain margin was far less well known than that west of Galicia, and consequently the objectives less focussed. Although it was anticipated that the same techniques applied to the Galicia margin would prove successful on this margin, the key structures to investigate were unknown at the beginning of the project. Seismic data were combined with the results from drilling recently on ODP Leg 149 across the ocean-continent transition of the Iberia Abyssal Plain margin. Although analysis of drill samples is not complete, an integrated, preliminary model for the evolution of this margin is developed and presented here (Chapter 5).

2 Seismic Data Processing

The multichannel seismic reflection data used for the studies described in the following chapters come from two different sources. The GP-series were recorded in 1975 and 1980 for the Institut Français du Pétrole, Paris, using 1-3 Flexichoc guns as source. The Lusigal-campaign under the leadership of G. Boillot (of the Gemco-group in Villefranche/Mer) shot the LG-profiles with an array of eight synchronised waterguns.

Whereas the GP-series were acquired with 48 channels on a 2.4 km long streamer (group interval 50 m), the LG-series were recorded with 96 channels (group interval 25 m), resulting in 25 m and 12.5 m CMP-distance respectively; both data sets had a shot spacing of 50 m. The offset range and CMP-coverage of 24/48 provide good velocity control and the chance to image strong reflections within the basement.

Seven of ten investigated profiles are margin-normal profiles. They thus show the extensional structures and have been successfully time- and depth-migrated. The north-south trending profiles provide connection and control between the east-west lines as a part of the profile grid exhibited in Figure 2.1. In the Galicia Bank area, the GP-profiles form a closely spaced grid, and thereby provide the opportunity to map out the S reflector in depth for the first time. In contrast, the LG12 line in the Iberia Abyssal Plain stands somewhat alone in this study, but passes through three recently drilled locations (ODP Leg 149; Sawyer, Whitmarsh, Klaus et al., 1994) within a distance of 160 km along the profile. Consequently, its interpretation is further controlled by additional geological information about the nature of the basement. This offers the possibility of combining discrete geological sampling with seismic data, thus leading to the development of a new model for lithospheric extension in this area.

All imaged profiles were first analysed by standard seismic processing, as described in section 2.1. Parts of the west-east trending GP-series and the LG12-profile were also investigated by the depth migration before stack, the principle of which is explained in section 2.2. This powerful tool reveals the geometry of the key structures in depth; one of the main topics of this work. Finally, the crustal detachment faults, the most prominent features of the investigated continental margin segments, are analysed in more detail regarding their reflection coefficients and physical properties (see section 2.3 and also Figure 2.2).

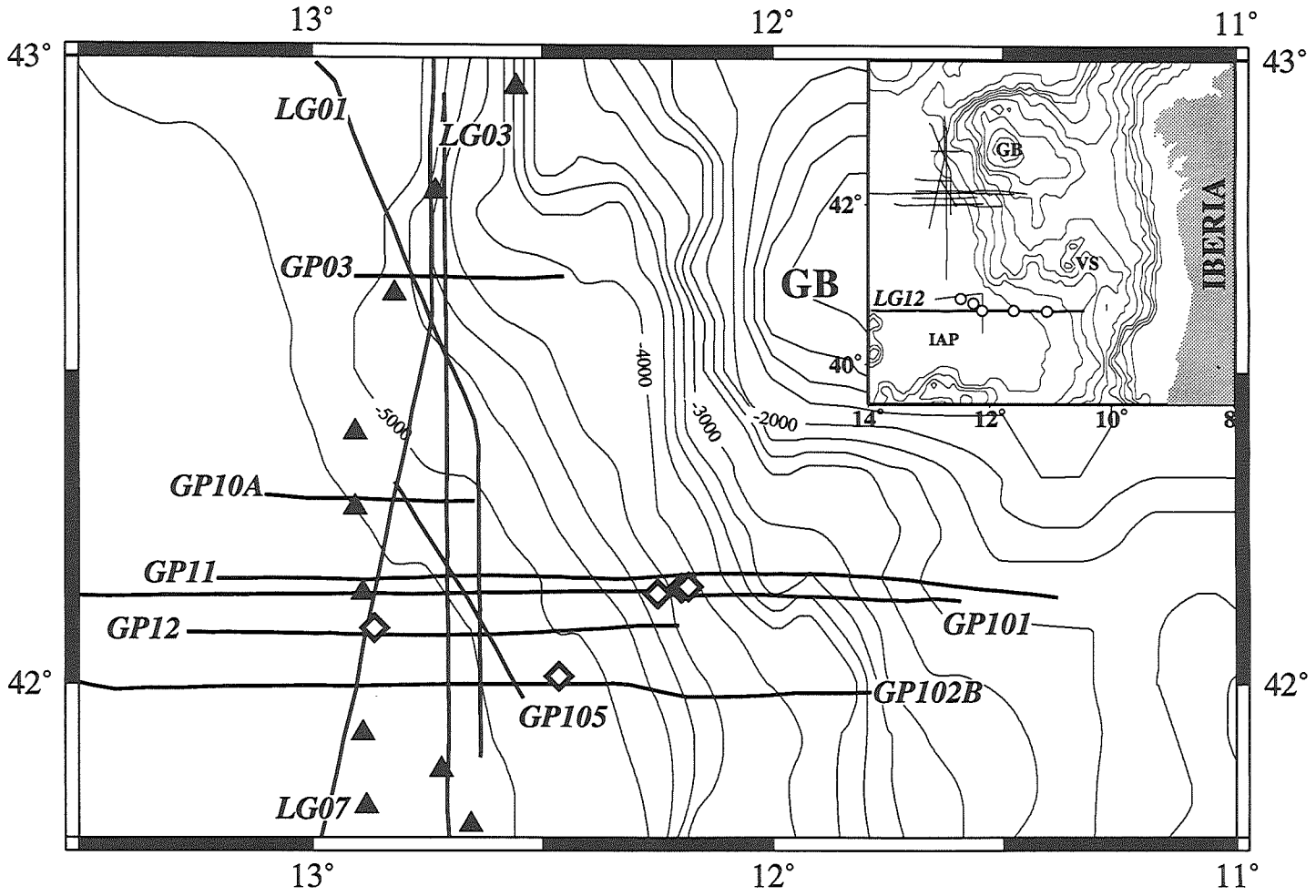

Figure 2.1: Bathymetric map of the investigated area with the profile locations of the GP-series and profile LG12 (inset). Also marked are drill sites from ODP Leg 103 (diamonds), Leg 149 (circles), and the Peridotite Ridge (triangles). GB-Galicia Bank; VS-Vigo Seamount; IAP-Iberia Abyssal Plain.

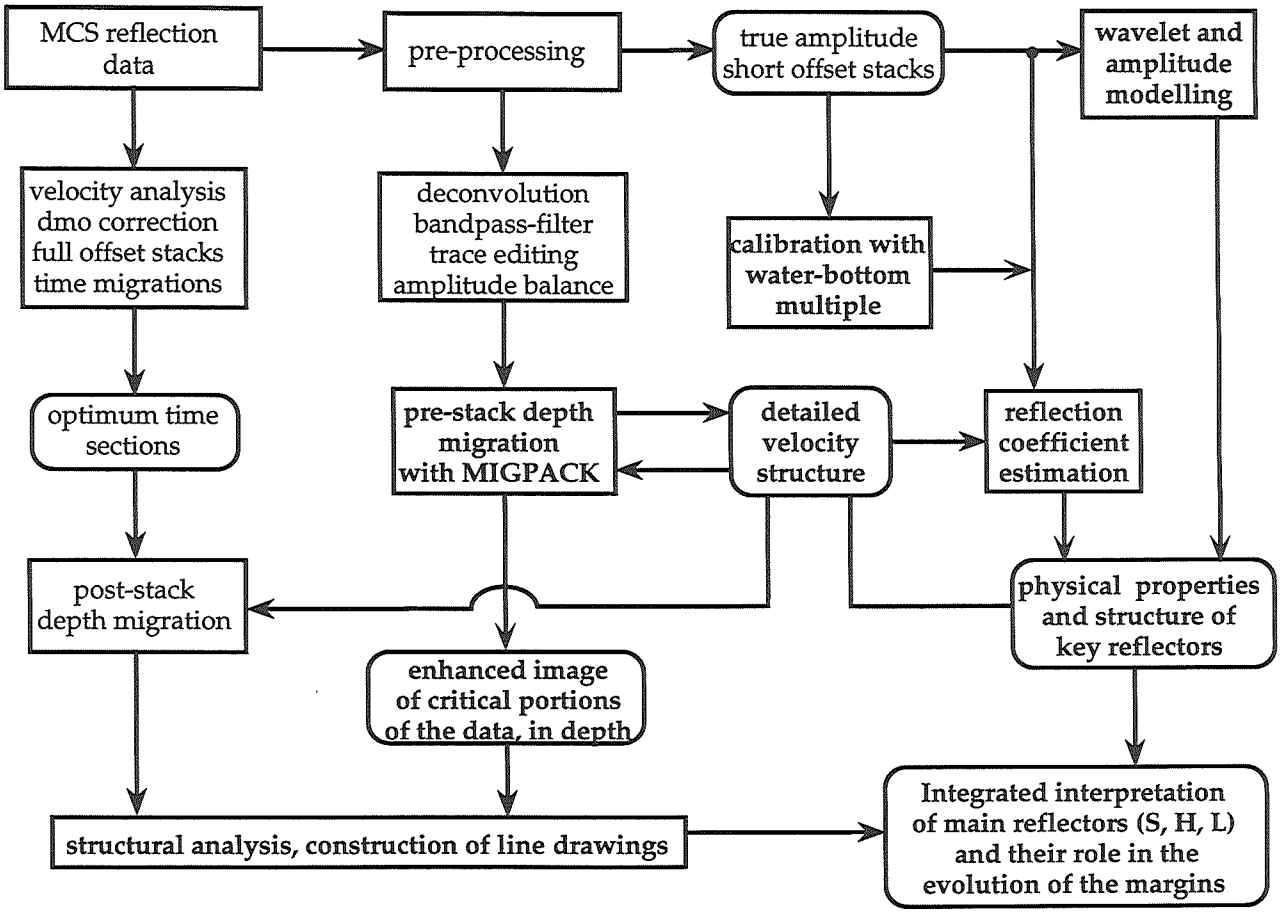

Figure 2.2: Flow-chart of single processing steps and their interaction during analyses of seismic reflection data from the Galicia Bank and Iberia Abyssal Plain margins.

2.1 Standard Processing

The GEOMAR Processing-Centre has a Convex-based system, which uses Geco-Prakla´s GEOSYS seismic software. This software package offers all modules necessary for a complete seismic analysis, including migration in time and depth. Hence, all available data first underwent the processing procedure described within this chapter, providing time-migrated stacked sections. These provided the data base for the selection of the relevant sections for the depth migration before stack (Figure 2.2).

The first step analysing the multichannel seismic reflection data was a standard processing scheme described here briefly (e.g. Hatton et al., 1986; Yilmaz, 1987). As available data were field tapes (SEG-B or SEG-D), pre-processing started with demultiplexing, specification of field geometry and writing this information into the header. At the end of this procedure, the data were sorted and output as shot- (48 or 96 channels) and CMP-gathers (24- and 48-fold). These gathers contained bad traces and had a high noise level, and thus need trace-editing, despiking and appropriate bandpass-filtering. Where appropriate a deconvolution was also applied to remove the earth's filter effects (Meissner & Stegena, 1977), thus compressing the seismic wavelet to increase the vertical resolution. Figure 2.3 shows an example of the near offset trace from profile LG12, which demonstrates the noisy and unclear seismic image of the raw data. The filter parameters were chosen after spectral analysis of the data. In general, the interesting frequency range lay between 10 and 70 Hz, with the main signal at about 15-35 Hz, depending also on depth. In practice, the data were bandpass filtered with ramps of different dips to avoid ringing at the filter edges, and also created time-variant.

The CMP-sorted gathers were used for velocity analyses picking the relevant CMPs for velocity analyses from the near offset stack (Figure 2.4). This analysis uses velocity panels (Figure 2.5) and constant velocity stacks to determine the velocity needed to correct the normal move-out of the data in the full offset stack (Figure 2.6) before DMO correction. Repeated velocity analyses after DMO and inverse NMO correction (Figure 2.2) results finally in optimum full offset stacks, which were then time-migrated (Figure 2.7). The analyses had on average an increment of every 50-250 CMP (0.6-6 km) along the profiles depending on basement topography and complexity. The deeper basement reflections with higher velocities were picked with a larger increment than in the sedimentary succession, as velocity analyses are not that sensitive in deeper

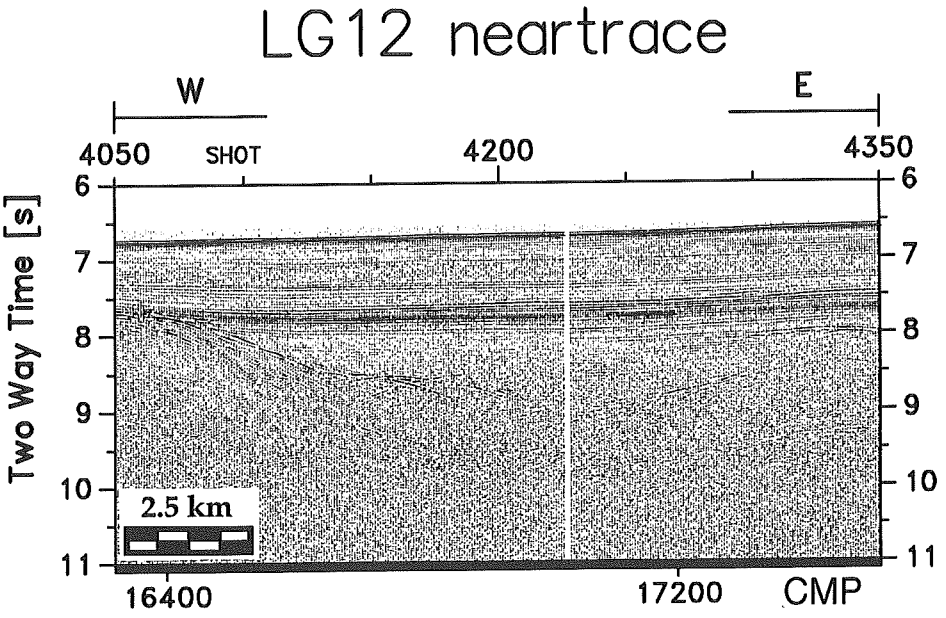

Figure 2.3: Part of the near trace seismic section from profile LG12, demonstrating the noisy and raw character of the unprocessed data.

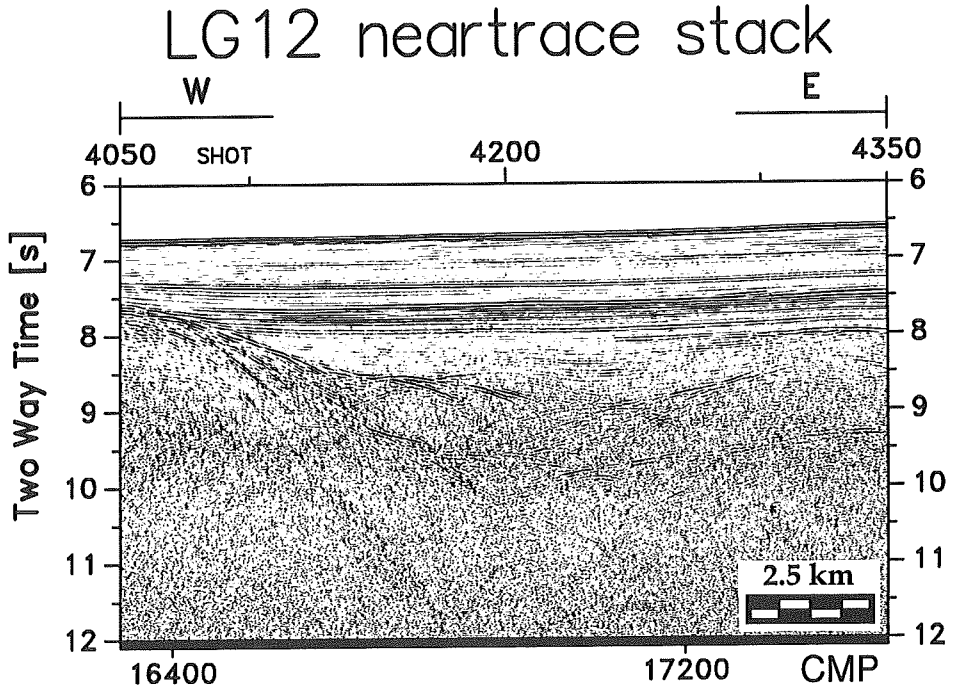

Figure 2.4: Part of the near offset stack from profile LG12 imaging the section clearer, but without good display of deep structures.

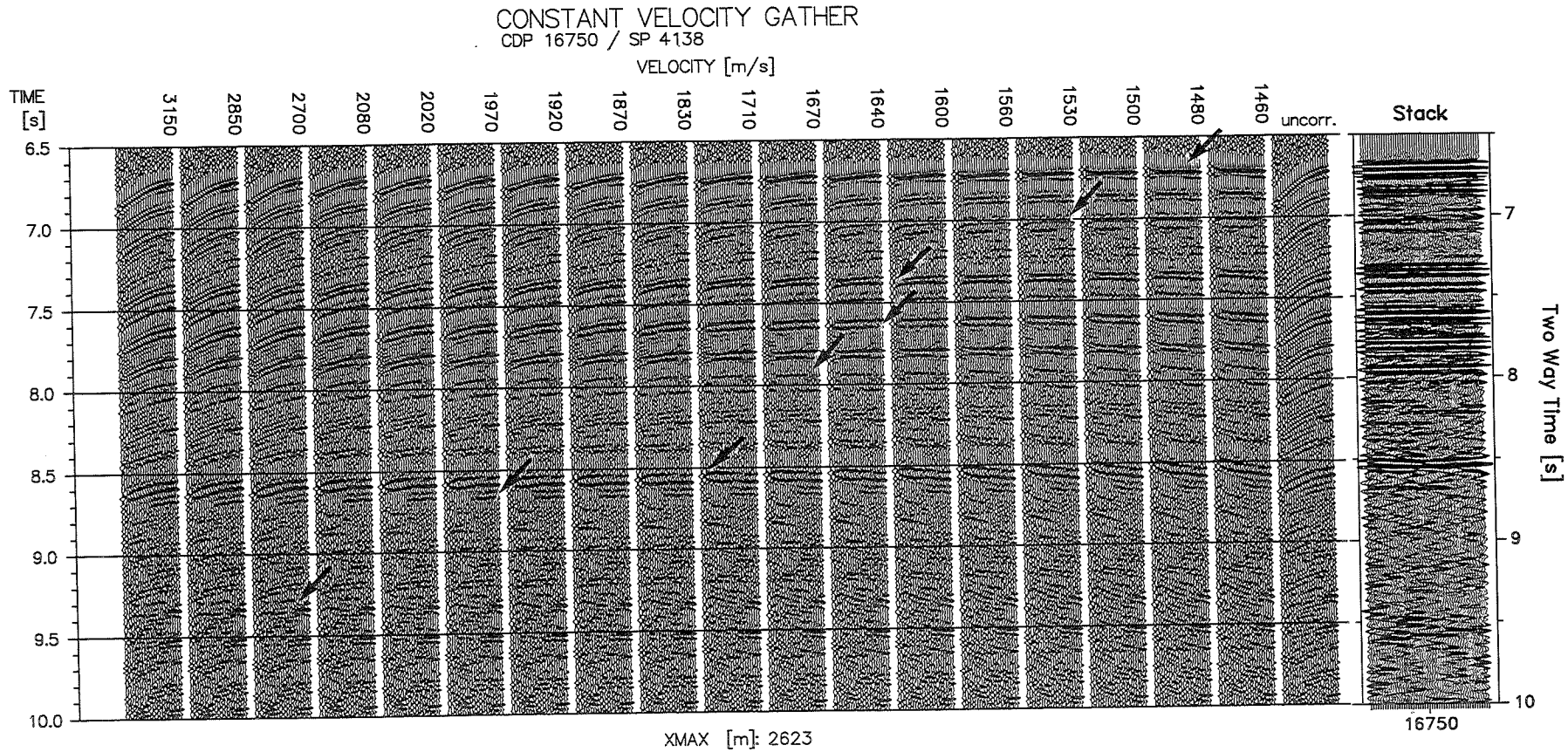

Figure 2.5: Example of a velocity panel used for determining the stacking velocities for dynamic correction on profile LG 12 at CMP 16750. Arrows mark the velocities picked for different sedimentary and basement horizons. Test stack with 50 CMPs displays to the right the result of the applied velocity function.

layers. Thus, the described processing steps correct the data dynamically, and improve the seismic image (compare examples from Figure 2.3 to 2.7).

In processing the data, particular care was also taken to keep steeply dipping reflections. For instance, in the time migrated sections neither trace mixing nor trace summation are applied, and fk-filter was only locally used. Dip-moveout corrections prior to final velocity analysis improved the image of steep events on the stack section. As will be seen below, imaging of steep events greatly facilitates interpretation of the data.

The edited and amplitude balanced shot-gathers are in a subsequent step the input for prestack depth migration, which continues downward both source and receiver gathers in the frequency domain.

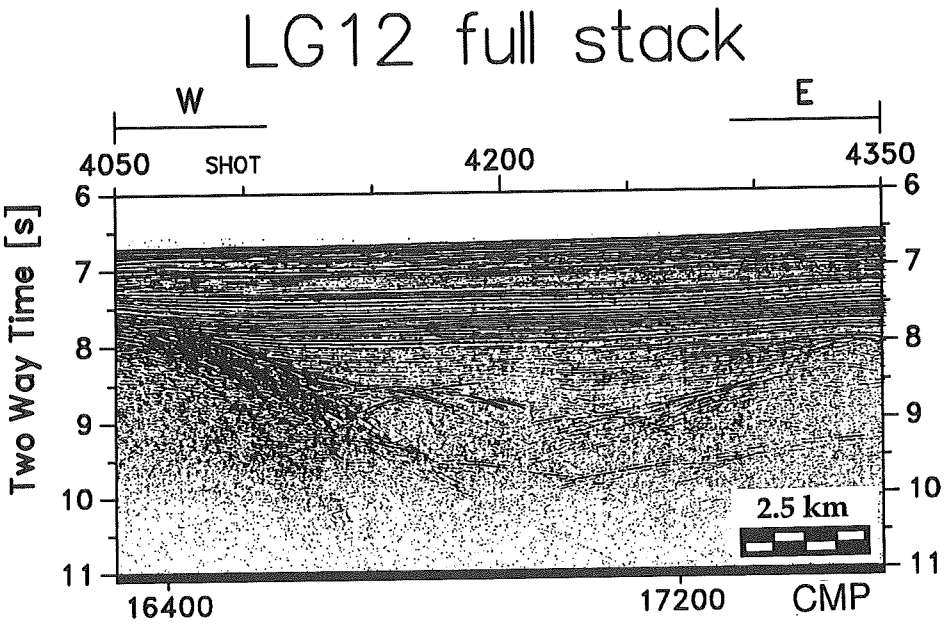

Figure 2.6: Part of the full offset stack from profile LG12 after velocity analysis and normal move-out correction. In comparison to the near offset stack, this seismic section images the deeper structures much clearer and needs in a last step only the migration of the data.

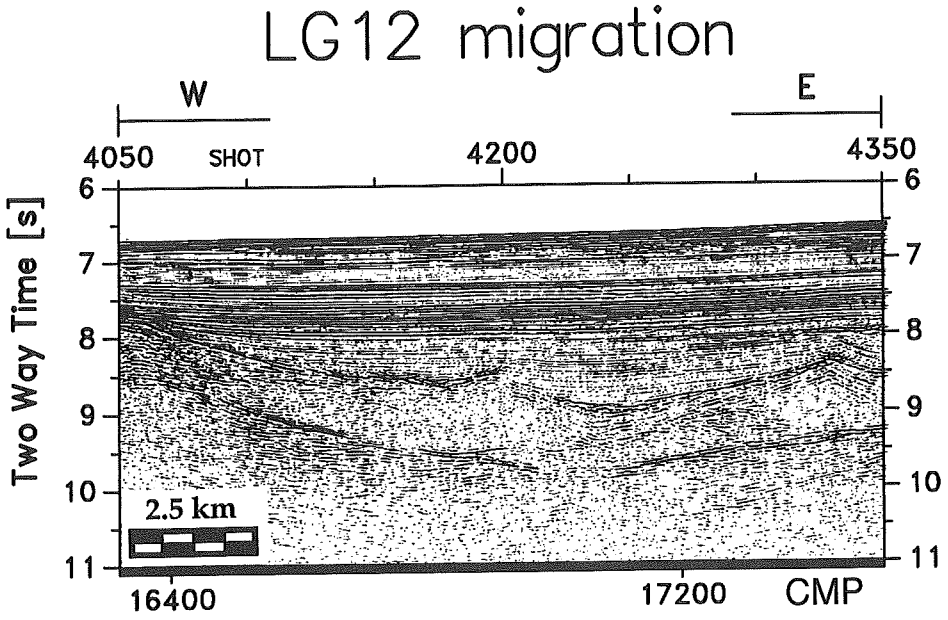

Figure 2.7: Migration of the full offset stack from profile LG12 from the same profile segment as shown in Figures 2.3-2.6. In comparison, this seismic section images the deeper structures much clearer and without the diffraction hyperbolas from the top of the basement.

Removal of noise is necessary for a successful migration: the sharper the signal and less noisy the input, the better the energy focussing and thus the resulting section. Therefore, the data were also filtered and where appropriate deconvolved prior to prestack depth migration. The extremely detailed velocity models resulting from prestack depth migration (see below) were used to construct the velocity field used for the depth migration after stack of the complete seismic sections (Figure 2.2).

The last branch of the processing flow-chart demonstrates the components needed to estimate reflection coefficients and determine physical properties of key reflectors. To address this issue, relative amplitude short offset stacks without any further processing that might have changed amplitude or phase characterisics are analysed after calibration of the system with the waterbottom

multiple.

Having optimised in this way the seismic sections, a reliable structural analysis was combined with physical attributes, geological and drilling information to provide an integrated model for the evolution of lithospheric extension, and the role of the main reflectors, which are subject of this study.

2.2 Prestack Depth Migration

One of the main aims of the processing was the depth migration of the seismic data, to better reveal the true geometry and geometrical relationships of key structures. For instance, interpretations of the S reflector had always been uncertain regarding its relationship to the overlying block-bounding faults, because only crude velocity information was available to convert time sections into geologically more meaningful depth sections. Indeed prior to this study, most interpretations have been based on time migrations. To address this issue, the seismic sections were depth migrated before stack.

As stacking velocity is not suitable for depth-migrating seismic data (Hatton et al., 1986), a detailed velocity function may better be constructed by the technique of depth-focussing error analysis (Denelle et al., 1986). This analysis is a byproduct of performing depth migration before stack and results from the importance of velocity both in converting a time section to depth, and in the migration of diffraction and reflection hyperbolae at different offsets to produce a final section (Figure 2.8).

Prestack depth-migration has two main advantages compared to standard migration. First, as a migration before stack, it avoids the smearing effects of CMP-stacking (Sherwood et al., 1989). This is an important factor in regions of complex geology, where normal faulting has juxtaposed tilted slabs of high velocity basement rocks against low velocity sediments, or even water (Peddy et al., 1987). Additionally, as a depth migration it counts for effects like raypath bending and velocity pull-up/push-down (e.g. Judson, 1980) according to Snell's law, in particular in areas with rapid lateral velocity changes as given by the complex geological structures on passive rifted margins. Thus, applying the depth migration before stack can produce a much more constrained and accurate image of the structures with their true geometry in depth than possible on time sections. The depth migration before stack was only applied to seismic reflection profiles normal to the continental margin, because 3-D effects and contamination by energy from side echos from the tilted crustal blocks and

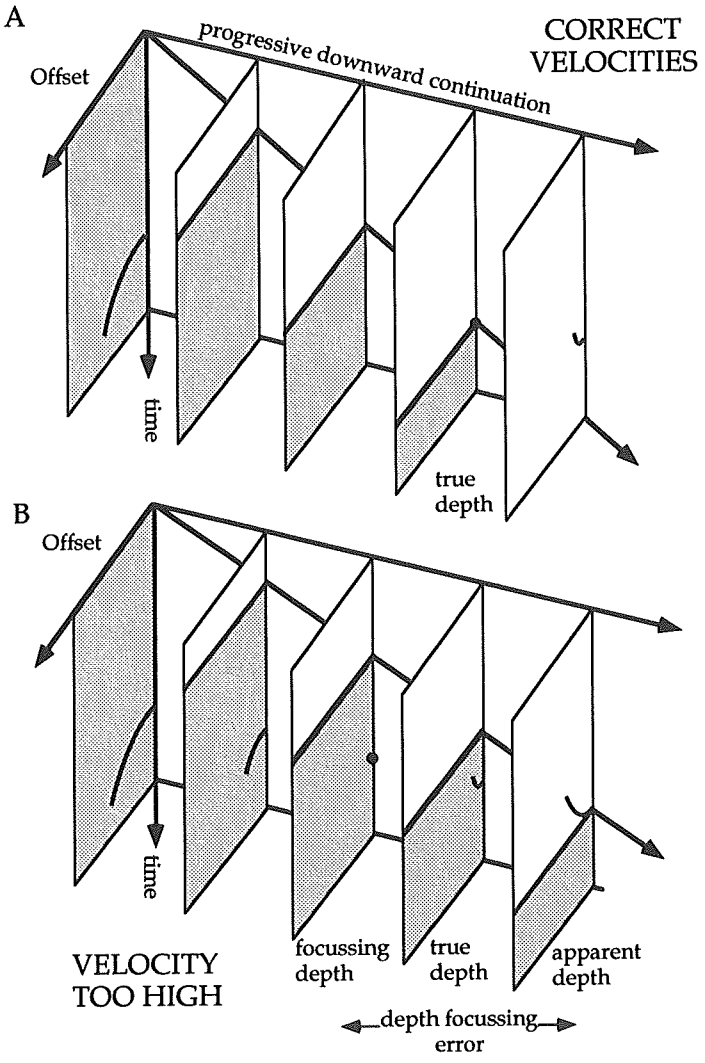

Figure 2.8: Schematic diagramm illustrating the principle of depth focussing error analysis (adapted from Denelle et al., 1986). During simultaneous migration in both shot and receiver domains with the correct velocity function A) maximum focussing occurs when the downward continuation operator reaches the actual depth of the reflector. If an incorrect migration velocity is used B) there is a discrepancy between the depth of maximum focussing and the depth to the reflector. Analysis of this discrepancy allows correction of the velocity model.

half-graben structures are thus minimised.

Using the Migpack® software (Denelle et al., 1986) the velocity model is created iteratively down from the oceanbottom to deeper levels through depth-focussing error analysis (Figure 2.8), which compares apparent and focussing depth of reflected and diffracted energy with a spacing of 10 shotpoints (analysis interval of 500 m) along the profiles. Both source and receivers are continued downwards to the depth of the reflector using a defined propagation velocity. If the propagation velocity is the same as the medium velocity, the energy is perfectly focussed when the operator reaches the depth of the reflector. If an incorrect velocity is used, maximum focussing occurs either before or after the downward continuation operator reaches the reflector. Determining the difference between the depth of focussing and the apparent depth of the reflector with the used velocity function (the depth focussing error) allows the velocity error to be calculated and a new, correct velocity model to be defined. The model is created from top to bottom of the section, determining velocity in one layer at a time because the velocity structure of the upper layer affects the accuracy of the velocity determination from the deeper levels.

Therefore the correct water velocity is determined first (and within the process the geometry of the data checked), then the velocity in the uppermost sedimentary layer is determined in the next iteration. These steps are repeated until the whole section and all specific layers have been analysed through depth-focussing error analyses.

As this method needs clear and strong reflections for reliable focussing of reflected and diffracted energy, it is difficult to define different velocity layers within the basement where reflections are limited or in areas of discontinuous, unclear reflections. Basement is migrated with an assigned half-space velocity, revealed by the reflections present within the basement, approximately 5.5-6 km/sec in most cases. In contrast, the sedimentary layers above provide a clear image as long as lithological boundaries or high reflectivity interfaces are picked. For the data analysed here, the postrift sequence generally comprised three or four velocity layers, the synrift II another, the synrift I and prerift one layer, and the basement above the S, H and L reflections another layer.

Velocity within the layers can vary both vertically and horizontally, allowing the construction of a detailed velocity model with relatively few layers. Experience proved that the use of compaction factors (allowing for vertical velocity variation) within a few sedimentary layers works more

efficiently, and provides clearer seismic images with fewer artefacts, than introducing a large number of different, narrowly spaced velocity interfaces with a constant velocity function.

This procedure yields a depth migrated section, which images the geological structures with their true geometry, and results in a detailed velocity model. This velocity model not only allows the correct migration of the data, but strongly constrains the lithologies present, e.g. sediment layers within the tilted fault blocks.

2.3 Amplitude and Waveform Analysis

In general, seismic reflection data only provide relative amplitudes, causing problems to determine absolute values. Some kind of calibration is needed to enable calculation of absolute values from the relative ones. Warner (1990) described such a calibration method, which is based on the comparison between the waterbottom multiple and the waterbottom reflection. The calibration procedure is as follows:

The amplitude of the primary waterbottom reflection in deep water is given by

$$A_p = Rx/d$$

where R is the unknown reflection coefficient of the seafloor, d a factor related to geometrical spreading, and x the calibration factor. By analogy, the amplitude of the corresponding first waterbottom multiple is

$$A_m = R^2x/2d.$$

Hence, by calculating the ratio of the primary to the multiple amplitude, the value of the reflection coefficient R can be determined easily from the ratio of the relative amplitudes:

$$R = 2\,A_m/A_p.$$

This analysis assumes that the seafloor is smooth and horizontal, that the seabed is a simple reflector between two half-spaces, and that energy is reflected at normal incidence, in other words that the water depth is large

compared to source and receiver size.

According to these assumptions, analyses are carried out on the near offset stack for the following reasons. In stacking only the traces of offsets between 300 and 1100 m (the near offset traces within this geometry), random noise is strongly removed, and second, effects of waveform distortion related to inexact NMO corrections in full offset stacking are also avoided. Furthermore, as the angle of incidence is less than eight degrees at the seabed, the near-vertical assumption is adequate. Consequently, analyses were carried out on those parts of the near trace stacks, where both the waterbottom reflection and its multiple are flat and smooth, and are imaged continuously, extending over a range of about 600 CMPs (7.5 km) along the profile.

A second condition for the application of this calibration method is that the reflections are not affected by other subsurface reflections, keeping the wavelet shape almost undisturbed. To exclude this influence, the amplitudes of the waterbottom reflection and its multiple are compared not only for the first peak-trough, but also for the second, which was always the largest, and third peak-troughs of the wavelet. Lastly, the peaks of the envelope functions were compared for the waterbottom reflection and its multiple. Within error, all gave the same value, with the envelope function showing the smallest standard deviation (as expected), giving for example a reflection coefficient for the waterbottom of 0.23 ± 0.04. According to Warner (1990), this value lies within the range of values for a soft waterbottom in deep water, where acoustic impedance is mainly dependent on the density contrast between water and sediment (e.g. Reston et al., 1995).

After calibrating the amplitude of the waterbottom reflection, its average amplitude is compared to that of the deeper seismic structure examined. For this type of estimation it is important to check in advance the waveform of the investigated structure to prove that the wavelets represent reflections from single interfaces and not from a thin layer or series of thin layers, for example.

On the base of the near offset stack of the data, including a correction for geometrical spreading, the maximum amplitude of the investigated reflector is compared to that of the water bottom by picking the maxima from the envelope functions of both the seabed and the relevant reflection. This ratio does not allow for anelastic attenuation (Q) and for transmission losses: these were estimated using the values from Boillot et al. (1995b), who calculated the Q factor along the profiles of the Galicia Bank area. They define in the upper postrift sediments a value of 10, increasing to 600 down towards the basement

(Boillot et al., 1995b).

To check that diffractive energy was included, both unmigrated and migrated data were analysed. Lastly, the length of the reflection investigated should be at least as large as the Fresnel-zone, so that the reflected energy is independent of the reflectors shape (Raynaud, 1988).

2.4 Synthetic Calculations

To check the reliability of the velocity model created for migration of the seismic reflection data, a synthetic seismogram was calculated for comparison with the real data. The velocity function generated with the depth focussing error analysis during prestack depth migration represents here the input for the synthetic calculation of a seismic section.

In the first step, a velocity grid is generated based on the developed velocity model and its associated interval velocities. This model is converted to a seismic section in depth where each reflector is represented by a spike at the corresponding depth of the defined velocity interface. This reflectivity series thus provides reflectivity values based on the velocity contrasts of the input model.

This section needs in a second step transformation of the spike into a wavelet similar to the waveform of the real data. Therefore, a bandpass filter is applied, whose characteristics should resemble those of the seismic reflection data in providing for instance the same frequency content. On each side of the defined frequency interval a ramping function is applied to avoid sharp truncations of the spectrum, in other words to reduce the ringing noise. This procedure yields a reflectivity series serving as input for the synthetic modeling.

Zero-offset modeling, the opposite of poststack migration, generates finally a zero-offset section in time. The Migpack-software (© Elf-Total & Dataid Technologies) offers an additional module for this purpose, which calculates synthetic sections in the frequency-space domain using either a 45-or 65-degrees diffraction operator. Hence, the synthetic section resulting from modeling is compared to the corresponding stack of the near offset traces to evaluate the quality of the velocity model.

3 Detachment Tectonics and Continental Break-up: the S Reflector offshore Galicia

3.1 Abstract

The west Galicia rifted margin is a non-volcanic rifted margin, characterised by landward tilted fault blocks bound by oceanward dipping faults. The fault blocks are underlain on time sections by an undulating group of bright reflections, the so-called Galicia S reflector. A variety of advanced processing techniques is used to constrain the nature of S, including prestack depth migration to construct detailed velocity models of the section overlying S, and to provide optimum images of portions of the data in depth. The results show that S passes continuously beneath the tilted fault blocks of the deep margin. S and associated reflectors are interpreted as a brittle detachment fault system, similar to those observed in the western USA. It is inferred that the detachment was active during the last phase of extension immediately prior to continental break-up. To the west, S appears to be truncated by east-dipping reflections from a ridge of peridotite. This ridge, drilled during ODP Leg 103 is characterised by top-to-the-east shear structures. These east-dipping reflections, not S, are related to this shear zone, thus suggesting that this east-dipping structure (rather than S) was responsible for the exhumation of the mantle rocks. The results are discussed in the context of the evolution of the margin.

3.2 Regional Setting and Objectives

The highly extended continental margin to the west of the Galicia Banks (offshore Spain) is crossed by a series of old (1975-1980) but remarkably high quality seismic reflection profiles (Figure 3.1 - Mauffret & Montadert, 1987). These lines, which are supplemented by the results of drilling on ODP Leg 103 (Boillot, Winterer, Meyer et al., 1987; 1988) and subsequent sampling from submersible (Boillot et al., 1988b), reveal the detailed stratigraphy and structure of this margin.

The seismic profiles show that just east of a ridge of serpentinised peridotite, the margin is characterised by east-tilted blocks bound by west-dipping normal faults. Underneath these blocks, the so-called S reflector (de Charpal et al., 1978) is observed at about 8-10 s TWT (e.g. Figure 3.2).

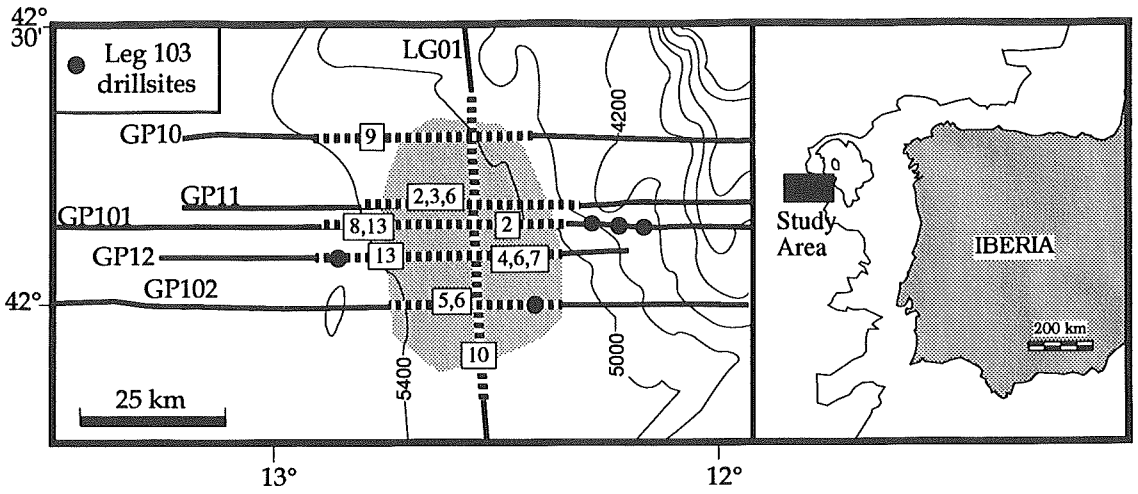

Figure 3.1: Map of the Galicia Bank margin with the location of the analysed profiles imaging the S reflector. Shading indicates the areal extent of S, striped lines mark data, shown and numbered by figure.

Drilling (Boillot, Winterer, Meyer et al., 1987; 1988) and submersible diving (Boillot et al., 1988b) proved that the S reflector is overlain by crystalline basement and does not represent an intra-sedimentary boundary. Sediments drilled within the tilted blocks on top of S identified the two sedimentary sequences Synrift I and Synrift II (Mauffret and Montadert, 1987), associated with two phases of rifting, one from 140 Ma to 125 Ma, the other from 125 Ma until eventual break-up at 114 Ma. Thus at least part of the synrift sedimentary sequence predates tilting and the accompanying normal faulting.

Although it is generally accepted that the S reflector is related to the extreme extension of the continental lithosphere, the precise nature of the S reflector is still the subject of much current debate (see Chapter 1), and more detailed studies are required to understand the evolution of this margin.

Previous interpretations of the S reflector, and of the structure of the margin, have been made on the basis of time sections, with only simple depth conversions based on general velocity models (Sibuet, 1992). On migrated time sections, S appears to undulate beneath the fault blocks (Figure 3.2): although it has long been recognised (Mauffret & Montadert, 1987) that some of this may

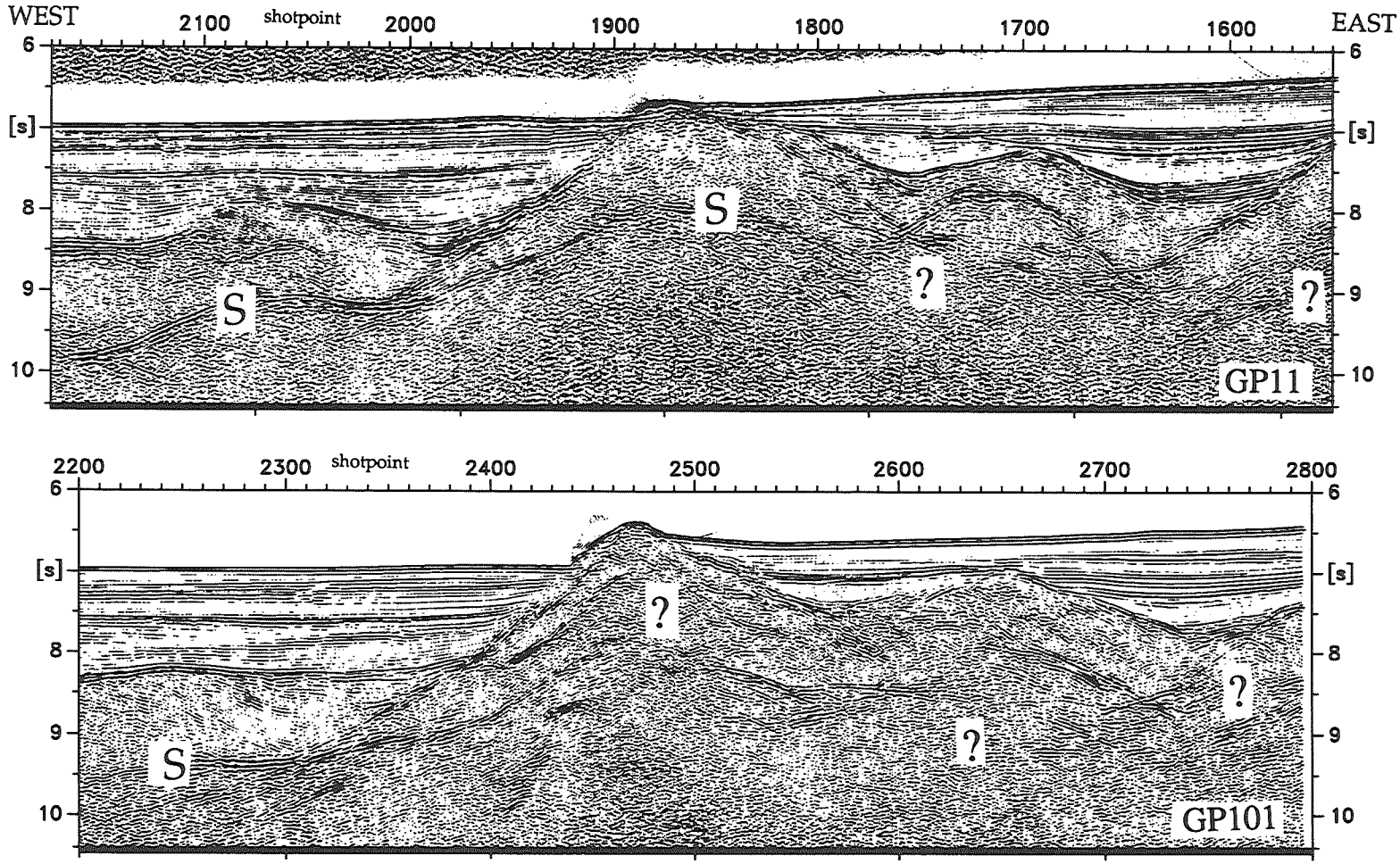

Figure 3.2: Time migrated seismic sections of profiles GP11 and GP101 (see Figure 3.1 for location). The S reflector is imaged as a complex, undulating group of bright reflexions beneath the tilted fault block topography, which is characteristic of this margin. Shot interval 50 m.

represent the effects of velocity pull-up and push-down, without detailed velocity information it has not been possible to determine the true geometry of S in two dimensions, let alone three. Furthermore, the image of the S reflector on some of the migrated time sections is discontinuous and complex: in places S appears as a reflection only a couple of cycles thick, but elsewhere S has been described (Sibuet, 1992) as a complex band of reflections up to a second thick: towards the eastern end of the profiles shown in Figure 3.2, no single S reflector can be identified with confidence, but rather a complex zone of reflectivity is observed. Finally, the relationship of S to the overlying block-bounding faults is far from clear on the time sections due to the complex, discontinuous image and the effects of velocity pull-up and push-down, leading to the suggestion that S could in places be offset by the block-bounding faults (Boillot et al., 1989).

The investigations discussed in this section set out to constrain the nature of S and its relationship to the overlying faults and other key structures of the margin by providing an improved image of critical portions of the data in depth and mapping of S. Furthermore, some key results from analysis of the waveform of the S reflector will be presented, as these demonstrate conclusively that S cannot be the brittle ductile transition. The results will then be placed in the context of the known geology of the margin, and a model for lithospheric extension leading to continental break-up advanced.

3.3 Method

Interpretations of the S reflector have until recently been hampered by its apparently variable character (Figure 3.2), the uncertainty regarding its relationship to the overlying block-bounding faults, and the lack of accurate velocity information to convert a seismic time section into a more geologically meaningful depth section. To address these problems the process of iterative prestack depth migration is applied to derive a detailed velocity model in the section overlying S (for explanation see section 2.2), and to provide an improved image of the structure in depth (e.g. Figure 3.3) rather than time.

Besides the depth sections, some time migrated seismograms are used for discussion. As the depth migration before stack requires bright and continuous reflections, this method provides no reliable focussing and hence no reliable velocity information in regions of weak and disrupted reflection events. Furthermore, without a detailed velocity model, the migration before stack

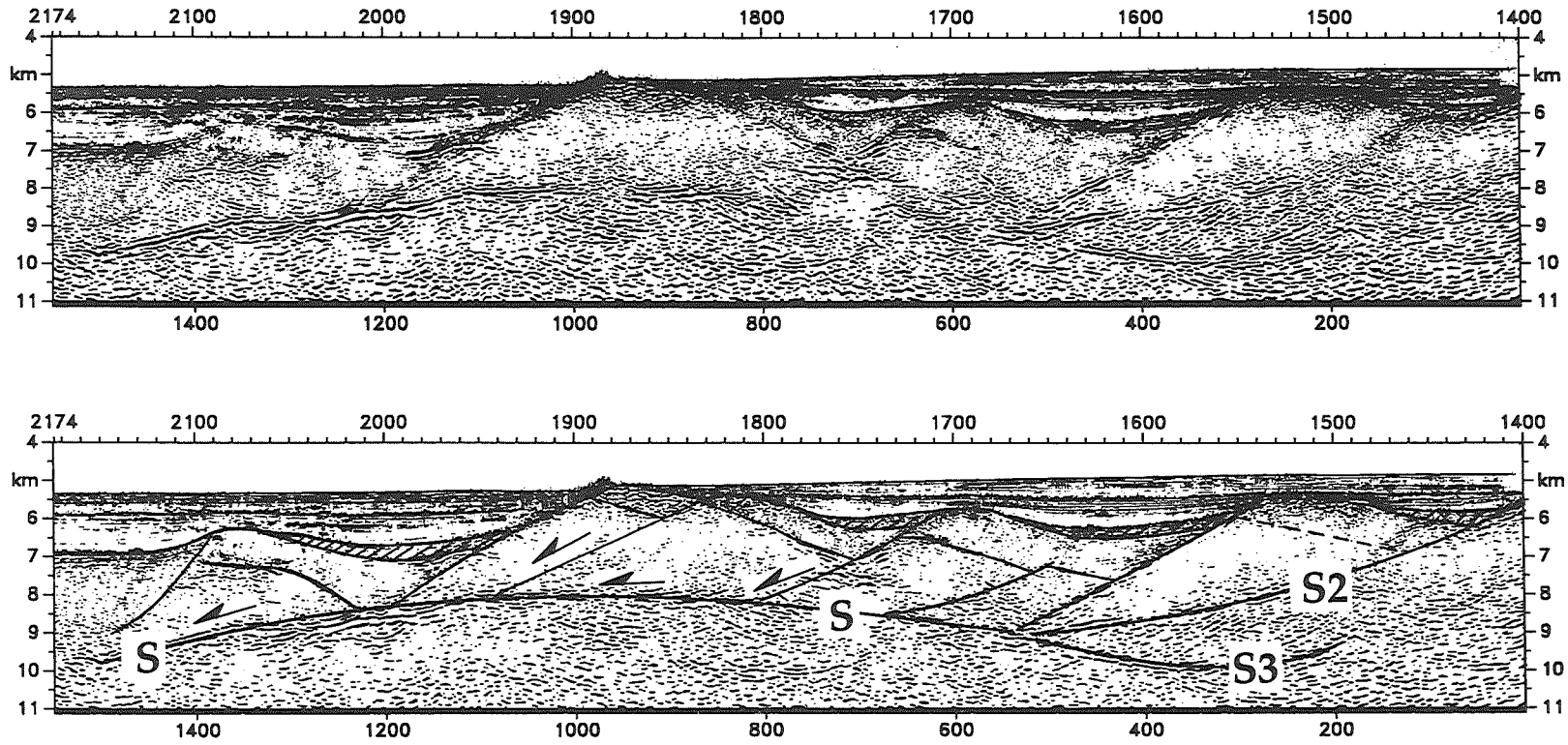

Figure 3.3: Prestack depth migration of profile GP11. The S reflector is imaged as a smooth and continuous structure with a domal shape, which splits into three separate features at the eastern end of the profile. The internal structure of the fault blocks is much clearer now, and identifies new fault structures, all of them detaching onto S (no VE). The corresponding velocity model is shown in Figure 3.6 (syn-rift II hachured).

could produce in those regions worse images than the less velocity-sensitive standard processing (see section 2.1). Furthermore, both stacked and time-migrated profiles are used for checking the intersections of the profiles and the correlation of the interpretation from one profile to another.

The calculation of the reflection coefficient of S and its amplitude analyses are based on the method described by Warner (1990), which is explained in detail in section 2.3.

3.4 Results

The benefit of applying iterative prestack depth migration is apparent in a comparison between Figure 3.2 (upper section) and Figure 3.3. Figure 3.2 is the result of optimum standard processing through to time migration after DMO stack of a portion of profile GP11. Note that on this section, although some faults are clearly imaged, others are not and can only be inferred from the tilted block - half graben structure of the margin. Furthermore, the internal structure of the fault blocks is not clear. However most fundamentally, the S reflector appears to undulate dramatically beneath the fault blocks and towards the east of the section, its image becomes very confused.

In contrast, Figure 3.3 is the product of eight iterations of prestack depth migration, resulting in the optimum section shown here. The most striking result is that S no longer undulates beneath the fault blocks but rather has a relatively simple domal shape. Furthermore, the clearer image reveals that rather than being complex and variable, S appears to have a remarkably consistent character, and hence presumably internal structure.

This result is further constrained by the depth sections of profiles GP12 (Figure 3.4) and GP102 from Hoffmann & Reston (1992 - Figure 3.5), which parallel line GP11 to the south. These two lines demonstrate further the smooth and undisturbed shape of the S reflector, instead of being cut by the overlying block-bounding faults as assumed from the time sections. In contrast to GP11, S has no significant domal shape here, but appears with a more pronounced gentle dip to the west.

The depth sections plus the velocity models (Figures 3.3-3.6) derived from depth-focussing error analysis reveal the internal structure of the fault blocks. In particular the combination of the improved image and the detailed velocity model allows the contact between the base of the tilted sedimentary sequence and the top basement to be picked with more confidence than before. This

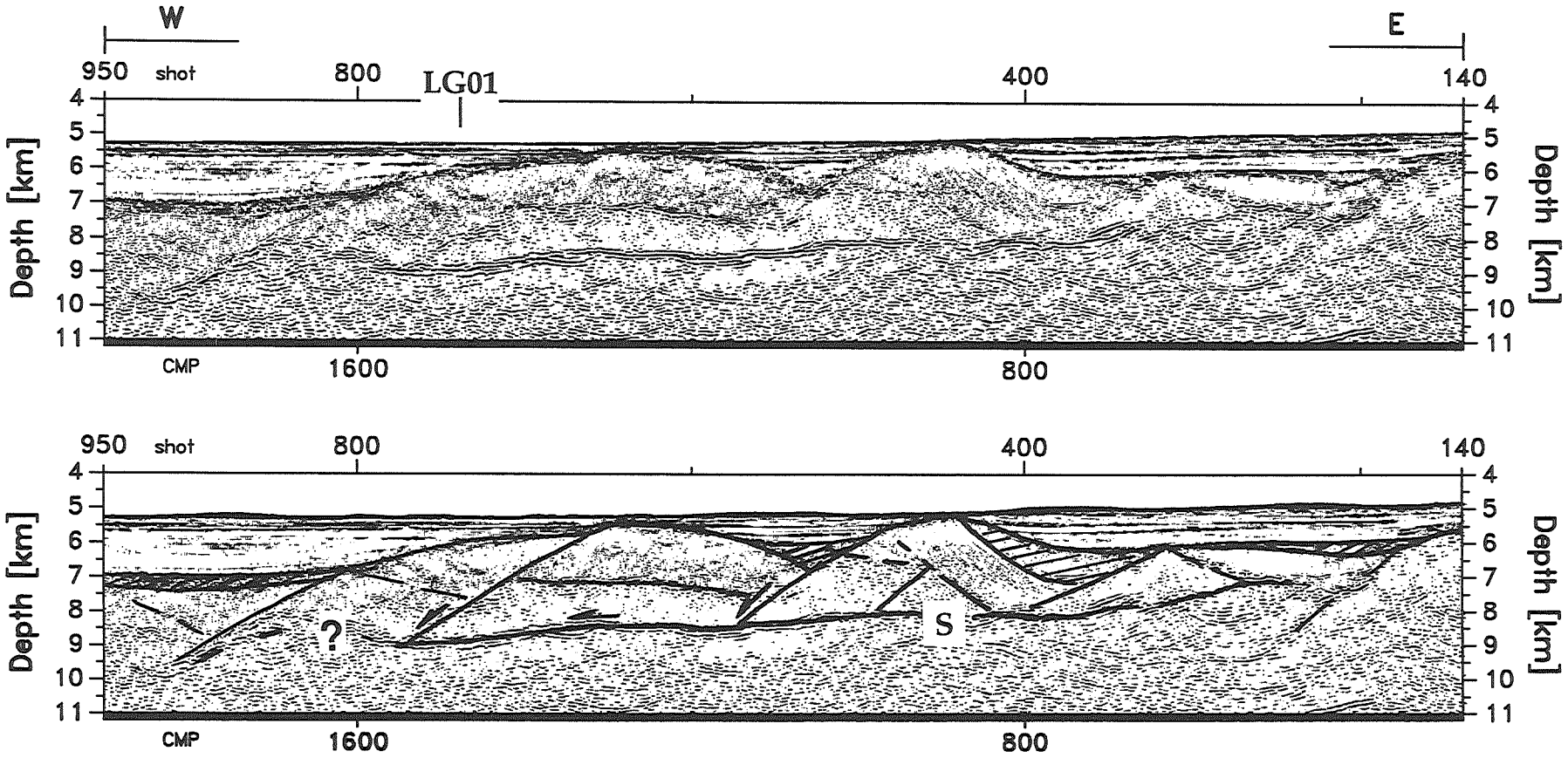

Figure 3.4: Depth section of profile GP12 migrated before stack. The S reflector exhibits a smooth and continuous shape with a gentle dip to the west. Again, at the eastern end of the profile, S seems to split into different features. Sediment sequences are identified within the fault blocks by their velocity (compare Figure 3.6; syn-rift II is hachured), and the block-bounding normal faults detach onto S (no VE).

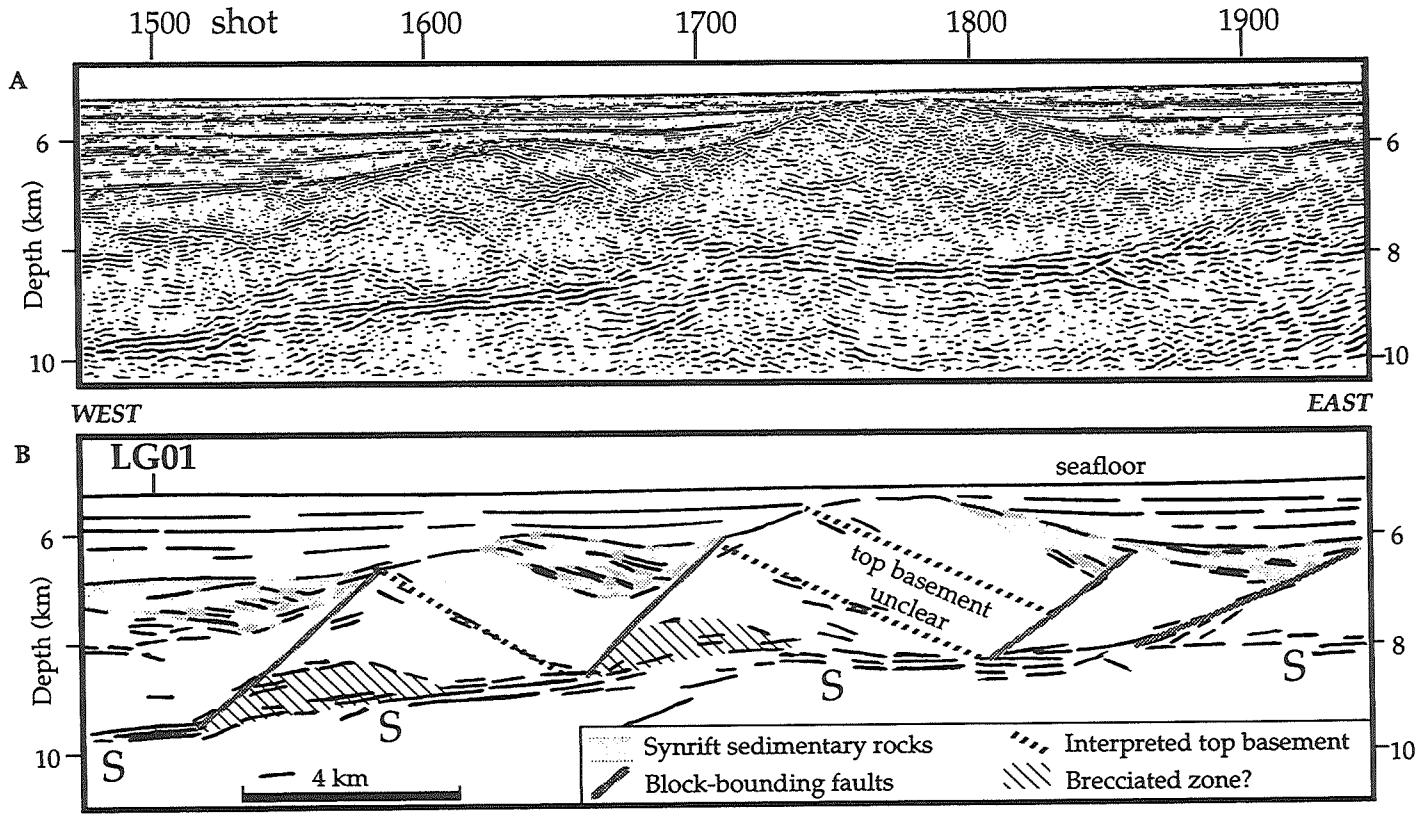

Figure 3.5: Prestack depth migration of profile GP102 (Hoffmann & Reston, 1992). The S reflector passes continuously beneath the tilted crustal blocks with a gentle westerly dip. The overlying normal faults detach onto S (no VE), and sediment sequences are identified by their velocities (Figure 3.6).

enabled the identification of further two faults on lines GP11 and GP12 that had not previously been recognised from the time sections.

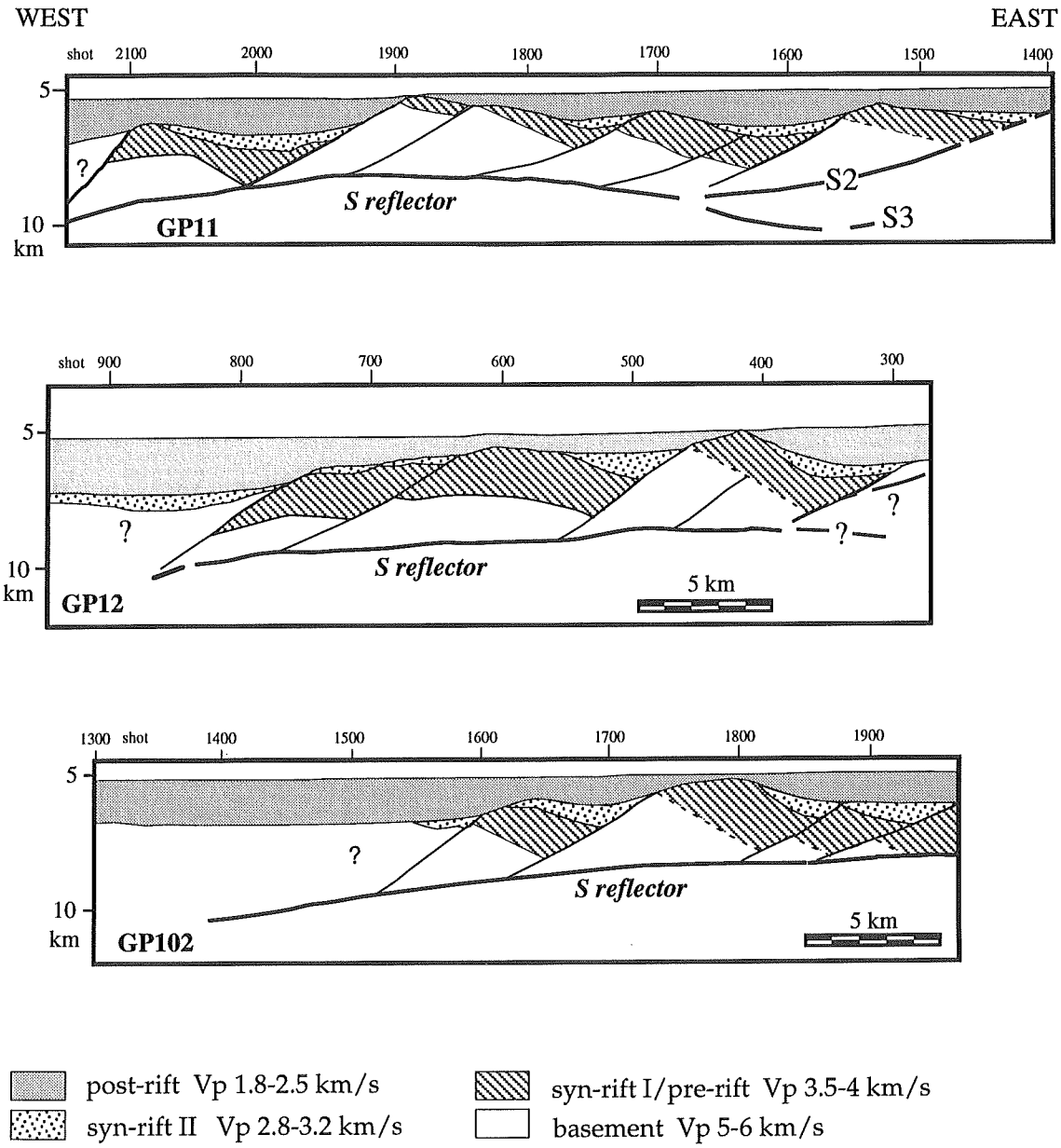

Figure 3.6: Schematic diagramm of profiles GP11, GP12 and GP102, combining the velocity model produced by prestack depth migration and interpretation. The velocity information allows the identification of the various units, and structural interpretation of S and other fault structures (no VE).

There remain patches of the sections, perhaps regions of poor signal penetration where the image of S is discontinuous. However, the simple shape of S on the depth sections means that S can be extrapolated through these patches with confidence. It is pointed out here that the S reflector itself is not considered discontinuous but only the reflection from it is. The smooth overall shape of S is rather interpreted as an indication that the reflector is a continuous feature, passing beneath the fault blocks without disruption.

The only portion of the data where the identification of S remains ambiguous is at the eastern end of the profiles. On GP11, where the time section shows a complex and discontinuous image of S, the improved imaging from prestack depth migration has resolved three separate structures (Figure 3.3), of similar continuity and character, all of which are connected to S at shotpoint 1670. One rises at c. 25° towards a half-graben (Figure 3.6) and is probably a normal fault, another (S2) rises more gently towards the east, but again to the boundary between two fault blocks and is thus also probably a normal fault, whereas the third (S3) dips to the east, flattens at about SP 1550 and then appears to turn up towards the surface, before disappearing at about SP1500.

For profile GP12 the ambiguity at the eastern end of the line is less pronounced and solved by depth migration before stack (Figure 3.4). S is characterised by a bright and continuous reflection, passing below the tilted blocks with only gentle westerly dip. It seems to cut up to the surface below the easternmost tilted crustal block (east of shotpoint 400) into a half-graben structure (Figure 3.6), instead of being split into separate features (Figure 3.4). Although east-dipping reflections imaged beneath S may be traced further down from 8 to 10 km depth (Figure 3.4 - east of shot 350), they are much weaker and less correlatable than the possible continuations of the S reflector on profile GP11 (Figure 3.3).

The same technique has also been applied to part of profile GP102 (Figure 3.5 - Hoffmann & Reston, 1992). This profile had been interpreted as showing that the block-bounding faults cut and offset the S reflector (Boillot et al., 1989). Although on this profile the faults are not themselves unambiguously imaged even after depth migration, the detailed velocity structure derived from depth focussing error analysis, coupled with the geometry of the tilted sedimentary units show that this profile is characterised by similar features to GP11 and GP12: S passes as a continuous feature beneath the blocks, which contain both basement and tilted sedimentary units (Figure 3.6). Critically, S does not

appear offset by the block-bounding faults on any of the profiles. It is now relevant to consider what sort of structure S might represent.

3.5 Discussion

The debate about the nature and sense of motion along the S reflector has still not abated, and occasionally new models and interpretations are suggested by different authors (see Introduction). The results from depth migration and waveform analyses of the S reflector along the profiles where it is best imaged provide further evidence relevant to this debate. In the light of this new information, former theories are discussed in the following section.

3.5.1 Nature of the S Reflector

A number of bright intracrustal reflections from a variety of settings, including the western United States (Goodwin et al., 1989; Litak & Hauser, 1992) and the Southern Appalachians (Pratt et al., 1991; Barnes & Reston, 1992), have been shown to be reflections from thin high velocity layers, interpreted as igneous intrusions. Several such bright features have been drilled in the Siljan structure of Sweden (Juhlin et al., 1990), and shown to be igneous intrusions. Hence one possibility that must be considered is that the S reflector represents a thin igneous intrusion of some kind. If so, it must have intruded at or after the end of rifting, as it is not offset by the block-bounding faults.

A simple comparison (Figure 3.7) of the waveform of S with that of the seafloor demonstrates that this interpretation is rather unlikely. S has a waveform virtually identical to that of the seafloor reflection, which can be shown by a comparison with the seafloor multiple to represent a reflection from a single interface. Hence S can also be taken as a reflection from a single interface rather than from the thin layer expected for an igneous intrusion.
It is also unlikely that S represents the top of a large igneous intrusion, again intruded at the end of rifting as it is not offset by block-bounding faults. First, no reflection corresponding to the base of such an intrusion is observed (Reston et al., 1995), second, no volcanics were sampled during drilling (Boillot, Winterer, Meyer et al., 1988), and third, it seems unlikely that the base of the fault blocks/top of the intrusion would be such a smooth surface in depth. Instead one would expect that as the overlying fault blocks floated on top of the crystal mush of such an intrusion, the thicker portions of the blocks

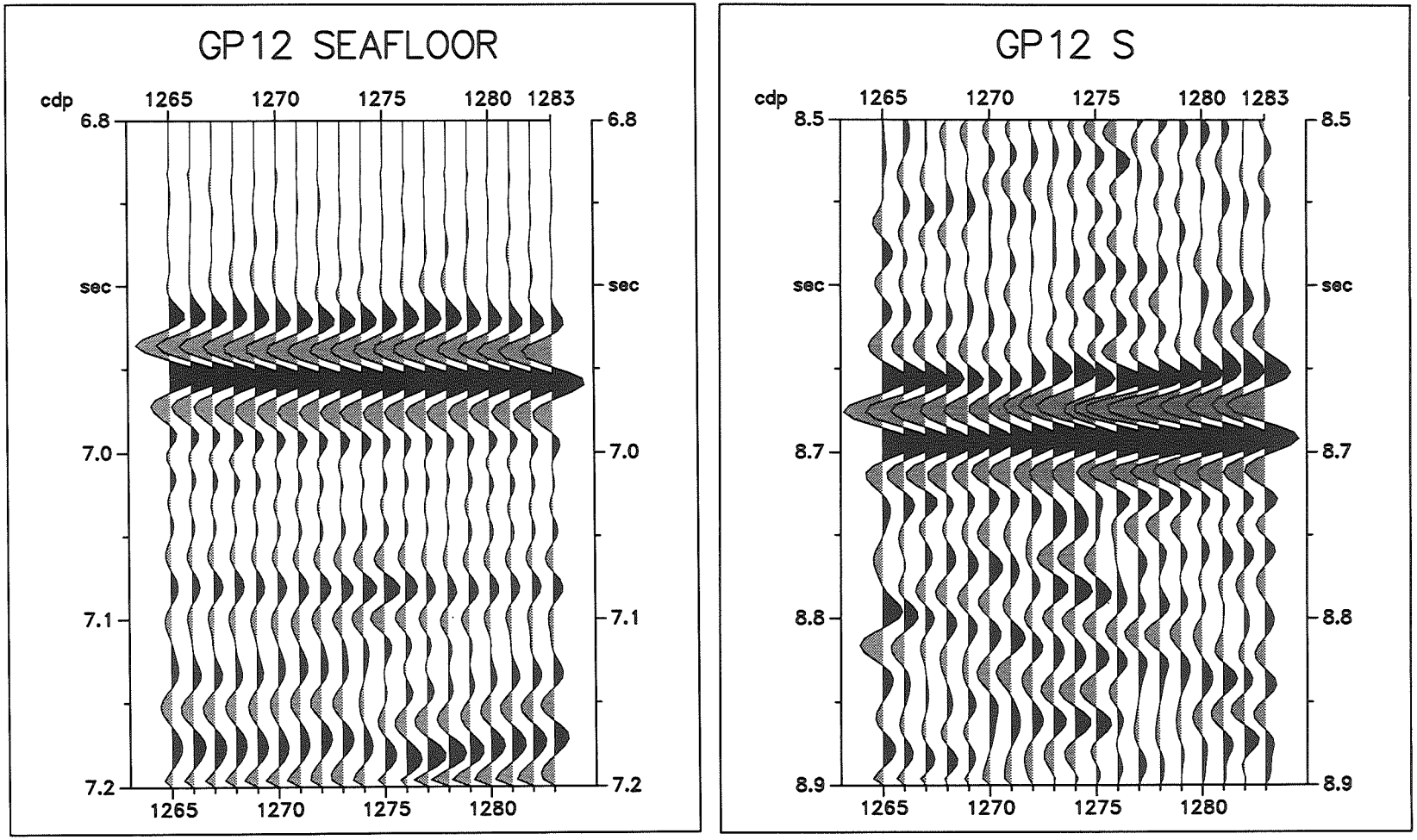

Figure 3.7: Comparison of waveforms of the S reflector and the seafloor from profile GP12 (minimum-phase filtered to the same bandwidth as S, simulating the effects of attenuation). The waveforms are almost identical, thus S is positive polarity as the seafloor, and also probably a reflection from a single interface. S may represent the tectonic contact between an upper plate of upper crustal rocks and a high velocity and density lower plate.

would have developed keels relative to the thinner portions of the blocks, according to the principle of isostasy. Instead, the remarkably smooth shape of S indicates that the lower plate to S may possess significant flexural strength.

It has been suggested that S represents a transition between brittle and ductile deformation (de Charpal et al., 1978), with deformation above S accommodated by block faulting, and that beneath S by ductile flow. Such a boundary would be transitional rather than a sharp interface and at depths greater than 5-10 km (Jackson, 1987). However, three lines of evidence argue against this hypothesis. First, analysis of the amplitude and waveform (Figure 3.7) of the S reflector shows that the brightest portions of the S reflector (e.g. profile GP12 shotpoints 450-750; Figure 3.4) represent a sharp increase in acoustic impedance (a reflection coefficient of c. 0.2 - Reston et al., 1995), in effect a single interface. Further analysis of the instantaneous frequency of S on profiles GP11 and GP12 (Berndt, 1994) reveals additionally that no rise of the instantaneous frequency can be observed at the S reflector. In other words, the frequency range of S lies within the dominant signal frequency (between 18 and 25 Hz for the GP-series). This observation implies a single interface at S, which is thus not a series of several subordinate reflections with a spacing smaller than a quarter wavelength. These investigations are hence consistent with a sharp tectonic boundary of some form, separating quite different lithologies above from below (the lower plate to S might be continental lower crust, or perhaps serpentinised upper mantle), but not with a transition zone. Second, the depth sections show that at the end of rifting S was in places less than 1 km beneath the seafloor, and is never more than 3 km beneath the top of the fault blocks. Even in regions of extreme extension, this is within the shallow seismogenic zone (e.g. Meissner & Strehlau, 1982; Jackson, 1987) where brittle deformation should dominate. Finally, as for the igneous intrusion hypothesis, if S were a brittle-ductile transition it would seem unlikely that the fault block topography could be supported, as the ductile lower crust would presumably have little flexural strength. S is however a remarkably smooth feature, passing beneath lateral changes in fault-block thickness without distortion (Figures 3.3-3.5). Because of these objections, it is most unlikely that S represents the brittle-ductile transition. Instead, the relationship between S and the overlying faults may be most consistent with an interpretation of S as a brittle detachment fault, probably similar to those mapped in the western United States.

The relationship between the block-bounding faults and the S reflector is

particularly important as it provides one of the strongest constraints on the role of S during rifting. On the depth section of profile GP101 (Figure 3.8) and the corresponding portion of line GP10 further to the north (Figure 3.9), it can be seen that some of the block-bounding faults (which detach onto S) also bound wedge-shaped packets of sediments, which thicken towards the faults. These have been identified as Synrift II sediments (Mauffret and Montadert, 1987; Winterer et al., 1988) deposited immediately prior to break-up during extension along that fault structure. As it is precisely those faults active during the last phase of rifting (i.e. those that cut the Synrift I sequence and bound the Synrift II sequence) which appear to detach onto S, it is suggested that at least S was active right up to continental break-up. The seismic images of profiles GP10 and GP101 closely resemble that of profile GP11 between shotpoints 1900-2150 (Figure 3.2), thus revealing that this relationship between the block-bounding normal faults and the S reflector is not a local feature, but valid in a broad area.

The profiles further south image the S reflector somewhat clearer, but up to line GP10 the structures are still representative. Profile LG01 provides a good cross-check (Figure 3.10), as it passes from north to south, thus cutting the margin-normal profiles, which are the data base for mapping S (Figure 3.11).

S appears on LG01 relatively flat and slightly domal, with the dome occuring at the intersection with profiles GP11 and GP101 (Figure 3.10). S deepens to the north, before it disappears north of line GP10, and it also deepens to the south, cutting down to at least 10 sec TWT at the intersection with profile GP102. In this area, S is probably covered by a thick tilted basement block, whereas at the intersection with GP11 and GP101 mainly sediments comprise the hanging wall.

This seismic data base, which consists of closely spaced lines and depth images of good quality, allows now the mapping of the extent of the S reflector (as already indicated by shading in Figure 3.1) and the construction of depth contours to S (Figure 3.11) from the depth migrated sections. This map shows that S shallows from 10 km depth to at least 8 km, and documents its domal shape on line GP11. A further shallowing to 7 km depth closer to the continent may be possible, because on the eastern segments of profile GP11 and GP12 S splits into different structures, cutting up to the surface with different angles. This would imply that the breakaway (the location where the detachment approaches the surface) of S lies to the east. The next step of investigation considers the direction of motion along the S reflector and where it might reach the surface.

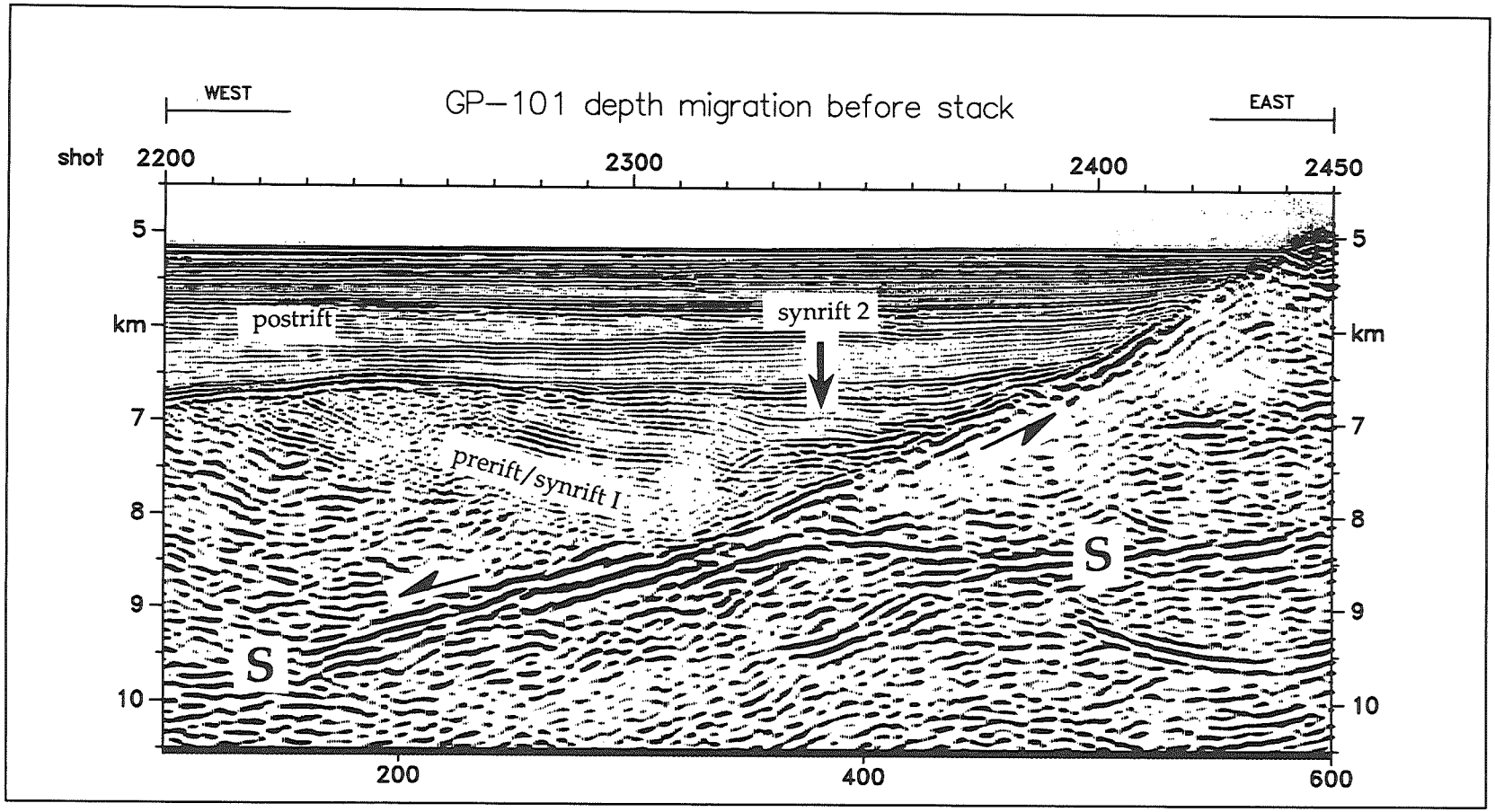

Figure 3.8: Depth-migrated part of profile GP101, showing in detail a block-bounding normal fault detaching onto the west-dipping S reflector. Sediments of syn-rift age are located in the hanging wall to this fault, and were deposited during the latest phase of rifting, as they show no disturbances (no VE).

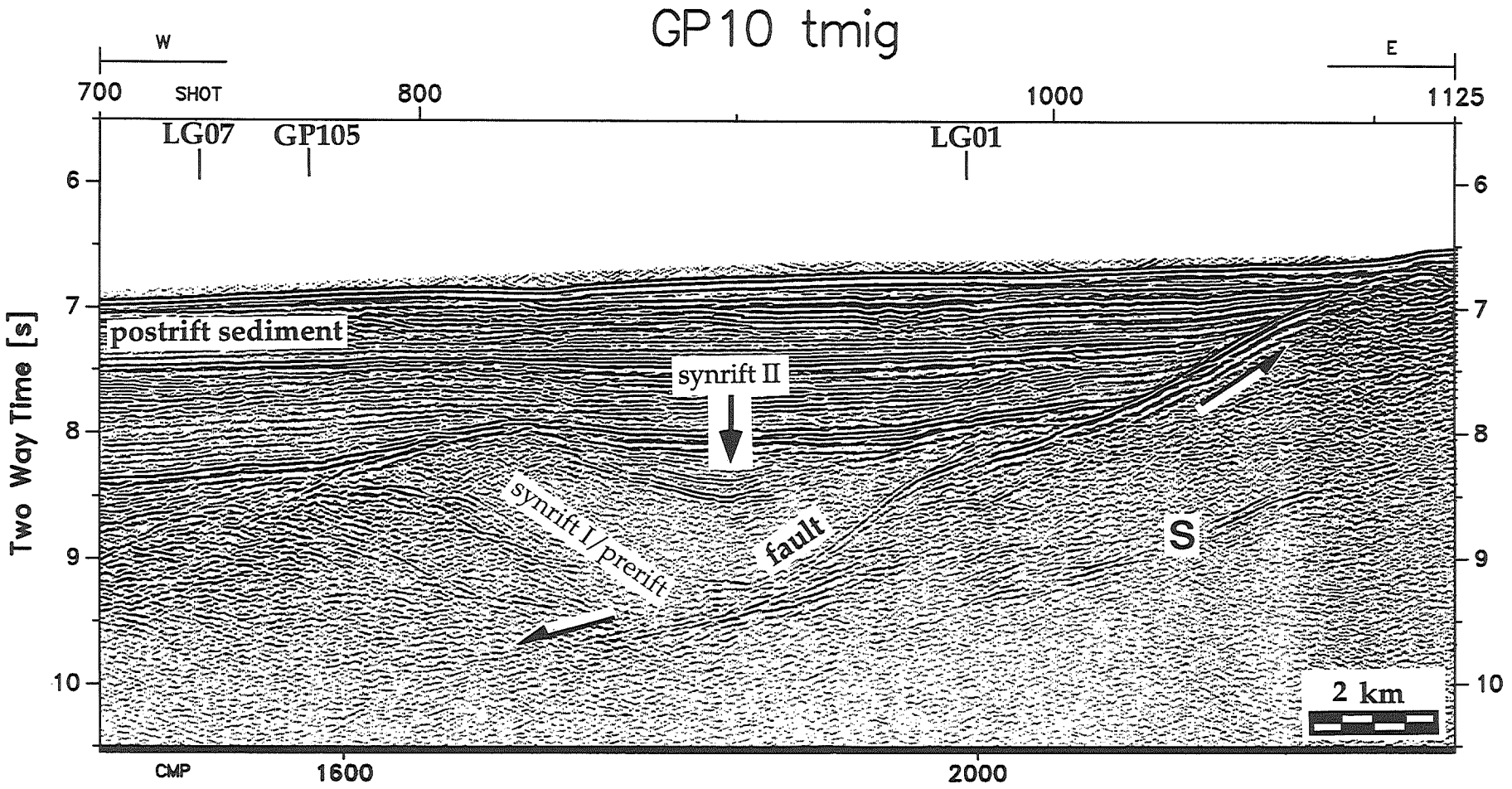

Figure 3.9: Time migration of profile GP10 (for location see Figure 3.1). This section reveals in the northern part of the investigated area fault structures corresponding to those observed in detail on GP101 (Figure 3.8). Sediment sequences of syn-rift age overlie a block-bounding normal fault detaching onto S, which gets less pronounced further to the north. Shot interval 50 m.

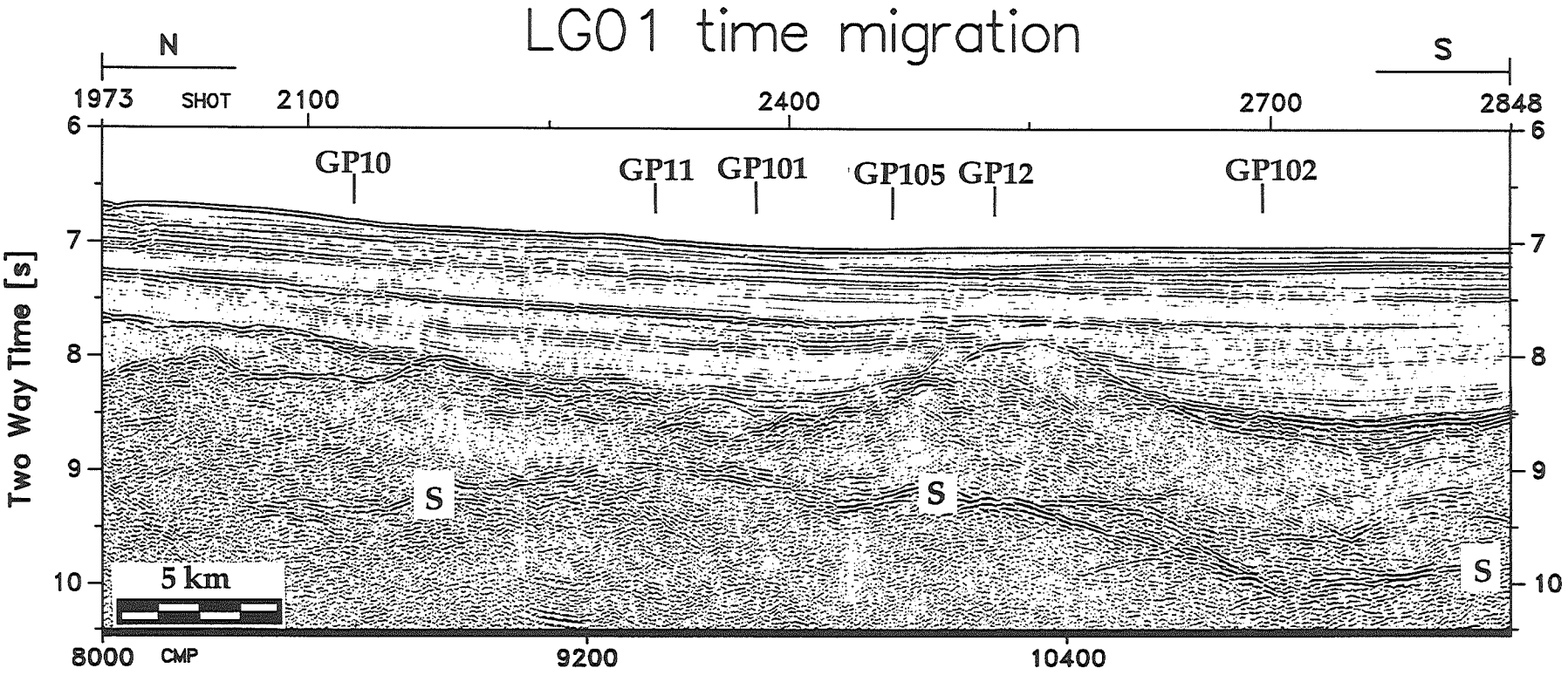

Figure 3.10: Migrated time section of the north-south trending profile LG01 (see Figure 3.1 for location), cutting across the margin-normal profiles of the GP-series. S appears relatively flat and slightly domal neart the intersection with lines GP11 and GP101, reaching its maximum depth of 10 sec TWT in the southern part of the line. Shot interval 50 m.

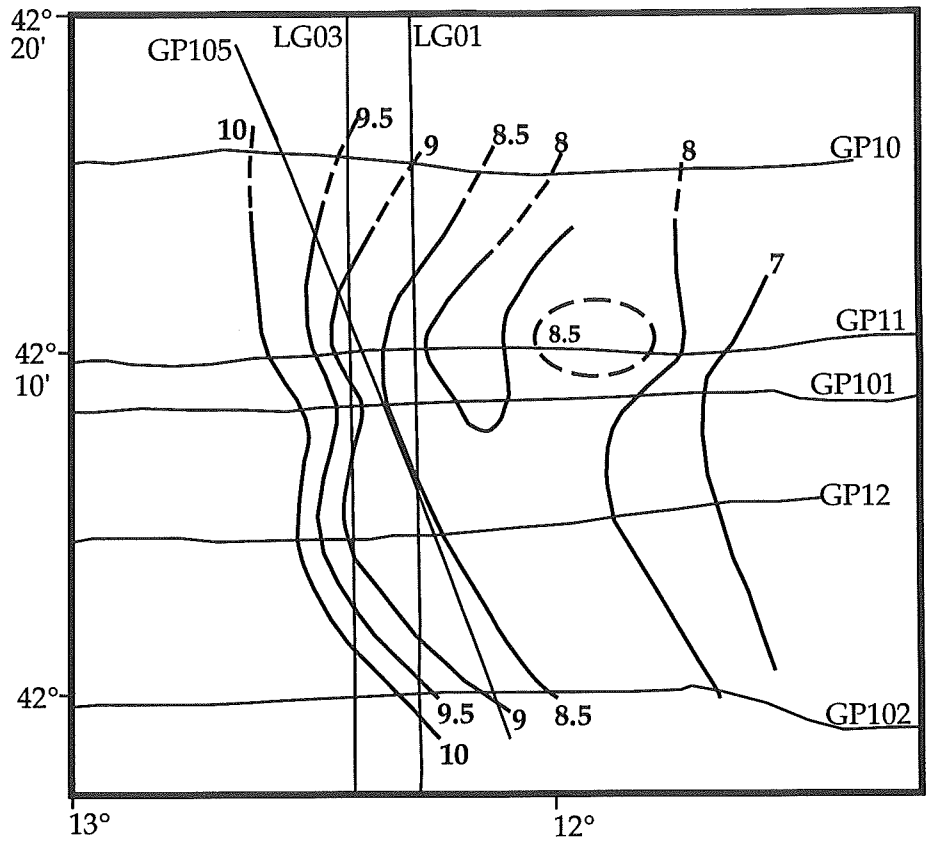

Figure 3.11: Depth contours to the S and S2 (cf profile GP11) reflectors in km, constructed from the depth migrated sections. Contours are drawn where S is unambiguously defined, and where crosslines facilitate the connection between the east-west profiles.

3.5.2 Sense of Movement along S

If S is a detachment fault analogous to those observed in the western United States (e.g. Lister & Davis, 1989), then movement along S should have a consistent sense. Some have interpreted this to be top-to-the-west (Winterer et al., 1988) but most recent workers (Boillot et al., 1988a; Sibuet, 1992; Reid, 1994) propose that S accommodated top-to-the-east movement. As this controversy is clearly important to an understanding of the evolution of this margin, the evidence about the sense of shear along S is the subject of discussion here. Various lines of evidence have been proposed, ranging from its relationship with the peridotite ridge located west of S, the structural dip of the Biscay S, the

measurable extension and subsidence of the Galicia margin, the structure of the conjugate margin off Flemish Cap, and analogies with detachment faults.

The faults bounding the basement blocks above S all dip to the west (e.g. Figures 3.3-3.5), and all accommodated top-to-the-west normal movement. If S accommodated top-to-the-east shear, all the block-bounding faults would be antithetic to S; if S accommodated top-to-the-west shear, the faults would be synthetic to S. Mapping of detachment terranes has shown that faults overlying a detachment are generally synthetic to that detachment (Lister & Davis, 1989): by analogy the S detachment would have accommodated top-to-the-west motion and would cut up to the surface to the east, the breakaway (Figure 3.12). Although on profile GP11 (Figure 3.3) it is not clear if S2 (which cuts up to the surface to the east) or S3 (which cannot be traced east of shotpoint 1500) is the continuation of S, it is clear that S does cut up towards the surface to the east on profiles GP12 (Figure 3.4) and GP102 (Figure 3.5). Hence the evidence points to a breakaway to the east, implying top-to-the-west motion along S.

LePichon and Barbier (1987) used the thickness of basement within fault blocks overlying the Biscay S reflector to infer that the Biscay S cut to depth under the margin, that is to the north-east. If the Galicia S were to do the same it would cut down to the east. However, although the features are similar, there is no *a priori* reason to believe that they should both cut down towards the margin. On the west Galicia margin the evidence is somewhat equivocal as the basement above S does not increase consistently either east or west. This is perhaps not surprising: studies of detachment terranes show that fault block thickness above the detachment does not generally increase in the transport direction, but rather varies irregularly (Lister & Davis, 1989). This observation may be explained by multiple generations of faults (Lister & Davis, 1989) or by the rolling hinge model of Wernicke and Axen (1988) and Buck (1988).

Sibuet (1992) pointed out a discrepancy between the amount of extension measured from faulting, and that determined from subsidence: in the region of the S reflector, the crust was thinned far more than would be predicted by the observable faults, particularly towards the ocean-continent boundary. Although as he noted that this discrepancy could be explained by multiple generations of faulting, he also proposed that it could be caused by differential extension above and below the S detachment if S accommodated top-to-the-east shear. He also interpreted a master fault parallel to the continental slope of the SE Flemish Cap margin as part of a large crustal detachment fault

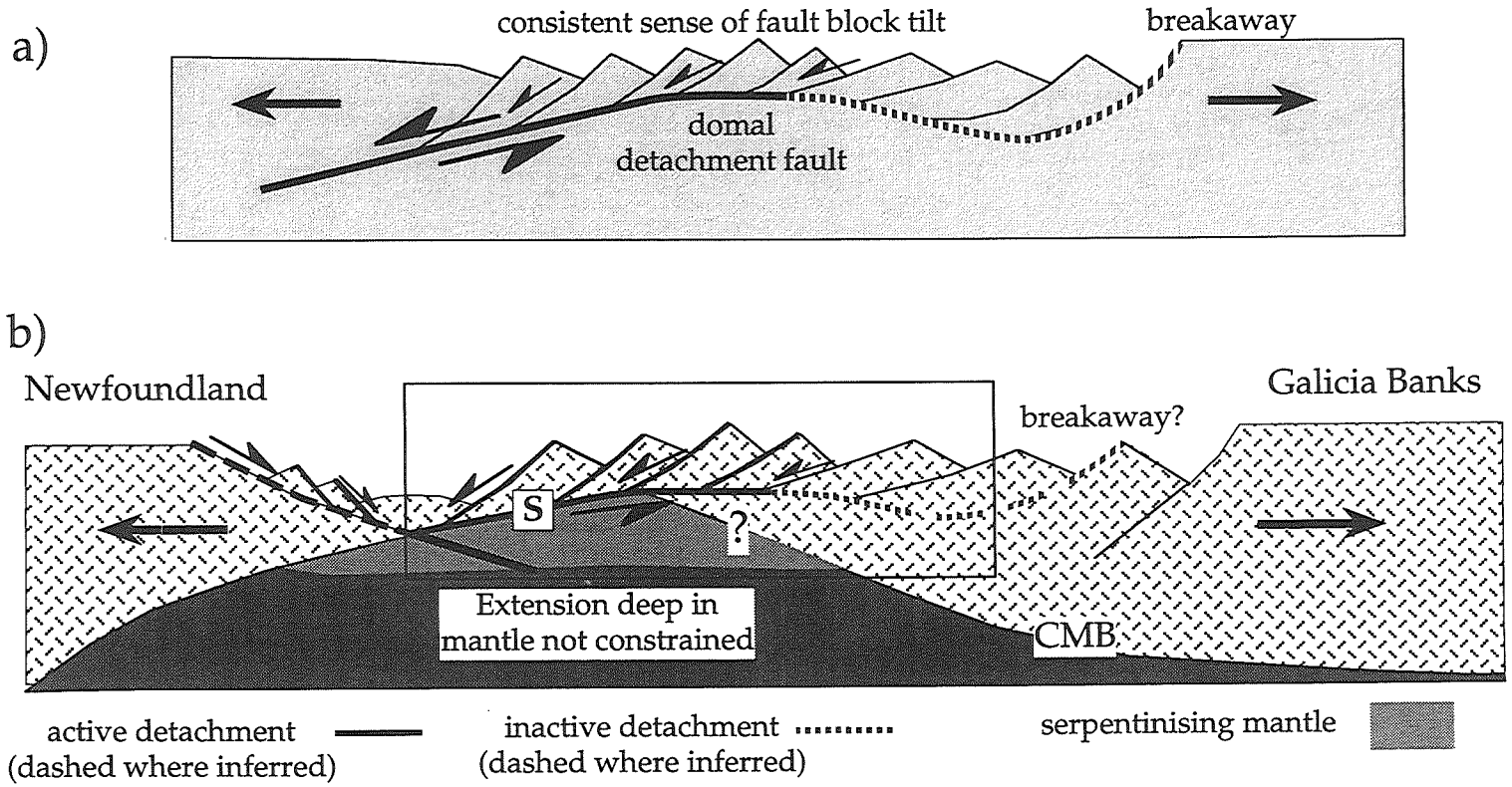

Figure 3.12 a) Cartoon (from Lister & Davis, 1989) summarising geometry of detachment fault terranes. Note that detachment is synthetic to overlying block-bounding faults. b) Modified detachment model applied to the Galicia Banks margin, shortly before break-up. Box marks portion of system imaged by profiles discussed here. S acts as detachment overlying faults but is cut by an east-dipping shear zone linked with the emplacement of peridotites sampled at the surface. This east-dipping structure may be the continuation of a detachment interpreted on SW Flemish Cap margin (Sibuet, 1992). Location of crust-mantle boundary (CMB) beneath rift unclear because of probable serpentinisation.

(compare Figure 3.12). Although Sibuet (1992) could not follow the eastward continuation of this structure towards the continent-ocean boundary, he proposed that this fault represented the westward continuation of the S reflector, and therefore located the breakaway to S on the Newfoundland side. However, as discussed below (Chapter 4), it is possible that such an east-cutting detachment can be present but not be a continuation of the S reflector.

Another argument that has been used to infer top-to-the-east shear along S is the discovery of top-to-the-east shear structures on the top of the Peridotite Ridge, interpreted as the westward continuation of an east-cutting S (Boillot and others, 1988; 1989). The migrated sections show that S cannot be directly traced onto the Peridotite Ridge. For instance on profile GP12 (Figure 3.13) S cannot be convincingly identified west of shotpoint 900 and instead appears to be truncated by east-dipping reflections coming off the peridotite. This relationship can also be seen on the corresponding portion of profile GP101 (Figure 3.13). These east-dipping reflections are interpreted as a top-to-the-east shear zone, corresponding to that sampled by diving and drilling on the Peridotite Ridge itself. This is clearly a different structure to the S reflector, indicating that the S reflector does not crop out on top of the Peridotite Ridge. Hence, the sense of shear determined for shear zones within the peridotite has no bearing on that of S: they can have opposite sense of shear as they appear to be different structures. This is the subject of further investigation and discussion in Chapter 4.

3.6 Conclusions and Outlook

The results of the analyses of the margin-normal profiles show that the block-bounding faults appear to detach onto the underlying S reflector, which nowhere appears offset, but instead displays a smooth, simple geometry. The block-bounding faults represent only the last phase of extension, as the sediments tilted within the blocks include earlier syn-rift units. From these observations it is inferred that S was a detachment fault, active just before break-up. Towards the east, S appears to split into a couple of separate features, which may be parts of the same low-angle normal fault/detachment fault system. Towards the west, S appears to be truncated by east-dipping reflections related to the Peridotite Ridge at the ocean-continent boundary. These may have been responsible for the emplacement of the peridotite, and may be related to the master fault described by Sibuet (1992) from the

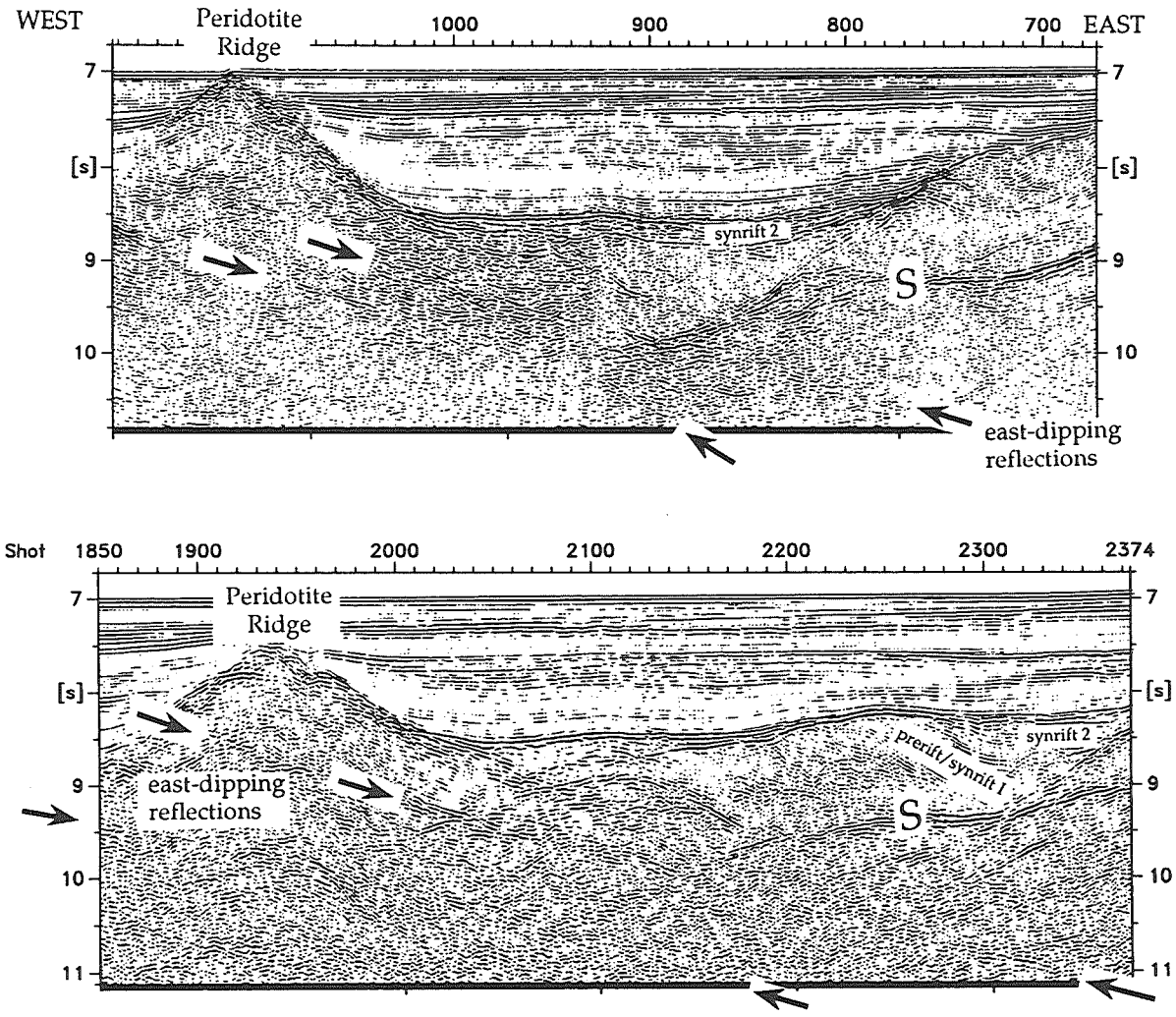

Figure 3.13 Region between the S reflector and the westerly bounding Peridotite Ridge on migrated sections from profiles GP12 and GP101. S dips to the west and appears to be truncated by east-dipping structures cutting down from the Peridotite Ridge. These may represent shear zones related to the exhumation of the mantle ridge. Shot interval 50 m.

conjugate Flemish Cap margin.

The sense of shear of S is not fully constrained, and much of the evidence regarding the sense of shear along S is equivocal: the sense of tilt of the fault blocks suggests also by analogy with detachment faults from the western United States that shear along S was top-to-the-west, whereas other workers have presented a variety of arguments that shear was top-to-the-east. Although it is considered most likely that S accommodated top-to-the-west shear and cuts down to the west, as also indicated by mapping the depth contours to S, this issue can perhaps only be fully resolved by drilling S (Reston et al., 1993). Clearly this is a topic of considerable importance, as it has implications not only for the structure of this margin but also for that of the conjugate SW Flemish Cap margin. Unfortunately, S is out of reach with current technology, but will nevertheless remain an important target of future work. Another goal in the near future will also be the investigation of this margin by detailed wide-angle reflection measurements, to better reveal the velocity structure below the S reflector and provide more information about crustal nature and the crust-mantle boundary.

4 Analyses of bright Crustal Reflections on the West Galicia Continental Margin and the Relationship of S to the Peridotite Ridge

4.1 Abstract

Near the Galicia Bank at 42° N, the S reflector, a bright crustal reflection below a series of tilted fault blocks, is regarded as the key for understanding the evolution of the Iberian continental margin. Here, its regional extent to the north is determined by testing the hypothesis of a possible northern continuation of the S reflector (called S´reflector near 43° N). Another point of investigation is the relationship of S and S´ to the westward bounding Peridotite Ridge.

Using prestack depth migration to derive detailed velocity information, it is shown that the S reflector is overlain by probable basement rocks (Vp > 5 km/s) whereas the S´ reflector may be overlain by lower velocity syn-rift or pre-rift sedimentary units (Vp < 4 km/s). S´ is clearly underlain by mantle peridotites, and may be associated with the emplacement of those peridotites at the surface.

In contrast, E-W and NW-SE trending profiles reveal that east dipping structures cutting down from the Peridotite Ridge cut across the S reflector. The relationship between these features can be interpreted in two ways: S may be antithetic to a mantle shear zone (perhaps S´) or this may postdate and cut S. In either case, S does not crop out at the Peridotite Ridge and is a structure different to S´ and to the high temperature mylonites drilled on the Peridotite Ridge. Hence the sense of shear observed within the peridotite is not necessarily the same as that along S.

4.2 Regional Setting and Objectives

As described above, the west Galicia rifted margin immediately landward of the ocean-continent boundary (marked by the Peridotite Ridge) is characterised by landward tilted fault blocks, bound by oceanward dipping faults, which appear to detach onto a bright intra-crustal reflection, S (e.g. Figure 1.3). The results of Chapter 3 revealed the S reflector as an important detachment active at depths ranging between 1-3 km below seafloor during continental break-up on the Galicia Bank margin. As such a major structure it

was suggested as a valid target for drilling (Reston et al., 1993) to address several outstanding questions: the confirmation of its nature, the determination of the sense, timing and conditions of movement along S, and the age of the overlying late syn-rift sediments.

A problem with drilling S has been so far its depth (c. 3 km below the seafloor - see Chapter 3). Because drilling technology is limited, a location has been sought where S might come up closer to the surface. A possible northern continuation of S, termed S´, was proposed by Boillot and others (1993) for drilling in an area of Cenozoic uplift of the margin (Figure 4.1). S´ was supposed not only to represent the continuation of S to the north., but also to be related to the east flank of the Peridotite Ridge at the ocean-continent transition (Figure 4.2).

The mantle ridge (e.g. Chapter 3 - Figure 3.13) consists of strongly serpentinised peridotite, cropping out at several places and sampled by drilling on ODP Leg 103 (Boillot, Winterer, Meyer et al., 1987 - Figure 4.1) near the ocean-continent transition. Analysis of samples obtained during drilling indicate that this peridotite was emplaced at the end of rifting, during final continental break-up (Girardeau et al., 1988; Beslier et al., 1990). In its southern part the ridge strikes north-south, parallel to the trend of the tilted fault blocks, and is believed to be bound to the west by oceanic crust (Malod et al., 1993).

The Peridotite Ridge itself was interpreted by Mauffret and Montadert (1987) as resembling a tilted crustal block bound by normal faults, and considered as a late extensional structure. However, drilling Site 637 revealed shear structures at the Peridotite Ridge of different sense. From the drill core, oriented by paleomagnetic techniques, Girardeau et al. (1988) identified mylonites and inferred top-to-the-east normal shear under high temperature conditions several km below the seafloor before serpentinisation.

The relationships between the S reflector and the Peridotite Ridge, between the S and S´ reflectors, and between S´ and the Peridotite Ridge are controversial. Boillot and others (1987) proposed that S, S´ and the drilled peridotitic shear zone are all the same structure, i.e. that the S reflector is the continuation of this east-dipping shear zone, and that S´ is the northern continuation of S. However, it has also been argued that S and the peridotitic shear zone may represent different structures (Krawczyk & Reston, 1995), and that the S reflector does not crop out at the Peridotite Ridge.

For this reason, the available reflection seismic data have been the subject of intense analyses to determine the relationship between S, S´ and the sampled

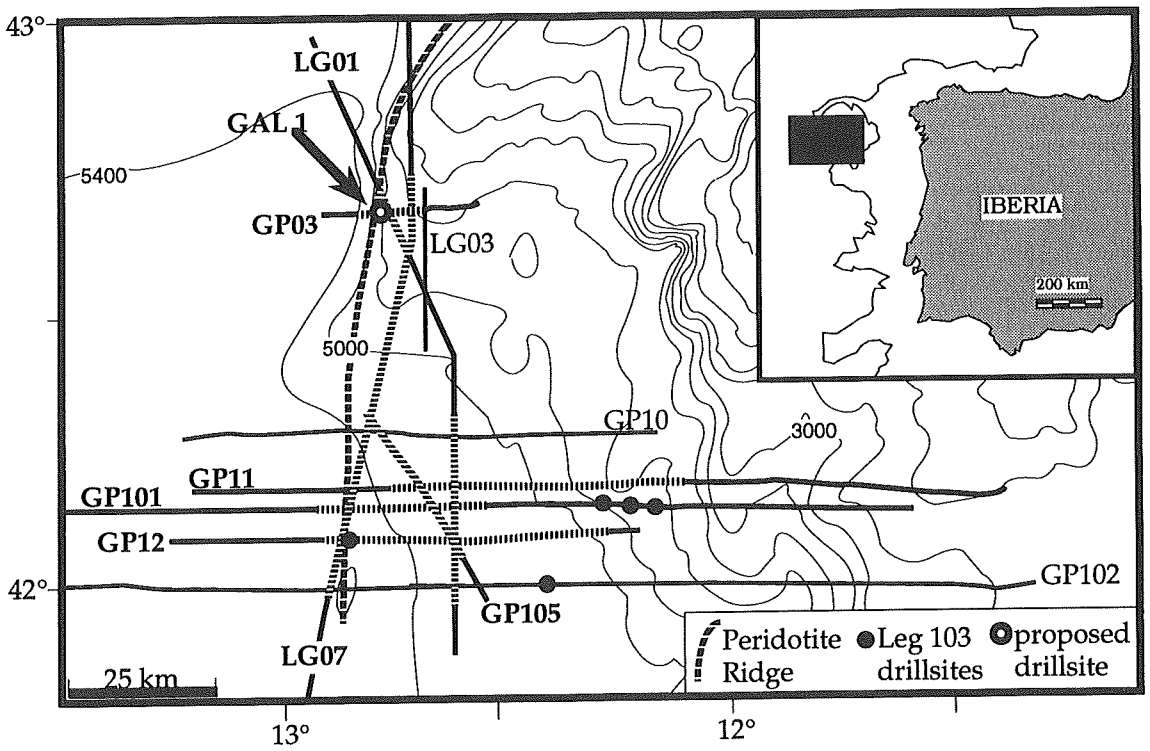

Figure 4.1: Map of the Galicia Margin showing the locations of the analysed MCS profiles; highlighted portions are shown in this Chapter. Marked are the Leg 103 drill sites, the proposed site GAL1, and the Peridotite Ridge.

peridotitic shear zone. Furthermore, the nature of the material directly above S and S´, termed in the case of S´ "enigmatic terrane" (Figure 4.2) has been compared: if the "enigmatic terrane" is sediment then S´ might simply be a reflection from top basement; if the "enigmatic terrane" is basement then S´ may be a major structure like S. To address this issue iterative prestack depth migration was applied to determine the true geometry of both S and S´ and also the velocity of the overlying units.

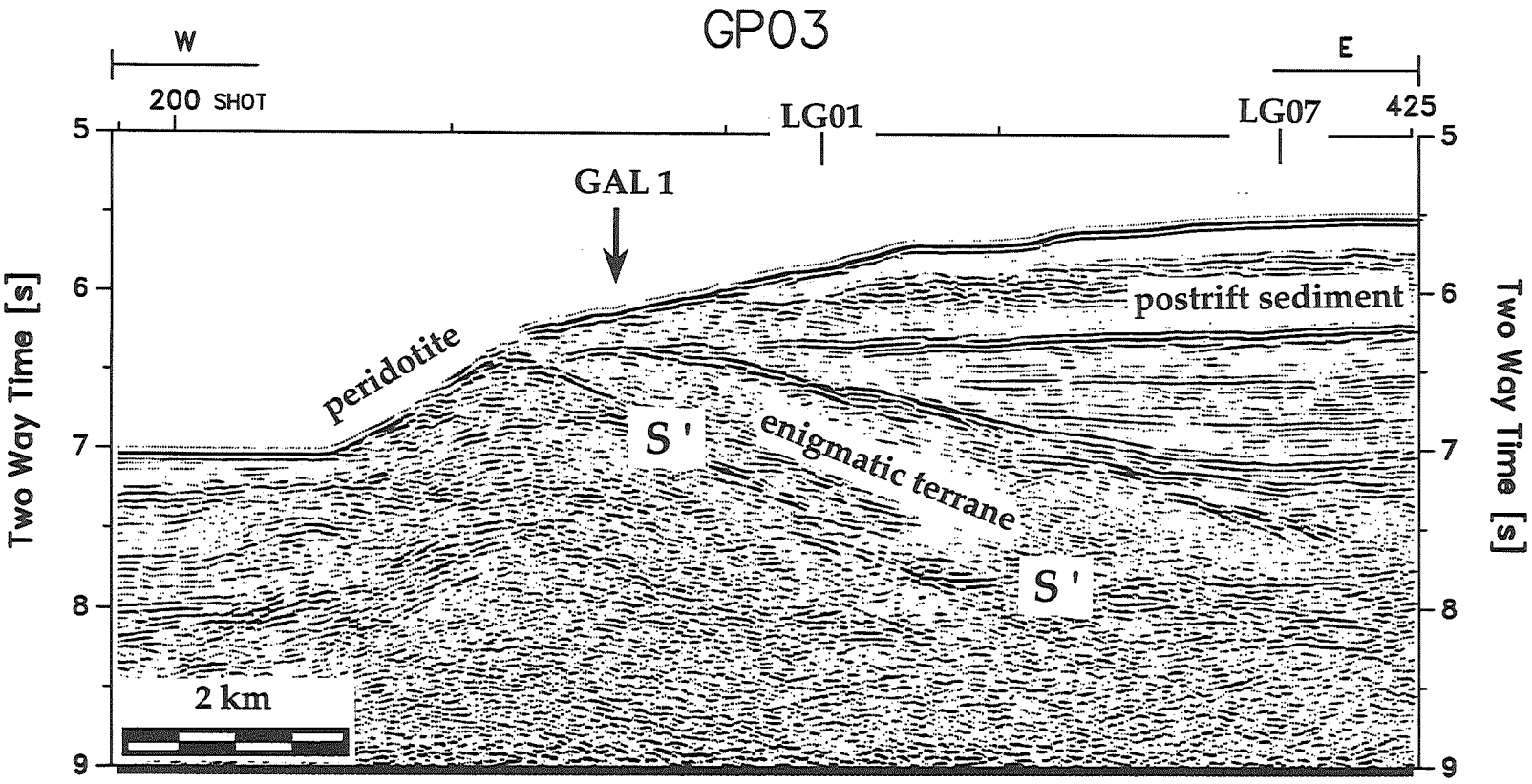

Figure 4.2: Time migrated version of profile GP03, showing the S' reflector, and its relationship to the serpentinised peridotites sampled by diving (Boillot et al., 1988). Below post-rift sediments, the so-called "enigmatic terrane" is directly overlying the S´ reflector, which is proposed for drilling at location GAL 1.

4.3 Relationships between S, S´ and the Peridotite Ridge

To investigate the relationship of the main structural features of the Iberian passive margin, the migrated time sections of all the seismic lines shown in Figure 4.1 were analysed. Here the results are discussed from the five profiles, which illustrate the relationship most clearly: GP03, GP12 and GP101, striking east-west (see Chapter 3), GP105 with a northwest-southeast trend, and LG07 in a north-south direction. Between the mantle ridge and the S reflector bright reflections are absent making the data unsuitable for analysis with the Migpack-software. So conventional processing was applied to the profiles for the structural analysis of S, S´ and the ridge to the west. Particular care was taken to keep steeply dipping events by dip moveout corrections and the local application of filters.

The north-south trending portion of profile LG01 (Figure 4.3) reveals that there is no direct connection between S (well imaged in the area of the southern GP-profiles) and the S´ reflector to the north. Line LG01 shows that the S reflector disappears north of the intersection with line GP10 (see Figure 4.1 for location) at a depth of approximately 9.5 sec TWT (shotpoint 2000). One possible explanation may be the Cenozoic uplift in the northern part of the west Galicia margin (Boillot et al., 1993), causing reverse faults and thus the interruption of structures.

The S´ reflector to the north is closely related to the peridotite exposures (Figure 4.2), cropping out between shotpoints 225-270, and sampled by submersible diving (Boillot et al., 1988b). S´ clearly marks the top of the east flank of this northern exposure of peridotite and dips towards the east between 6-8.5 sec TWT (shotpoints 250-425). This eastward dip may possibly be consistent with the sense of the shear observed in the mylonites sampled further south on top of the Peridotite Ridge during drilling on ODP Leg 103 (Boillot, Winterer, Meyer et al., 1987).

To analyse further the relationship between the east dipping S´ reflection and the Peridotite Ridge where this was drilled and where top-to-the-east mylonites were sampled, S´ was followed onto the north-south trending profile LG07 (Figure 4.4), which intersects profile GP03 at shotpoint 400 (Figure 4.2). At the profile intersection, S´ is imaged on GP03 at a depth of 8 sec TWT and can clearly be correlated with a band of strong reflections on LG07 (Figure 4.4 - shotpoint 1000). From this crossing point, S´ may be traced more tentatively to the south, deepening from 8 to 9.5 sec TWT (shots 1000-1700) and intersecting

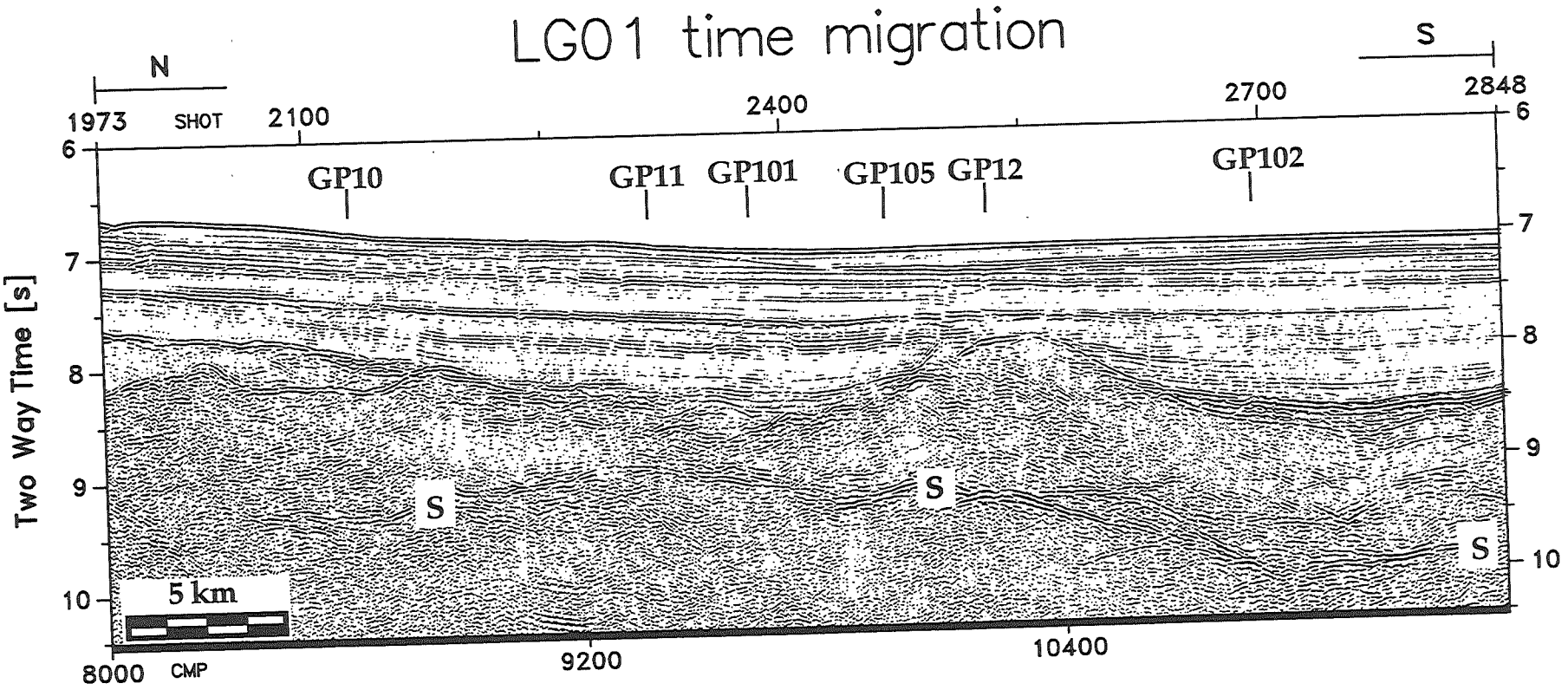

Figure 4.3: Migrated time section of the north-south trending profile LG01 (see Figure 4.1 for location), cutting across the margin-normal profiles of the southern GP-series. S appears relatively flat and slightly domal neart the intersection with lines GP11 and GP101, reaching its maximum depth of 10 sec TWT in the southern part of the line, but cannot be traced north of profile GP10. Shot interval 50 m.

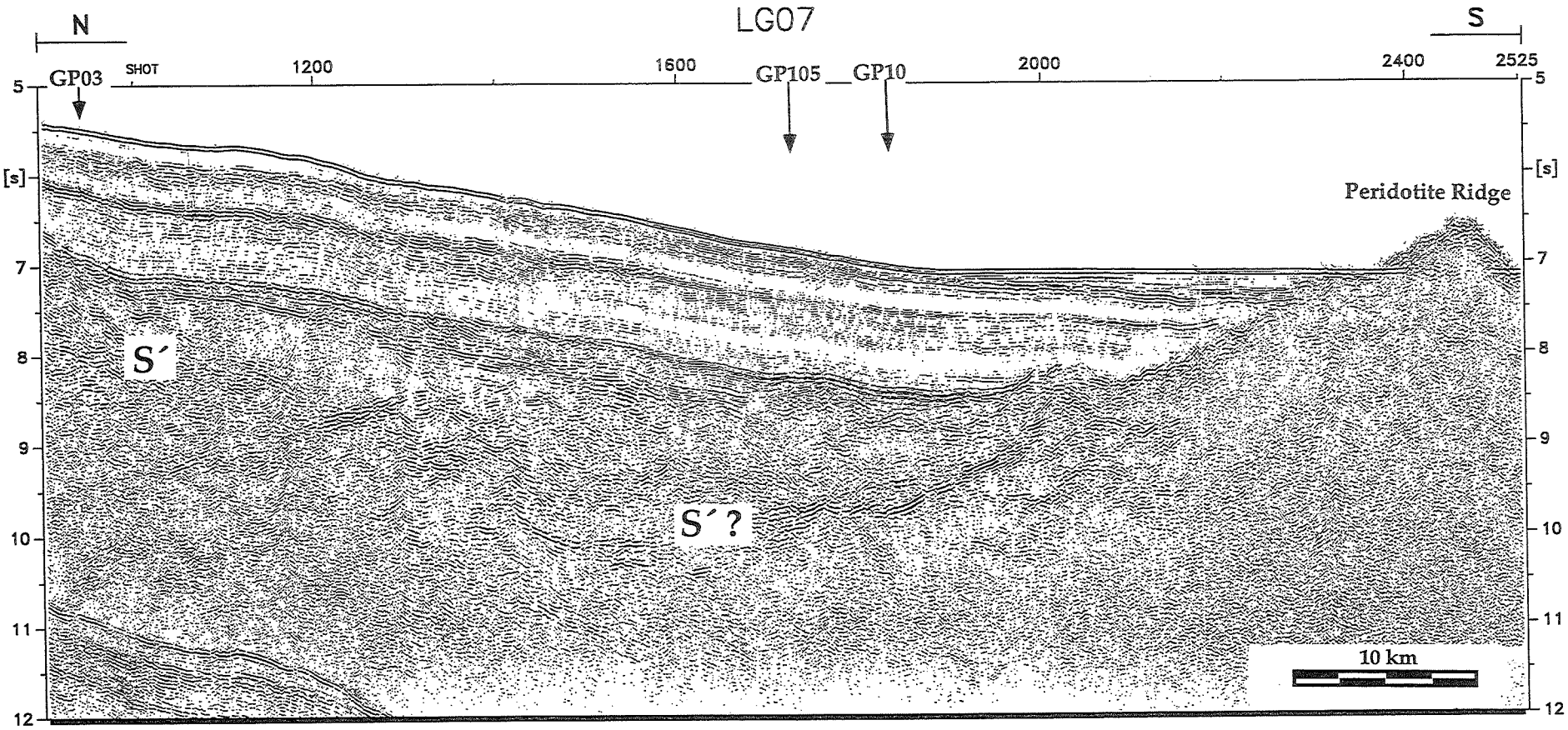

Figure 4.4: Time section of line LG07 after standard seismic processing (time migrated after DMO stack). S´ and eastward dipping structures are correlated to crosslines GP105 and GP03. The connection between these main structures is not completely clear, nevertheless suggesting that the eastward dipping reflections cutting down from the Peridotite Ridge are the continuation of S´.

with lines GP105 and GP10. If the bright series of reflections at c. 9.5 sec TWT (shotpoint 1700) and S′ represent the same structural feature (Figure 4.4), then S′ also marks the top of the peridotite in the southern part of line LG07 (shots 1700-2300) that is the east flank of the Peridotite Ridge. Although the connection between S′ and its southern counterpart flanking the Peridotite Ridge on LG07 is not completely proven, this relationship does seem plausible particularly as S′ demonstrably marks the gently-dipping east flank of the peridotite to the north (Figure 4.2). This is in agreement with the interpretation of Boillot and others (1987; 1995a). It is now considered if S might also represent an east-dipping structure coming off the Peridotite Ridge. To address this issue, the western portions of profiles GP12 and GP101 (Figure 4.5) are further investigated, and correlations with the intersecting profiles GP105 and LG07 are considered.

On profiles GP105 (Figure 4.6), GP12 and GP101 (Figure 4.5) the S reflector passes below the westernmost fault block, and is characterised by a bright and continuous reflection with a gentle dip to the west (Figure 4.5 - compare also Chapter 3). The down-to-the-west movement along the block-bounding faults overlying S implies a top-to-the-west movement along S itself, by analogy with the results of Lister and Davis (1989) from mapping detachment terranes in the western United States. (They show, that the faults overlying a detachment are generally synthetic to that detachment, in which case S and the normal faults both accomodated extension top-to-the-west. - discussed in Chapter 3) Second, the seismic depth sections (see Chapter 3, Figures 3.3-3.6) show that S cuts down towards the west and that the breakaway is probably located to the east, both consistent with top-to-the-west motion along S. This implies that S is a different structure to the top-to-the-east shear zones bounding the Peridotite Ridge.

Boillot and others (1995a) suggested that S might be traceable on the oblique line GP105 (Figure 4.6), to its intersection with profile LG07 near the flank of the buried Peridotite Ridge. However, it appears from Figure 4.6 that S cannot be traced to LG07 but rather dies out landward of the Peridotite Ridge. Instead, the most striking features are the apparently south-east dipping reflections, cutting across the S reflector at approximately 10 sec TWT (shotpoints 650-850) near the intersection with profile LG07. These east-dipping reflections cutting across S may be incompletely migrated, as line GP105 is oblique, and full migration of reflections would require unrealistically high velocities. Nevertheless, at the northern end of GP105 (Figure 4.6) at the

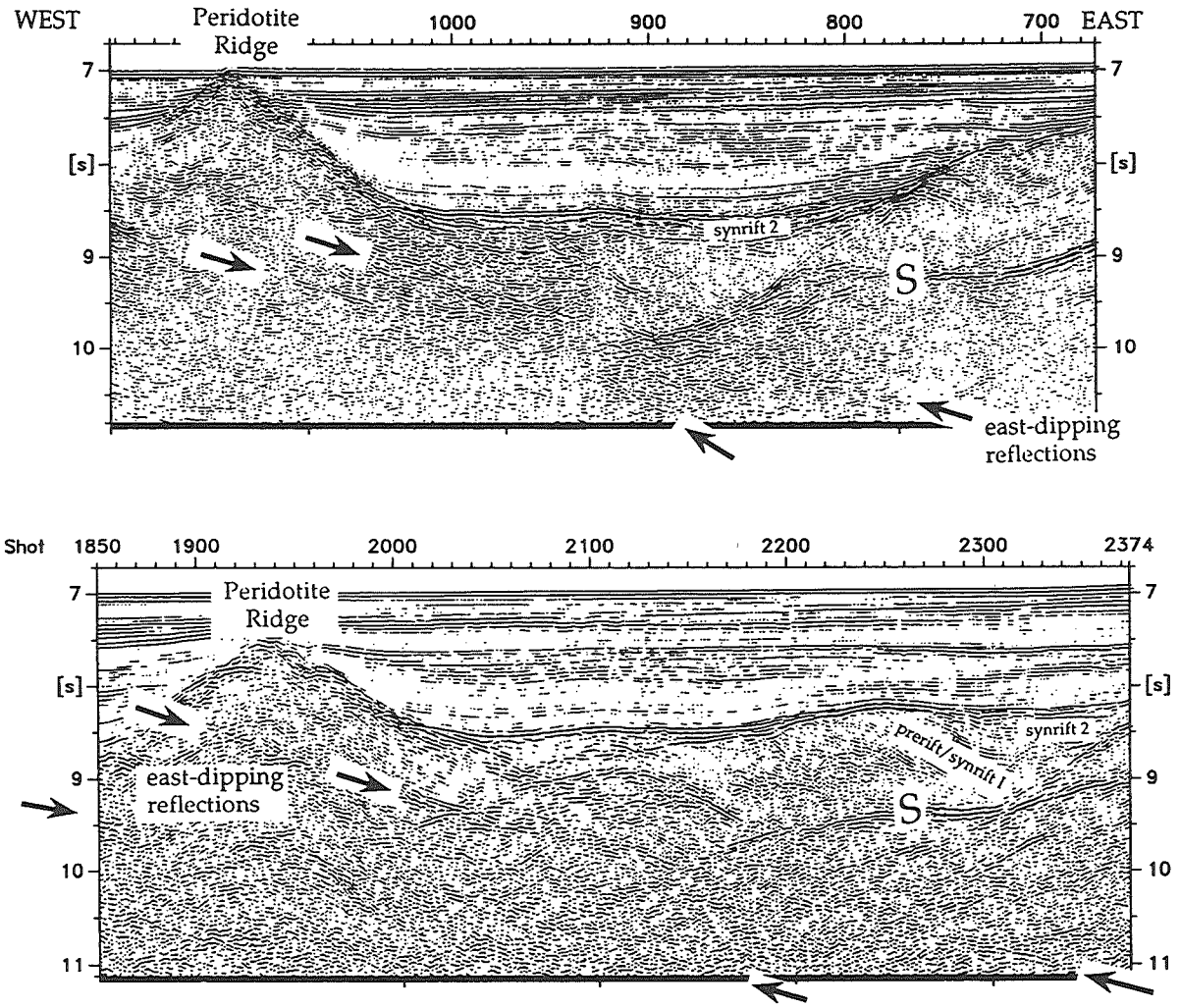

Figure 4.5: Migrated time sections of profiles GP12 and GP101 showing the relationship between the Peridotite Ridge and the S reflector. The S reflector dips to the west, and appears to be crosscut by east-dipping reflections coming down from the Peridotite Ridge, probably representing mantle shear zones.

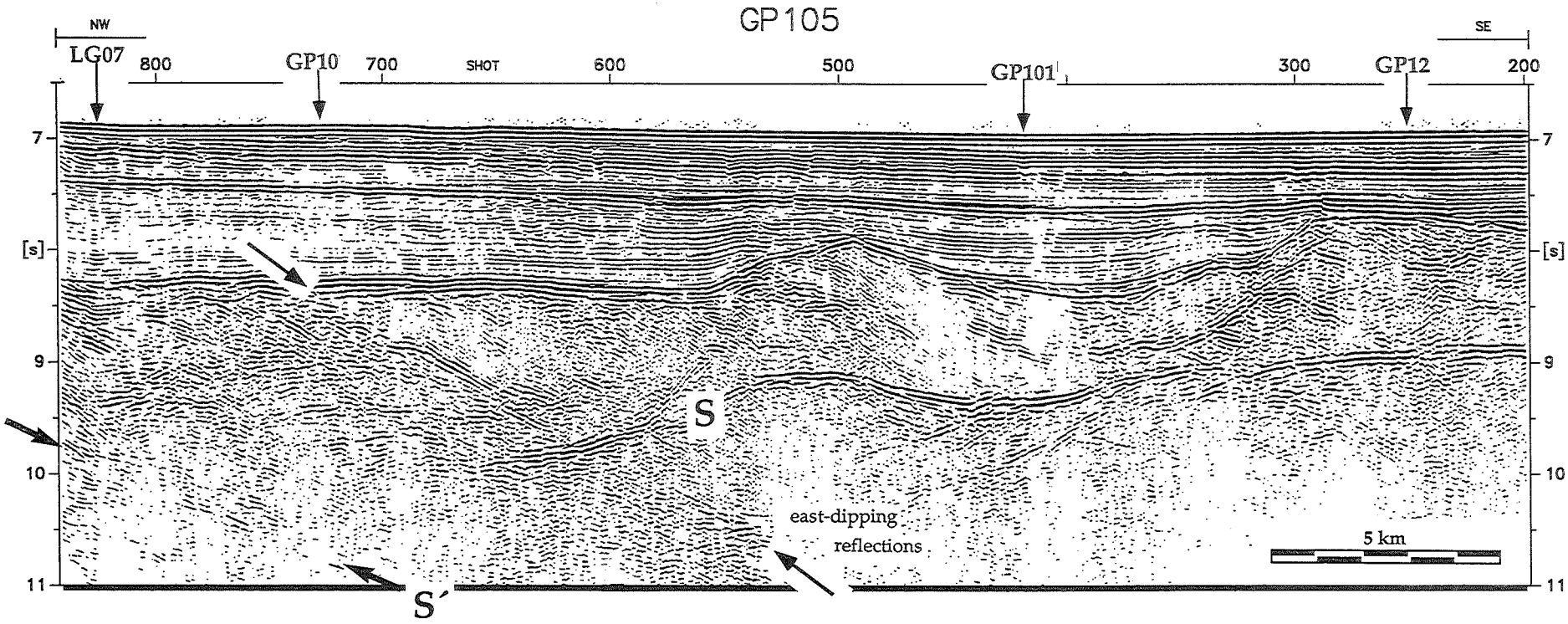

Figure 4.6 Time section of line GP105 derived from standard seismic processing (time migrated after DMO stack). To the east, S is clearly imaged below the break-up unconformity and a tilted block with a gentle dip to the west. Note in the western part of GP105 the apparently south-eastward dipping reflections, cutting acrossS. At the intersection with LG07, the apparently south-eastward dipping reflections may correlate at 9.75 sec TWT depth with those from the top of the peridotite (Figure 4.4).

intersection with LG07, the apparently south-eastward dipping reflections, which appear to cut across S, correlate with the strong reflection on LG07 from the top of the peridotite (shotpoint 1700 - Figure 4.4). As described above, this reflection can be clearly followed on LG07 south onto the top of the Peridotite Ridge (shots 1700-2300) and more tentatively northwards (shots 1700-900) towards the intersection of LG07 with profile GP03 (Figure 4.2) where it correlates with the S´ reflector marking the top of peridotite as identified by submersible sampling (Boillot et al., 1988b). Thus, the correlation of the northwestern part of GP105 with profile LG07 (Figure 4.4) suggests that the eastward dipping reflection, cutting down from 9.75 to 11 sec TWT (shots 750-825) may represent S´ but cuts across S.

This observation of east-dipping events cutting across the S reflector is more pronounced in the southern part of the investigated area. Here, the east-west profiles GP12 and GP101 (Figure 4.5) clearly image the S reflector dipping to the west below the tilted crustal blocks. A significant series of east-dipping reflections comes off the Peridotite Ridge, cutting down from the mantle outcrop and apparently cutting across S at a depth of c. 10 sec TWT between shotpoints 2050-2150 on profile GP101, and between shots 900-950 on line GP12 (Figure 4.5). Although the relationship between S and these east-dipping reflections is not fully resolved, it is clear that S cannot be traced onto the east flank of the Peridotite Ridge as had been suggested by Boillot and others (1995a). Instead, these east-dipping reflections are interpreted as an east-dipping extensional structure, which is associated with the shear structures observed on the Peridotite Ridge but not with S. S' is further regarded as the top-to-the-east shear zone bounding the Peridotite Ridge and was drilled during Leg 103 (Boillot, Winterer, Meyer et al., 1987), implying opposite sense of shear along the mantle ridge (top-to-the-east) and S (top-to-the-west).

In summary, the S´ reflector may not be the continuation of S because of the following reasons:

- there is no direct connection between S and S´.
- S´ dips to the east, while S dips to the west.
- S´ marks the dipping east flank of the peridotite to the north and may correlate with the similarly placed shear zones drilled on Leg 103 to the south. In contrast S appears to be crosscut by east-dipping reflections coming off the Peridotite Ridge.
- the available evidence favours top-to-the-west shear along S but top-to-the-

east shear along S´ and the drilled peridotitic shear zone. These relationships are summarised in Figure 4.7.

The relationship of S itself with the drilled peridotitic shear zone could be interpreted in different ways (Figure 4.8). One possible interpretation suggests two conjugate shear zones putting into contact mylonitized, sheared gabbro and peridotite: the east-dipping S´ structure accomodating top-to-the-east shear, and west-dipping S accomodating top-to-the-west shear. In this model, the portion of S´ above S may actually be a conjugate deformation zone (cf Reston, 1990; Beslier & Brun, 1991) predicting that the shear zone bounding the peridotite would have both top-to-the-west and top-to-the-east senses of shear. However, only top-to-the-east shear has been observed, perhaps because of the erosion of the mantle shear zone after denudation.

Alternatively, the Peridotite Ridge itself may have been emplaced along the top-to-the-east east-dipping shear zone (imaged as the eastward dipping reflections), which bounds the mantle ridge (Figure 4.8). This would have occured after break-up, and hence after movement along S had ceased. Such emplacement of peridotite after the end of crustal rifting has been previously proposed by Winterer and others (1988) and Sibuet (1992), invoking a diapiric origin. In contrast, Boillot and others (1988a) interpret sediments onlapping the ridge as Synrift II, deposited during final rifting, implying that the Peridotite Ridge was emplaced during the last phases of rifting and not after break-up.

Considering finally the results of Chapter 3 and the sense of movement along S, the east-dipping structures coming off the Peridotite Ridge might represent the continuation on the Galicia margin of the east-dipping master fault inferred by Sibuet (1992) from Flemish Cap (see Figure 3.12). In this case, the S reflector might be unrelated to the structure found on the Newfoundland margin.

4.4 Comparison of S and S´: the Nature of the S´ Reflector

To further compare S and S´, the velocity structures of the sequences directly overlying these reflections are investigated by depth migration before stack (MIGPACK-software), which provides a detailed velocity model by iterative velocity determination through depth focussing error analysis (Denelle et al., 1986 - see section 2.2). This method is applied to parts of three margin-normal profiles: GP11, GP12 (compare also Chapter 3), and line GP03

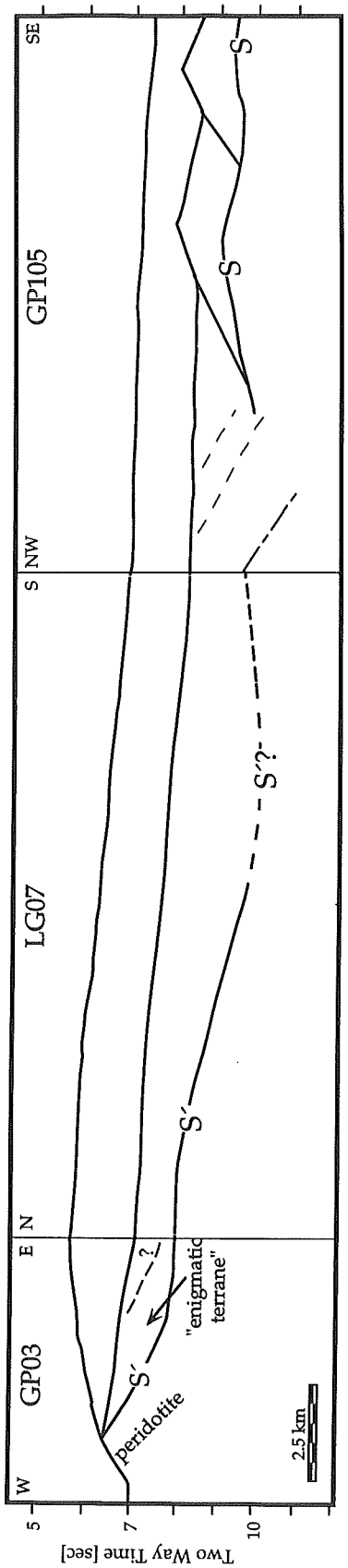

Figure 4.7: Line drawing of segments from profiles GP03, LG07 and GP105 (see Figures 4.2, 4.4 and 4.6) summarising the relationships of S, S´ and the peridotite exposure to the north. Even if S´ can be followed south along LG07, no direct connection with S is apparent.

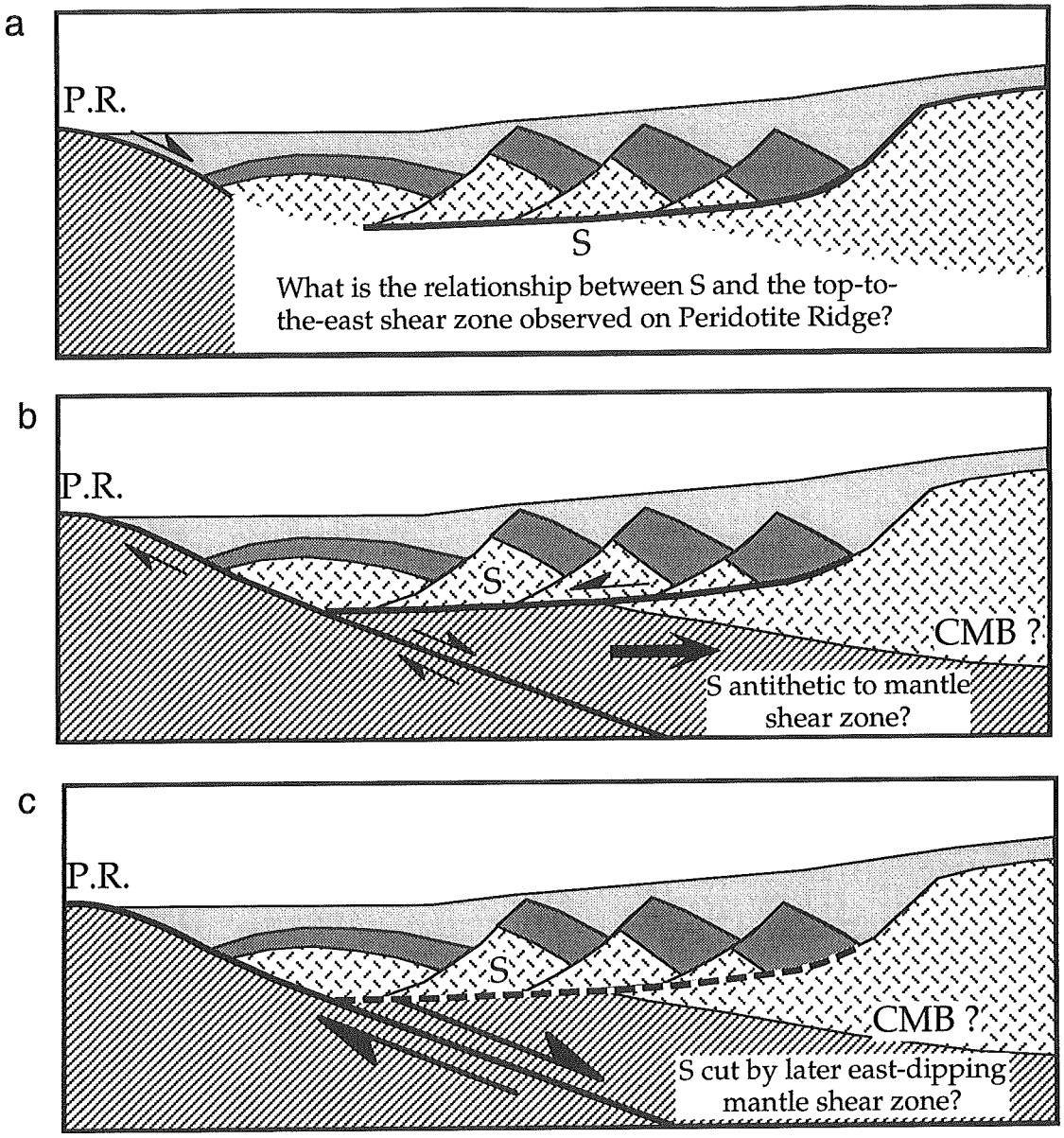

Figure 4.8: Schematic diagramm to illustrate the relationship between the S reflector, S´ and the Peridotite Ridge. a) the sense of shear observed in the peridotite is top-to-the-east, whereas the sense of the tilted fault blocks suggests above S a top-to-the-west shear zone. Seismic data (Figures 4.2 and 4.5) shows eastward dipping reflections cutting down from the Peridotite Ridge (PR) offering two interpretations for the relationship between S and the Peridotite Ridge: b) S may be conjugate to a mantle shear zone or c) it is cut by a later one (S´).

cutting normal to S´ (see Figure 4.1 for location). Profiles GP11 and GP12 are located in the area where S was originally defined (de Charpal et al., 1978), and profile GP03 (Figure 4.2) covers the location where S´ and the overlying "enigmatic terrane" have been described by Boillot and others (1993). The intersection with profile LG01 (Figure 4.9) provides additional geometrical control and images the S´ reflection as a band of subordinate reflections of approximately 300 msec TWT thickness as it cuts into levels deeper than 8 sec TWT (shotpoint 1250).

The velocity structures derived from prestack depth migration of the multichannel reflection seismic lines GP03, GP11 and GP12 imply that S and S´ may be overlain by different lithologies, as the sequences directly above S and S´ show different interval velocities (Figure 4.10). While the interval velocities of the post-rift sediments are in good agreement, ranging between 1.8 and 2.4 km/sec, the velocities of the terranes above the S and S´ reflectors show large differences varying between 3.5-5 km/sec.

Thus, the crustal blocks immediately above S on the margin-normal profiles (Figure 4.5) are interpreted as consisting of crystalline basement (with an interval velocity of approximately 5.5 km/sec) overlain by tilted pre-rift and early syn-rift sediment (Vp 3.5-4 km/sec). The sequence above S´ (Figures 4.11), which is the so-called enigmatic terrane, may in contrast be dominantly pre-rift sediment of about 3.8 km/s, as this velocity is similar to that of sedimentary units identified within the tilted fault blocks on GP11 and GP12 (e.g. Krawczyk & Reston, 1995). In conclusion, this analysis of the velocity structure of the "enigmatic terrane" overlying S' indicates that this may include little if any crystalline basement, but rather that it dominantly comprises the same type of sedimentary units tilted within the fault blocks further to the south.

However, this supports the possibility that S´ may represent a detachment fault: it is clear from the section GP03 that S' marks the contact between peridotite (it can be traced directly from the known outcrop of serpentinised peridotite to the east - Figures 4.2, 4.11) and the "enigmatic terrane" - i.e. rocks of probable pre-rift or early syn-rift age. A contact between peridotite and sediments deposited either before rifting or perhaps during early rifting is almost certainly due to tectonic displacements postdating the deposition of those sediments. It is for instance known that the peridotite was emplaced near the end of rifting (Boillot, Winterer, Meyer et al., 1987; 1988) and hence was overlain by crustal basement during the earlier deposition of the sediments that

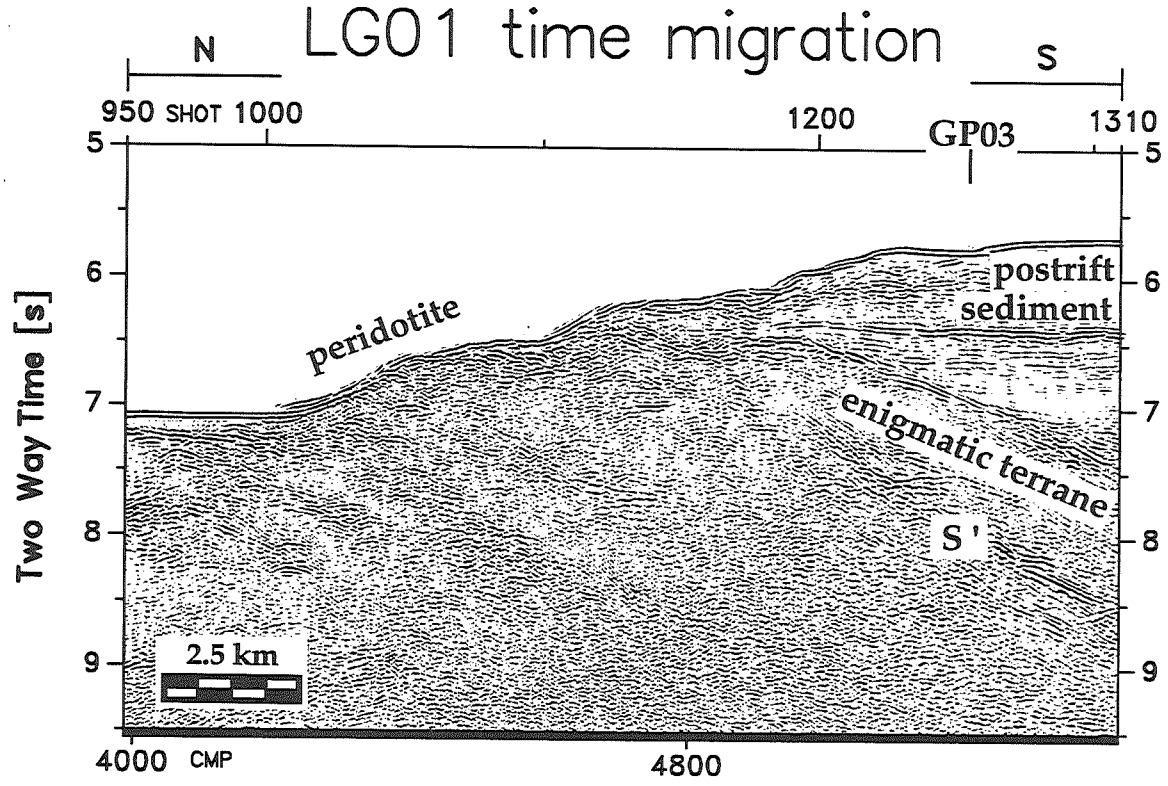

Figure 4.9: Detail of profile LG01 at the intersection with GP03 after time migration. Different sediment sequences, the "enigmatic terrane" and the S´ reflector are imaged east of the peridotite outcrop. Below 8 sec TWT, S´ is composed of a band of bright subordinate reflections of c. 300 msec TWT thickness.

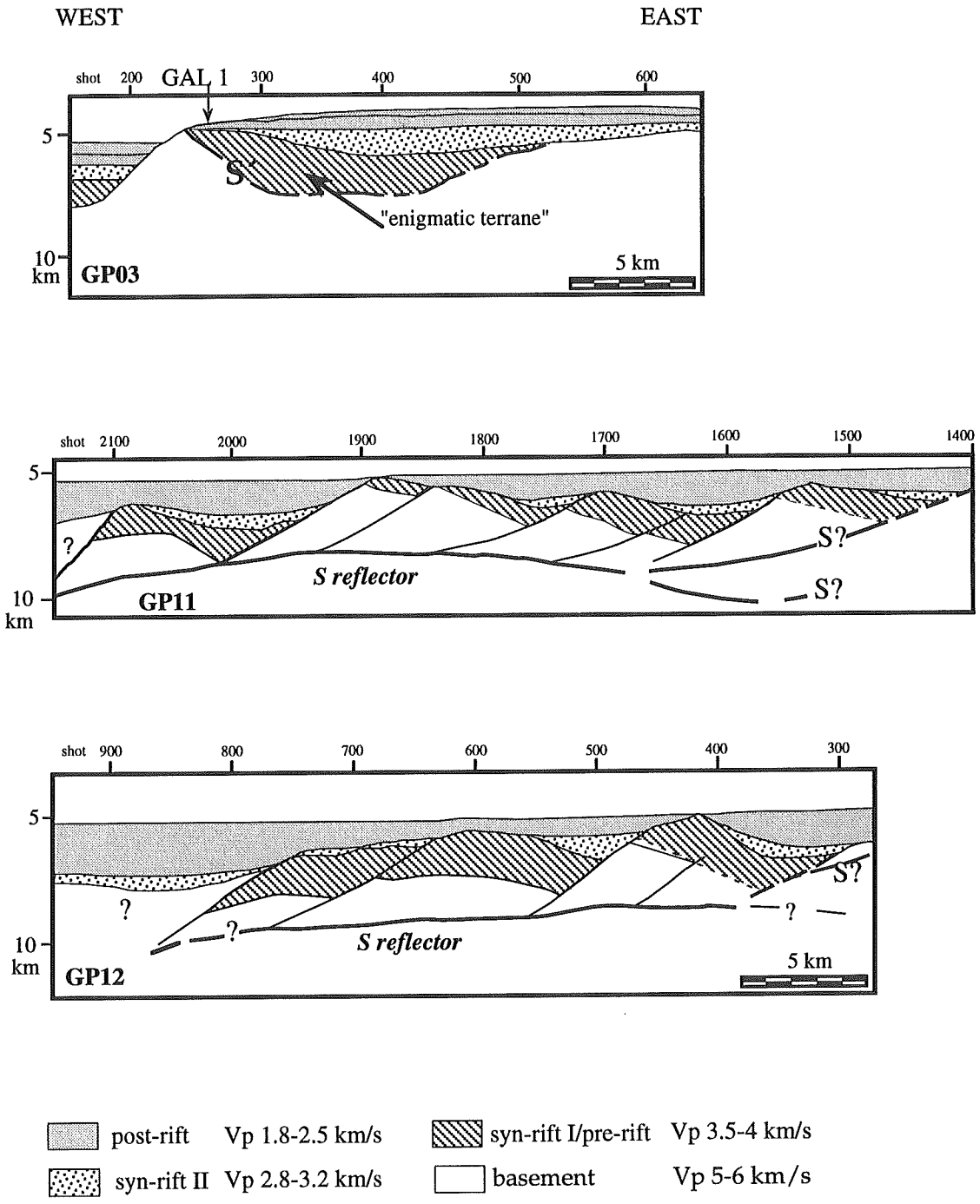

Figure 4.10: Interpretations and velocity models produced by iterative prestack depth migration in the area of S (GP11, GP12) and S´ (GP03). The enigmatic terrane overlying S´ is identified by its velocity as sediment, while the S reflector is overlain by basement.

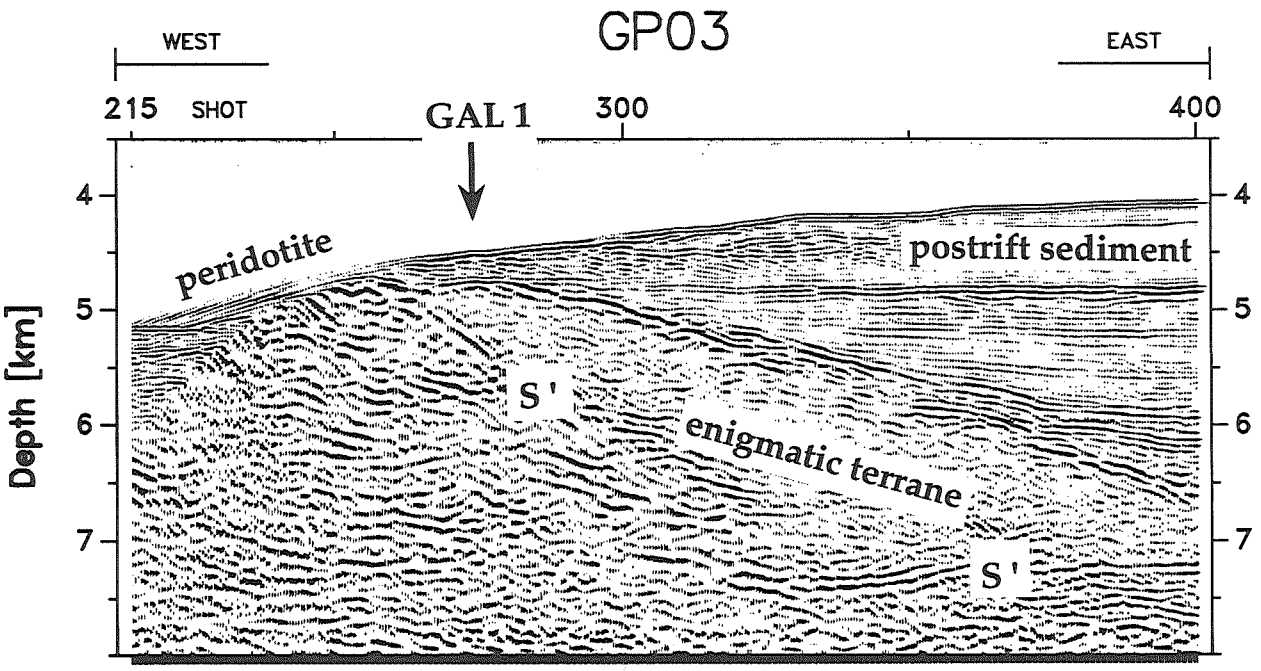

Figure 4.11 Depth section of line GP03 after prestack depth migration with the velocity model shown in Figure 4.5. The marked drillsite GAL 1 is proposed at a location where S´ approaches the surface. Interval velocities indicate that S´ may be overlain by early syn-/pre-rift sedimentary units (Vp < 4 km/s) in the "enigmatic terrane".

may comprise the "enigmatic terrane". Therefore, the contact between these sediments and the peridotite cannot simply be a depositional surface, and at no time could the S' reflector have been subject to erosion. In conclusion, S' may be a valid target for drilling a detachment fault (Reston et al., 1994).

4.5 Conclusions and Outlook

A detailed velocity model through iterative prestack depth migration reveals that the S reflector is overlain by probable basement rocks (Vp > 5 km/s), whereas lower velocity early syn-rift or pre-rift sedimentary units (Vp < 4 km/s) may overlie the S´ reflector. As the S´ reflector is underlain by peridotite, and as the contact between pre- or early syn-rift sediment and peridotite could not be depositional, S´ is interpreted as a major structure juxtaposing uppermost continental crust against mantle.

These analyses show furthermore that S is an intra-crustal reflection onto which the block-bounding faults detach. It exhibits a gentle dip to the west and does not come up to the surface like S´, being rather truncated by east dipping reflections close to the Peridotite Ridge. These appear to correlate with S´. S could have accomodated top-to-the-west extensional movement, being either antithetic to a mantle shear zone (S´) or cut by a later one. However, these results support the proposal that S' may represent a major detachment fault of some time, although perhaps not the same one as S.

These results constrain once again the importance of drilling detachment faults on continental rifted margins, to determine the timing, sense of movement, and the nature of the upper and lower plate rocks. As shown here, geophysical investigations constrain some of the nature of the different sequences deposited before, during and after rifting, and advance much of the discussion about lithospheric extension, but the last proof can only be given by drilling.

5 Indications for Detachment Tectonics in the Iberia Abyssal Plain

5.1 Abstract

The Iberia Abyssal Plain (IAP) segment of the western Iberian Atlantic margin is characterised by highly extended and thinned continental crust bounded westwards by a ridge of serpentinised peridotite within the transition zone between continental and oceanic crust (OCT). To better understand the evolution of this margin, the margin-normal profile LG12 between Sites 898 and 901 was analysed. After optimum processing, including prestack depth migration, the seismic sections image strong reflections below the break-up unconformity in this segment of the Iberian non-volcanic margin. These intra-crustal reflections are overlain by probable basement rocks (Vp > 5 km/s), whereas syn-rift or pre-rift sedimentary units exhibit generally lower velocities (Vp < 4.1 km/s). Between Site 901 (identified by drilling as probable continental crust) and Site 900 (amphibolite facies metamorphosed gabbro) to the west, basement is broken up into landwardward-tilted crustal blocks bound by normal faults. These block-bounding faults appear to detach onto bright intra-crustal reflections (structure H exhibits a reflection coefficient of c. 0.15), which thus mark the lower boundary of the single blocks. By analogy with the similar seismic image of the S reflector in the Galicia Bank area to the north , where continental break-up has been controlled by the detachment fault structure S (see Chapter 3), continental break-up in the IAP could have been also controlled by detachment faults active at different times during rifting. Extension of the upper lithosphere along the detachment system may have exposed a cross-section through the entire lithosphere from upper crust (Site 901), through the lower crust (Site 900) to the uppermost mantle (Site 897).

5.2 Regional Setting and Objectives

The Iberia Abyssal Plain (IAP) represents the central segment of the west Iberia continental margin located between the Galicia Bank and Tagus Abyssal Plain areas (Figure 5.1). The three rift phases, occuring on the Iberian margin (cf Chapter 1), influenced the IAP during Early Cretaceous break-up between Iberia and the Grand Banks. Rifting appears to have propagated northwards, occurring at c. 137 Ma in the Tagus Abyssal Plain (Pinheiro et al., 1992), at c.

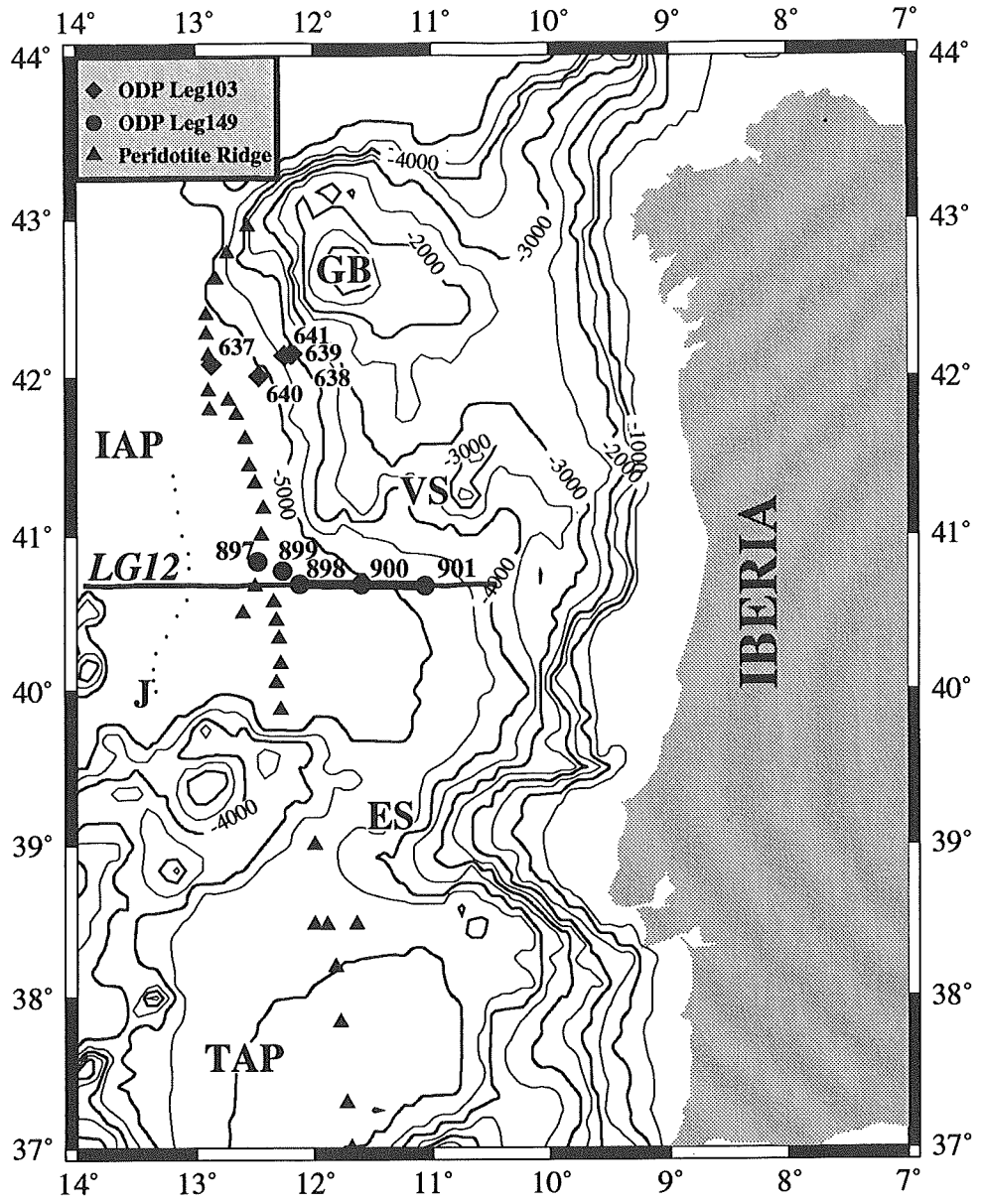

Figure 5.1: Bathymetric map showing the location of the analysed multichannel reflection seismic line Lusigal 12 (LG12) west of Iberia. The highlighted portions are shown here. Also marked are the drilling locations of ODP Leg 103 (diamonds) and 149 (circles); triangles trace the partially drilled ridge of serpentinised peridotite at the ocean-continent transition. Depth contours are in metres below sea level, contour interval is 250. Abbreviations: GB - Galicia Bank; IAP - Iberia Abyssal Plain; VS - Vigo Seamount; ES - Estremadura Spur; TAP - Tagus Abyssal Plain; J - magnetic anomaly, associated with chron M0.

130 Ma in the Iberia Abyssal (Whitmarsh et al., 1990) and finally at c. 114 Ma in the Galicia Banks area (Boillot, Winterer, Meyer et al., 1988). The timing of the onset of seafloor spreading is confirmed by the magnetic J-anomaly found just westward of the presumed ocean-continent transition (OCT). J is thought to be slightly older than chron M0 (Whitmarsh et al., 1990), indicating that seafloor spreading off the IAP margin started shortly prior to J´s formation in Hauterivian-Barremian time, and the break-up off Galicia must have occurred later.

In the Iberia Abyssal Plain, a basement ridge similar to the one on the Galicia Bank passive margin was interpreted by Beslier et al. (1993) to be serpentinised peridotite and to mark the ocean-continent transition like the mantle outcrop west of Galicia (Figure 5.1). This hypothesis was further supported by the analysis of refraction seismic data combined with the modelling of a single east-west gravity profile (Whitmarsh et al., 1993). These authors identify a layer of extremely thinned continental crust adjacent to thin oceanic crust, both underlain by a layer with seismic velocity of 7.6 km/sec, which may be interpreted in two ways. First, it may be underplated material, brought up by some kind of small-scale magmatism during rifting and/or break-up. This hypothesis has been considered unlikely because of the absence of volcanism on this passive margin (Sawyer, Whitmarsh, Klaus et al., 1994), the local extent of the thin layer and finally the relatively high velocity compared to those found on volcanic margins for underplated material (e.g. White et al., 1987). The second possibility is that this thin layer consists of peridotitic mantle material that was partly exhumed during lithospheric extension and was serpentinised directly after break-up when penetration of water may have been facilitated by the thin sediment cover and the highly fractured overlying section. In this hypothesis, the 7.6 km/s layer represents that portion of mantle material that was partly serpentinised at or close to break-up.

Landward of the peridotite ridge the crust is c. 4 km thick (Whitmarsh et al., 1993), and thickens gradually landward. Although the width of the transition from oceanic crust through serpentinised mantle to definite continental crust is four times wider on the Iberia Abyssal Plain (Beslier et al., 1993), the basic structure of the Iberia Abyssal Plain margin is similar to that of the Galicia Banks margin (Krawczyk et al., 1994).

5.2.1 Drilling Results from ODP Leg 149

ODP Leg 149 set out to drill a transect across the transition from oceanic to continental crust (OCT) off the west Iberia continental margin in the Iberia Abyssal Plain. One of the main objectives was to drill basement to reveal the nature and rock type of basement across the OCT (Figure 5.2a). As suggested by analogy with the west Galicia margin (Beslier et al., 1993), the existence of a peridotite ridge at the western end of the OCT in the IAP was to be tested. Second, geophysical modeling (Whitmarsh et al., 1993) identified a layer of extremely thinned continental crust adjacent to thin oceanic crust, both supposed to be underlain by partly serpentinised mantle material. Thus, drilling set out to confirm those hypotheses by sampling at different basement highs across the OCT (see Figure 5.1 for location of the drilled sites).

Drilling Site 897 on ODP Leg 149 (Sawyer, Whitmarsh et al., 1993 - Figure 5.2b) confirmed indeed that the basement ridge comprises serpentinised mantle rocks bounding the transition from oceanic to continental crust (OCT) to the west. Drilling also sampled serpentinites at Site 899 in the form of a mass-flow deposit (within three distinct breccia units), suggesting that serpentinised peridotite must form basement close to this location.

Further east, at Site 900, amphibolite-grade metamorphosed mafic igneous rocks were sampled. These are highly sheared and deformed gabbros, deformed at depths of 12-20 km (M.-O. Beslier, pers. comm.). They are perhaps best interpreted as either pre-rift or syn-rift lower crust.

Finally, Site 901, although failing to reach basement, encountered Tithonian strata dominated by mud and clay, interpreted as either very early syn-rift sediments, or perhaps more likely pre-rift sediments. A significant amount (in places almost 85%) of terrigeneous plant debris and other organic matter (Shipboard Scientific Party, 1994c) indicates the terrigeneous origin of the Tithonian sediments. Hence, even if these were early syn-rift sediments, it is considered very likely that these sediments were deposited on upper continental basement.

Leg 149 thus partly confirmed the existing geophysical model, but also left a number of questions unanswered and posed some new ones. The extent of the peridotite appears to be larger than previously supposed; the OCT may be of wider extent than previously thought (the first unequivocally continental crust occurs at Site 901 rather than at Site 898); and previously unsuspected lower crustal rocks were found at the intervening Site 900.

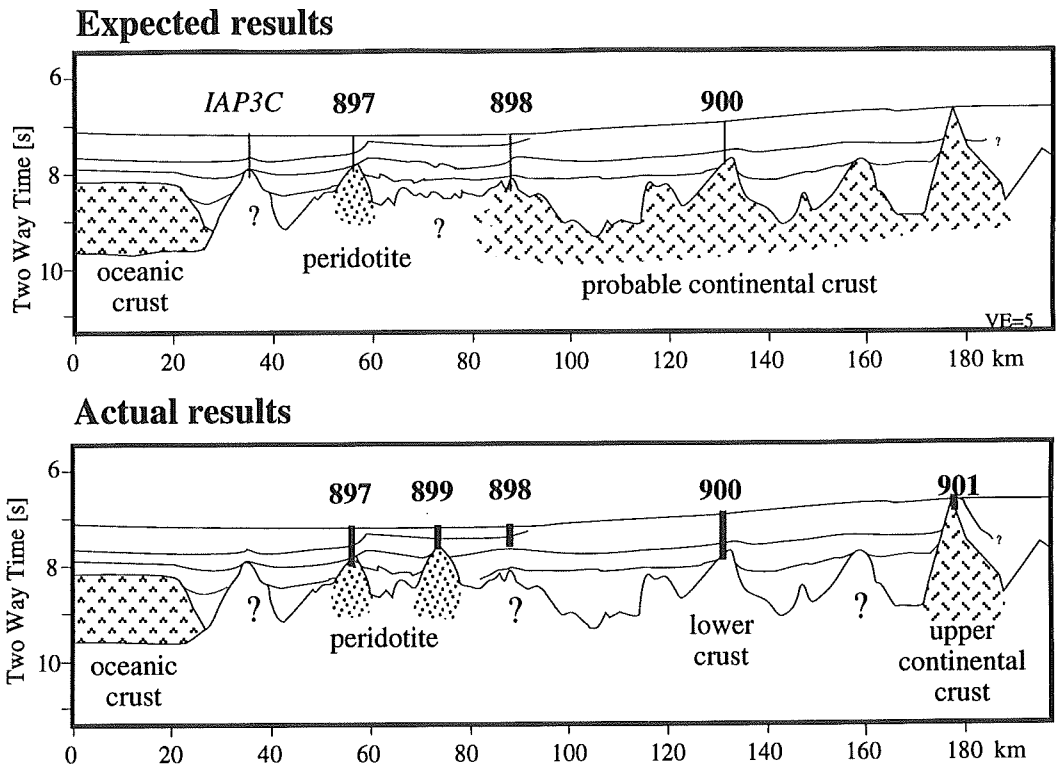

Figure 5.2: Predicted and actual drilling results from ODP Leg 149 (after Sawyer, Whitmarsh et al., 1993) with special emphasis on basement rocktype. From west to east this transect sampled in Sites 897 and 899 peridotitic basement, and lower crust in Site 900 (metamorphosed, mafic igneous rocks); Site 901 cored Tithonian sediments interpreted as pre-rift, so that basement here is very likely upper continental crust.

5.2.2 Aims

To provide a framework for the interpretation of the drilling results, the reflection seismic profile Lusigal 12 (LG12) was subject of reprocessing and intense analyses. As it crosses three of the Leg 149 drill sites, a correlation between results from drilling and seismic investigation is possible constraining the evolution of this margin in particular, and the mechanism of continental break-up in general.

Furthermore, having carried out a similar analysis in the north (see

Chapter 3), the opportunity exists to compare the results from the Iberia Abyssal Plain with those of the west Galicia Bank rifted margin. The presence of peridotitic basement on the Galicia margin (Boillot, Winterer, Meyer et al., 1987) marking the OCT indicates that the two margins have certain similarities, although the distance between peridotite and the first subcrop of upper continental basement is considerably smaller off the Galicia Bank (Beslier et al., 1993). There it has been shown that rifting leading to break-up was controlled by a detachment fault, the S reflector (Wernicke & Burchfiel, 1982; Reston et al., 1995; Krawczyk & Reston, 1995 - see also Chapter 3). Although no such detachment fault has been identified along the Leg 149 drilling transect before the beginning of the investigations carried out for this study, it is possible that detachment faulting played an important role in the evolution of the IAP margin as shown below.

To further constrain the nature of the key structures found, secondary aims like analysis of geophysical attributes were included. Thus the polarity, the reflection coefficient, and the internal structure of the main feature were also examined.

5.3 Seismic Data

The processed multichannel reflection seismic profile Lusigal 12 discussed here (for location see Figure 5.1) was acquired during the Lusigal campaign in 1990 under the leadership of the GEMCO working-group in Villefranche (chief scientist G. Boillot).

The source used for the LG series was an array of 8 waterguns (shot interval 50 m). A 2.4 km, 96 channel streamer (group interval 25 m) was used, resulting in a CMP interval of 12.5 metres. Profile LG12 was recorded from west to east normal to the Iberia passive margin and to the main structures, and so has been successfully time- and depth-migrated.

The standard processing of line LG12 followed the scheme described in Chapter 2 of this study. Here, it is pointed out that particular care was taken to retain steeply dipping reflections, as this profile is dominated by the basement topography. For instance, in the time migrated section (Figure 5.3), neither trace mixing nor trace summation were applied, and fk filter was applied only locally. Also dip-moveout was corrected prior to final velocity analysis, in order to improve the image of steep events on the stack section. As will be seen below, imaging of steep events greatly facilitates interpretation of the data.

Another aim of the processing was the depth-migration of the data, to reveal the true geometry and geometrical relationships of key structures for the first time in depth. Analysis of depth-focussing errors (Denelle et al., 1986) during prestack depth migration is the basic tool to create a detailed velocity model (see section 2.3 for explanation). As this technique is very expensive in terms of computer time, it was applied only to the most important parts of the seismic profile covering the drill locations from ODP Leg 149 at the outer and central basement highs of this section (Figure 5.2). With the resultant velocity information, a velocity model across the whole transect was constructed (Figure 5.4) for depth migration after stack.

This processing yields a depth migrated section, which images the geological structures with their true geometry, and results in a detailed velocity model. This model not only allows the correct migration of the data, but strongly constrains the lithologies present.

5.4 Results

The multichannel seismic reflection profile Lusigal 12 (LG12) covers part of the drilled transect across the ocean-continent transition (OCT) in the Iberia Abyssal Plain (see Figure 5.1 for location). The extreme ends of the analysed section (Figure 5.3) are marked by two basement highs corresponding to Sites 898 and 901, whereas the central high is at the location of Site 900, which sampled basement on ODP Leg 149 (Sawyer, Whitmarsh, Klaus et al., 1994).

Drilling at Site 901 encountered pre-rift sediment of Tithonian age, whereas at Site 900 highly sheared and deformed gabbro was sampled (Figure 5.2), which probably represents lower continental crust or material underplated during rifting (Krawczyk et al., 1994). Site 898 did not reach basement, but at Sites 897 and 899 further to the west, samples of serpentinised peridotite proved the existence of a mantle ridge marking the OCT. Thus, drilling points to a general deepening of lithospheric level from east to west along the drilled transect (and the seismic reflection data), sampling from east to west upper crust (Site 901), lower crust (Site 900) and mantle material (Sites 897, 899).

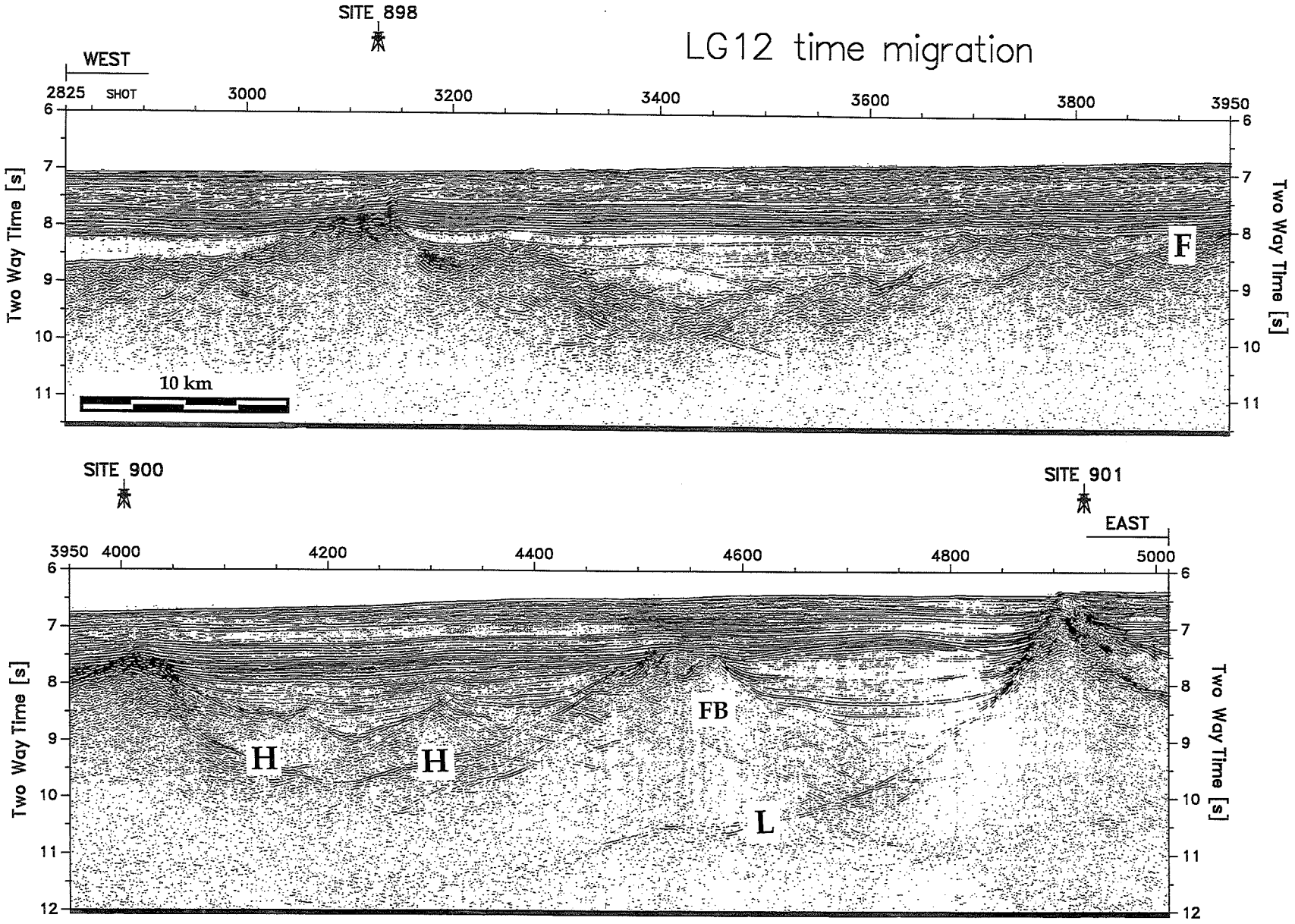

Figure 5.3: Time migrated seismic section of profile LG 12 covering from west to east ODP Leg 149 drill Sites 898-901 (50 m shot spacing). Interpretations, based on the depth section in Figure 5.8 are presented in Figures 5.16, 5.19 and 5.20. Note the detachment fault H, the listric fault structure L, and the low-angle fault F; FB-fault block.

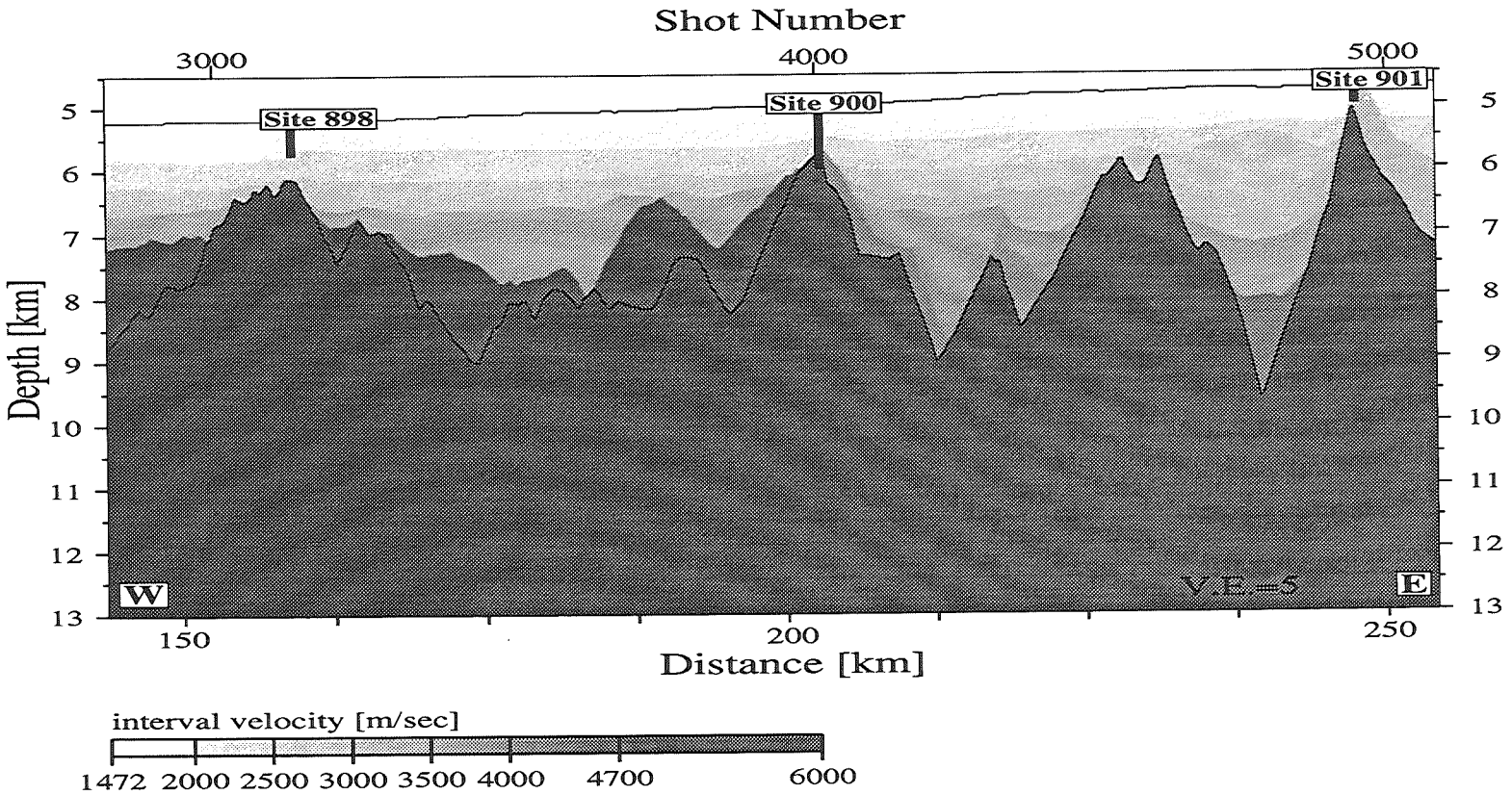

Figure 5.4: Velocity model of profile Lusigal 12 between Sites 898 and 901 derived from iterative prestack depth migration. The model allows the following units to be identified: basement (Vp 5.5 km/sec), post-rift (Vp 1.7-3.1 km/sec), syn-rift (Vp 3.2-4 km/sec) and pre-rift (Vp 4.1-4.7 km/sec) sediments capping the tilted block at Site 901, where pre-rift sediments of Tithonian age had been drilled (Shipboard Scientific Party, 1994c), and probably east of Site 900. Figures 5.5, 5.6and 5.11 show the model in more detail next to the drill sites.

5.4.1 Sediment Sequences

Between Sites 898 and 900, the post-rift sequence on the western part of profile LG12 exhibits a pattern of low-angle apparently westward inclined reflections, attributable to a progradational sequence (Figure 5.3). These are unconformably overlain by a sequence of mainly terrigeneous turbidites (Shipboard Scientific Party, 1994a). This unconformity (at Site 898 at 7.5 sec TWT depth and 750 mbsf) is correlated with a 10 Ma hiatus from middle Miocene to late Pliocene, and may be related to gentle regional deformation during the northwest-southeast compressional phase of the Rif-Betic Mountains in southern Spain and North-Africa. East of Site 900 the westerly inclined reflections are no longer imaged, and the post-rift sequence shows except for two places a regular and subparallel bedding; thickness varies from 750 to 2500 m, and interval velocities are not higher than 3.1 km/sec (Figure 5.4). Two mounded units east of Site 900 may represent contourites: one is a large sediment ridge extending over 14 km between shots 4600-4875, the other is a minor one between shots 4950-5025 (Figure 5.3). The break-up unconformity marks the lower boundary of a seismic more transparent sedimentary sequence and separates post-rift from syn-rift sediment or basement.

In the eastern part of the profile (shots 4000-4450, directly to the east of Site 900) thin sedimentary sequences of possible late syn-rift age overlie landward-tilted wedge-shaped units of early syn-rift sediments (Vp 4.1 km/sec). Further syn-rift deposits may be interpreted on top of the basement high between Site 901 and 900 (Figure 5.5) as well as east of it (Figure 5.6), all characterised by interval velocities between 3.2 - 4 km/sec (Figures 5.5, 5.6).

The only place where presumed pre-rift sediments are identified is where these were sampled by drilling (Shipboard Scientific Party, 1994c), i.e. at Site 901 at the eastern end of the profile. Here, the seismic section displays a more transparent layer of Tithonian strata tilted after deposition (Figure 5.7). The thickness of the different sequences varies from at maximum 3 km for the post-rift sediments to c. 1.75 km for syn-rift, and less than 1 km for the pre-rift sequence (Figure 5.8).

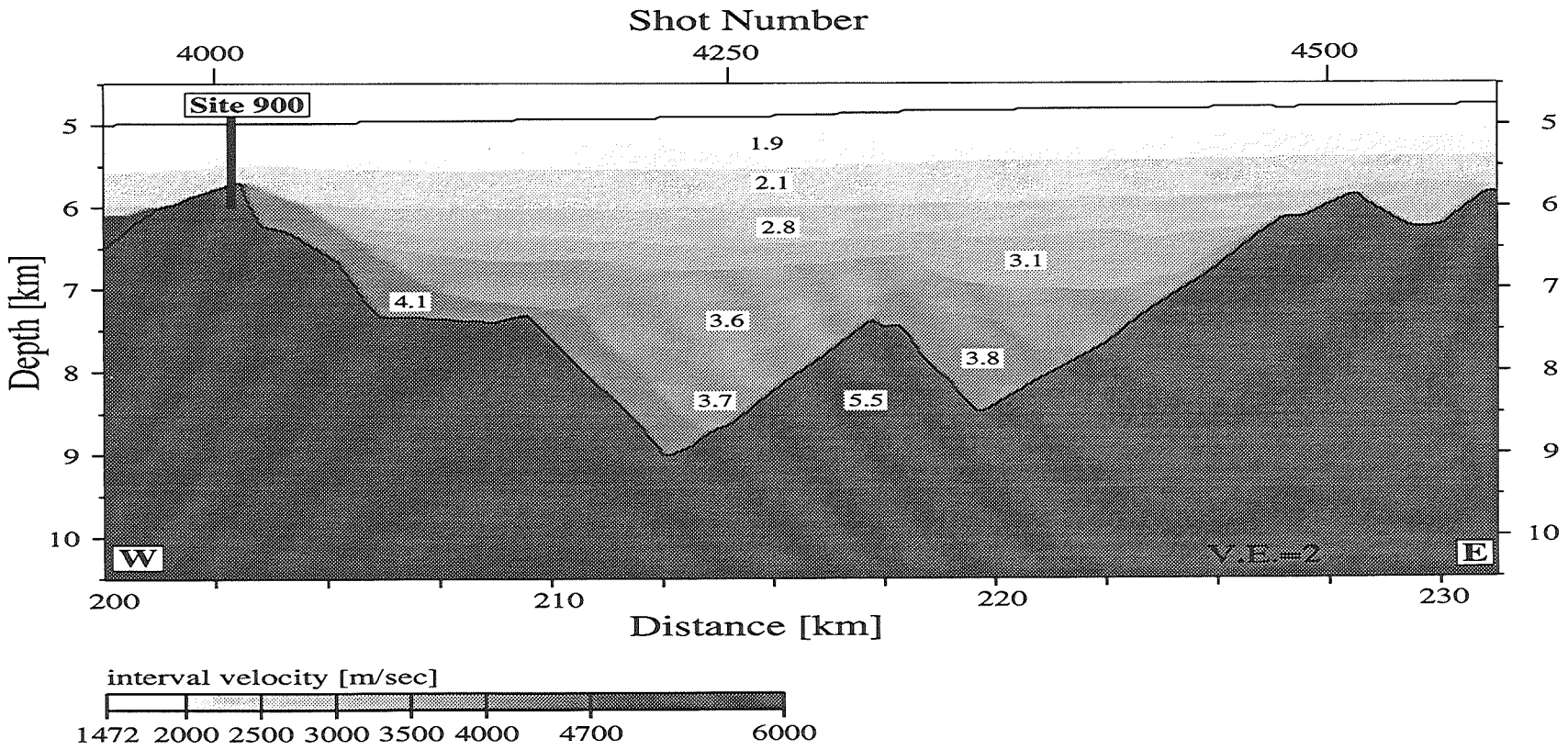

Figure 5.5: Interval velocities on profile Lusigal 12 east of Site 900 derived from iterative prestack depth migration. The different sedimentary sequences are clearly discernible by the velocities. The wedge-shaped sequences on top of the continentalward tilted blocks are interpreted as syn- and/or pre-rift. Sediments show velocities between 1.7 and 4.7 km/sec: Vp 1.7-3.1 km/sec for post-rift, Vp 3.2-4 km/sec for syn-rift, and Vp 4.1-4.7 km/sec for pre-rift sediments on top of the basement (Vp 5.5 km/sec).

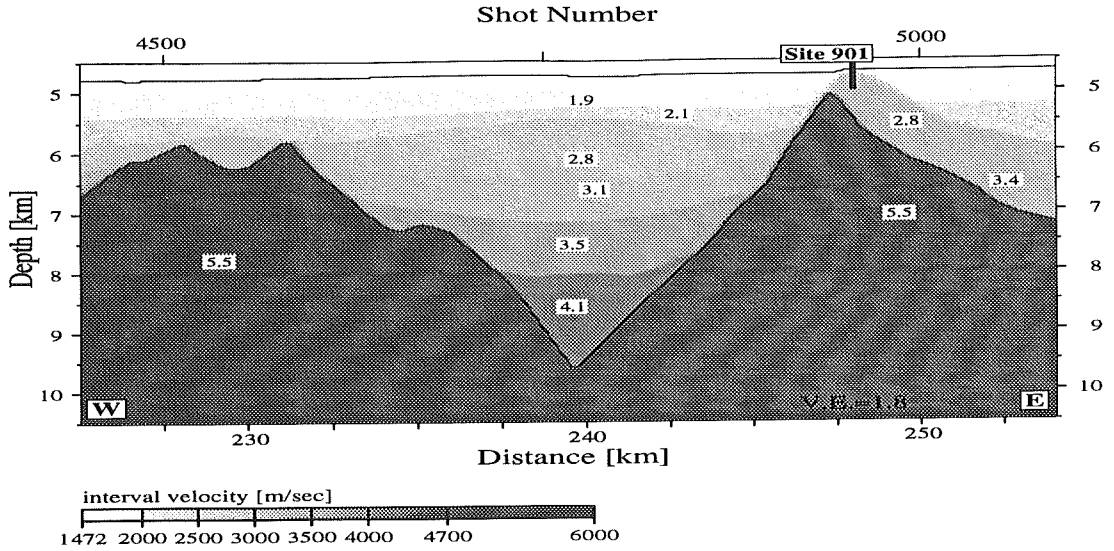

Figure 5.6 Velocity model of line LG 12 next to Site 901 from prestack depth migration. Sediment velocities increase (Vp 1.7-4.1 km/sec) from shallow to deeper levels, and those sampled on top of the tilted block (Vp basement 5.5 km/sec) are most likely of pre-rift age (Shipboard Scientific Party, 1994c).

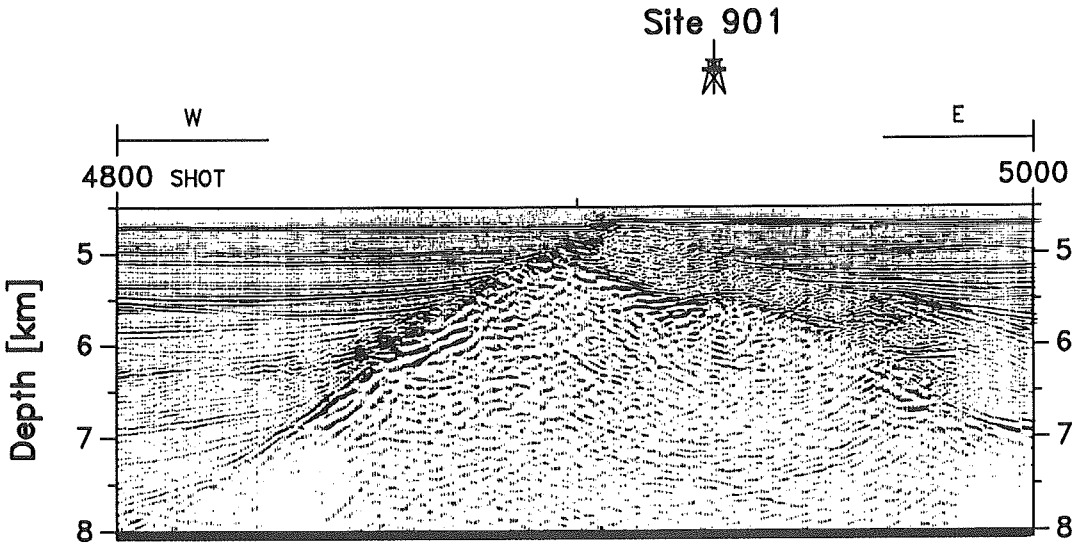

Figure 5.7 Seismic section at Site 901 migrated before stack with the velocity model shown in Figure 5.6. This basement high represents the most westward tilted crustal block drilled on this transect across the transition between oceanic and continental crust off the Iberian rifted margin. It is capped conformably by pre-rift sediments of Tithonian age (Shipboard Scientific Party, 1994c).

5.4.2 Basement Structures

It is within the basement that the profile images the most striking features relevant for discussing the transition between continental and oceanic crust and the mechanism of lithospheric extension on the IAP segment of the Iberian passive margin (Figure 5.8). Of particular importance are strong basement reflections imaged between Site 900 and Site 901 (Krawczyk et al., 1994). Other basement reflections east of Site 900 may also be important, but are less easily interpreted.

The easternmost high on LG12 appears to be a tilted fault block, capped by a 450-750 m thick seismically transparent layer of pre-rift or pre-tilting sediment (Figure 5.7). The basement itself exhibits velocities of 5.5 to 6 km/sec, whereas within the tilted sedimentary layer the velocity values between 2.8 - 3.4 km/sec are relatively low compared to approximately 4.1 km/sec close to Site 900 (Figures 5.5, 5.6). One reason may be the higher degree of probable basement fragments mixed with the directly overlying sediment during continued extension at Site 900, and a different lithology, described here as mud dominated clay and silty clay (Shipboard Scientific Party, 1994c). It is however also possible that this sequence is less compacted than the more deeply buried units to the west.

500 m west of drill location 901, the seafloor is marked by a 100 m high fault scarp (Figure 5.3). This is the surface expression of a fault forming the western side of the large fault block drilled at Site 901. The fault can be followed to depth as a bright reflection (L) between shotpoints 4400 and 4900, a distance of almost 25 km (Figure 5.8). L appears on the time section (Figure 5.3) to be a listric structure, flattening beneath the fault block (labelled here FB) immediately to the west of Site 901. Thus L is clearly a major structure, and probably controlled extension leading to break-up for this part of the transect. West of shotpoint 4400 L becomes hard to follow.

The east flank of the high between 901 and 900 (fault block FB) does not show many structures, but its central upper part appears faulted and may contain a small basin with up to 750 m of probably syn-rift sediment (Figure 5.8). More pronounced are the reflections between Site 900 and the basement high FB. West-dipping to sub-horizontal reflections (shotpoints 4075-4325) bound landward thickening wedge-shaped blocks, interpreted as strongly tilted fault blocks, overlain by landward-thickening wedges of sediments, interpreted as syn-rift. These reflectors end at the level of another bright

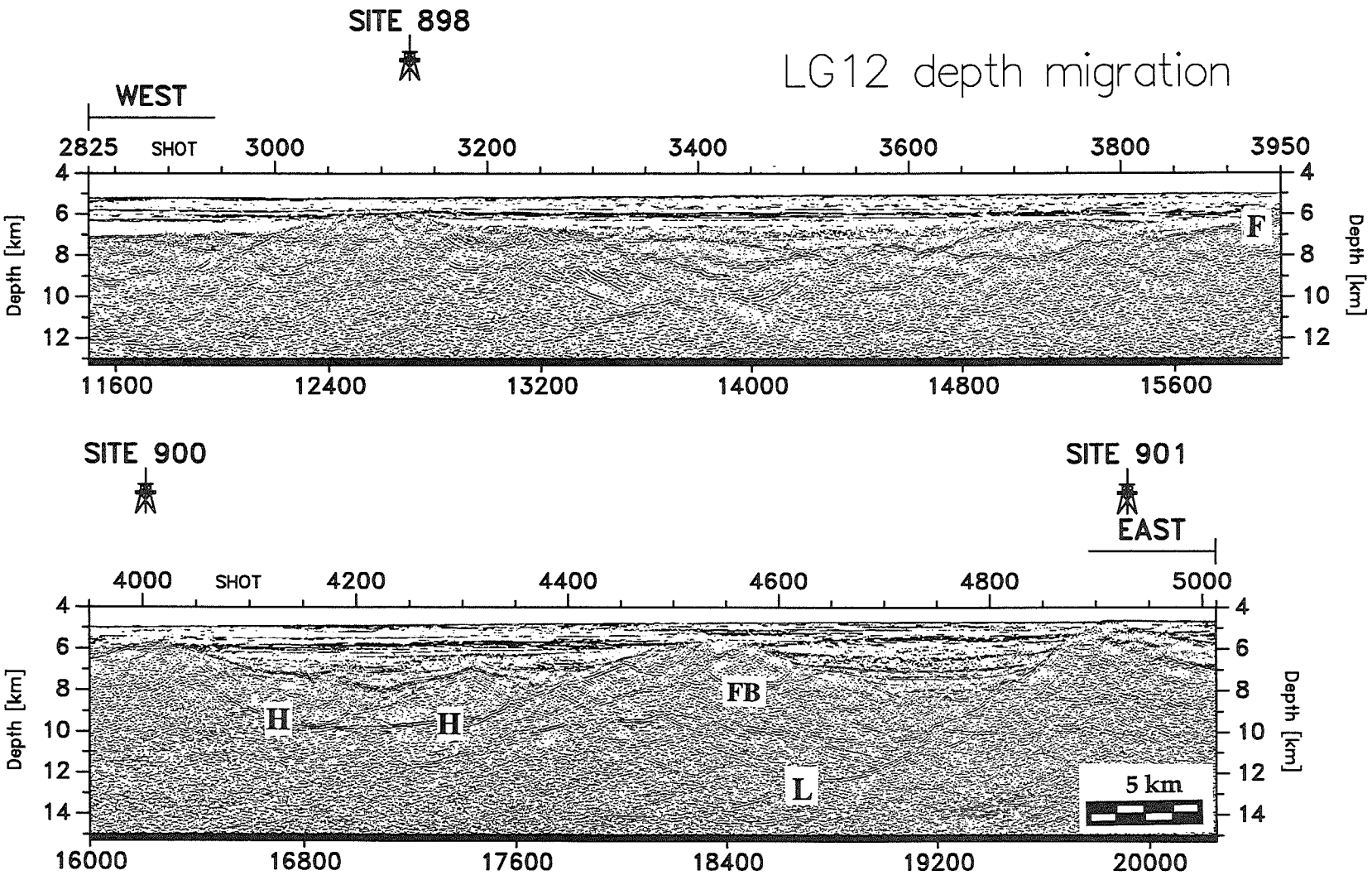

Figure 5.8: Depth-migrated section of profile LG12 between Sites 898 and 901 drilled during ODP Leg 149 (50m shotspacing, no VE). Strong reflections in the basement characterise this segment of the Iberian passive margin, showing different fault structures (H, L, F) of various dips; FB-fault block. For details see Figures 5.6, 5.11 and 5.16.

reflection (H), which extends between shots 4025-4425 at a depth ranging between 6-10 km. H cuts down from FB with an oceanward dip, but flattens, turns and cuts up towards the top of the Site 900 high as a band of strong, eastward dipping reflections.

The observation of landward tilted, wedge-shaped blocks overlying H is more pronounced on the detailed prestack depth migrated section (Figure 5.9). This section reveals furthermore, that the normal faults separating the blocks stop at the underlying reflector, thus appear to detach onto it. Therefore, H may be interpreted as detachment fault. The tilted blocks are identified by the interval velocities (Figure 5.5) to consist of basement covered by wedge-shaped sediment sequences thickening towards the block bounding faults.

Evidence for the presence of lower crustal material and H itself on top of the basement high of Site 900 is provided besides the velocity model (Figure 5.5) by the detailed seismic image from iterative prestack depth migration (Figure 5.10). H can clearly be followed from 9 km depth to the top of the fault block at 6 km depth, approaching the basement surface slightly east from the drilled position. There, it is probably overlain by early syn-rift sediments, and most likely the lower plate to H was drilled at Site 900. This is supported by the heavily sheared and fractured structure of the analysed samples (Shipboard Scientific Party, 1994b). The nature of H is discussed further below.

An alternation of small highs and basins within the basement topography appears west of Site 900 between shotpoints 2825-3900, also imaging some intra-crustal reflections with various dips (Figure 5.3). Between shotpoints 3300-3800 the seismic section exhibits three irregular lens-shaped features, each of them extending approximately 10 km along the profile. These are tentatively identified as basement, perhaps highly fractured, with a consistent interval velocity of 4.7 km/sec, and are clearly separated from the overlying sediment sequences with a maximum velocity of 3.5 km/sec (Figure 5.11).

In this western part of line LG12, deep reflections of various dip directions are also apparent (Figure 5.8). Cutting down from Site 900 towards the west, a reflection (labelled here F) deepens between shotpoints 3700-4000 from 6 km at Site 900 to at least 9km depth, but cannot be followed clearly further oceanward below the next basement block. The basement high next to Site 900 marks the proposed drill location IAP7 (shotpoint 3775; Reston et al., 1994). The major reflector below the IAP7 basement block to the west of Site 900 may be possibly the same structure as the H reflector east of it, as will be discussed further below.

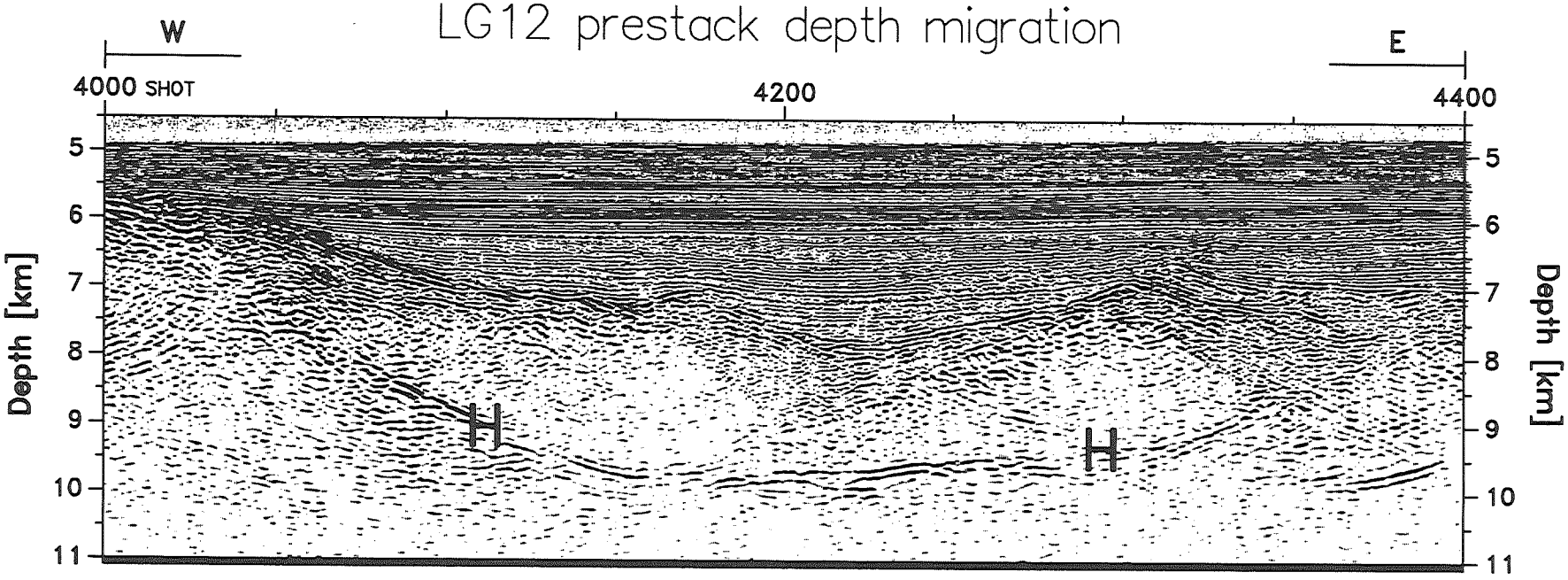

Figure 5.9: Prestack depth migrated seismic section east of Site 900, converted with the velocity model shown in Figure 5.5. The continentalward tilted blocks are separated by normal faults stopping at the underlying reflector H, which is therefore interpreted as detachment fault subcropping near Site 900. Wedge-shaped sedimentary sequences thicken towards the block-bounding faults and can clearly be identified as syn- and/or pre-rift sediments as also indicated by the changes in velocity. Above, the post-rift sequence shows regular and subparallel bedding.

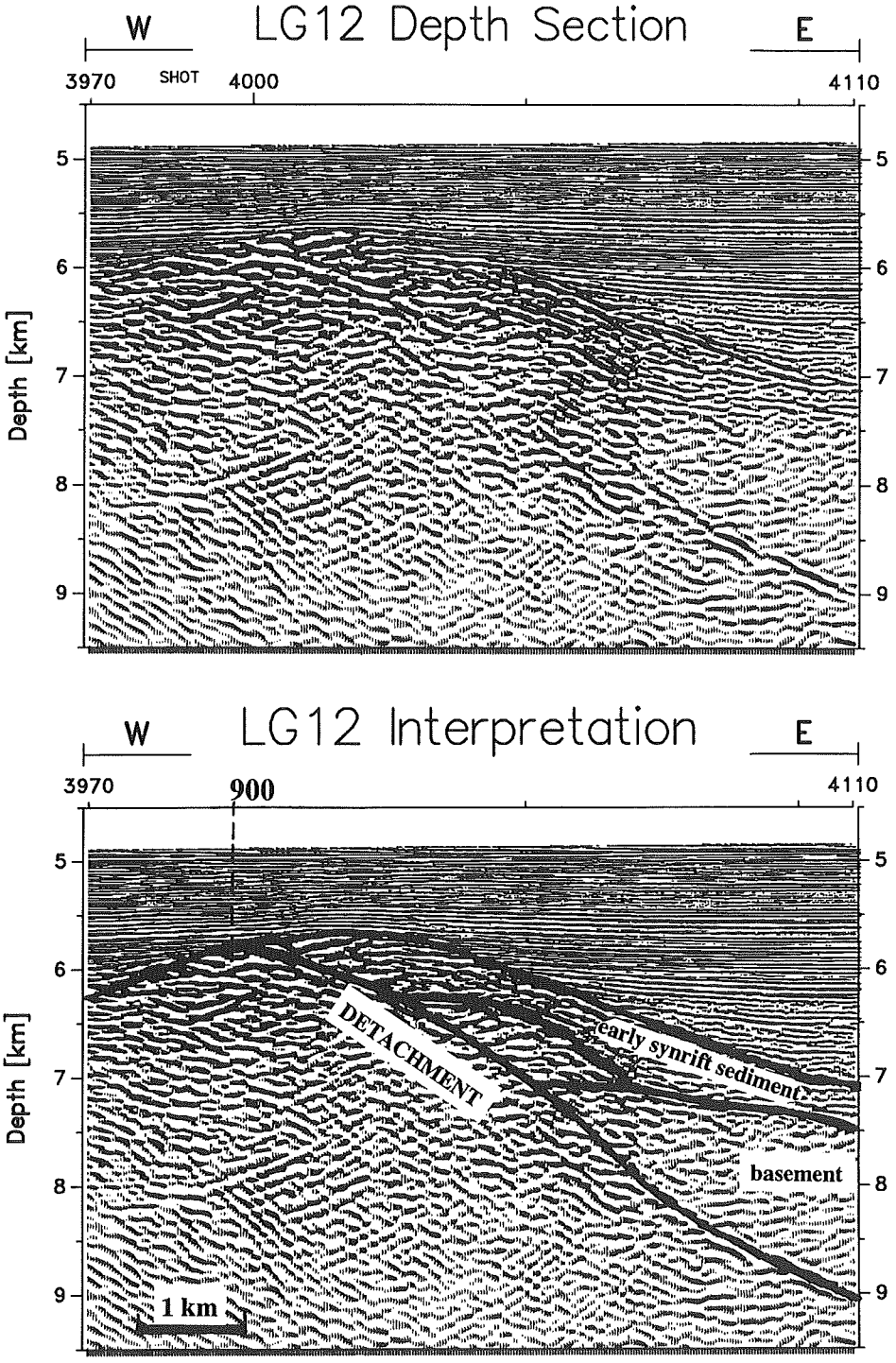

Figure 5.10: Detailed seismic depth section, migrated before stack, and its interpretation at Site 900. The probable detachment fault H subcrops just east of Site 900, which sampled highly deformed, amphibolite grade gabbro with shear structures between 10-40 degrees. The detachment is overlain by a small lens of crustal rocks (Vp > 5 km/sec), which is covered by probable early syn-rift sediment (Vp 4.1 km/sec).

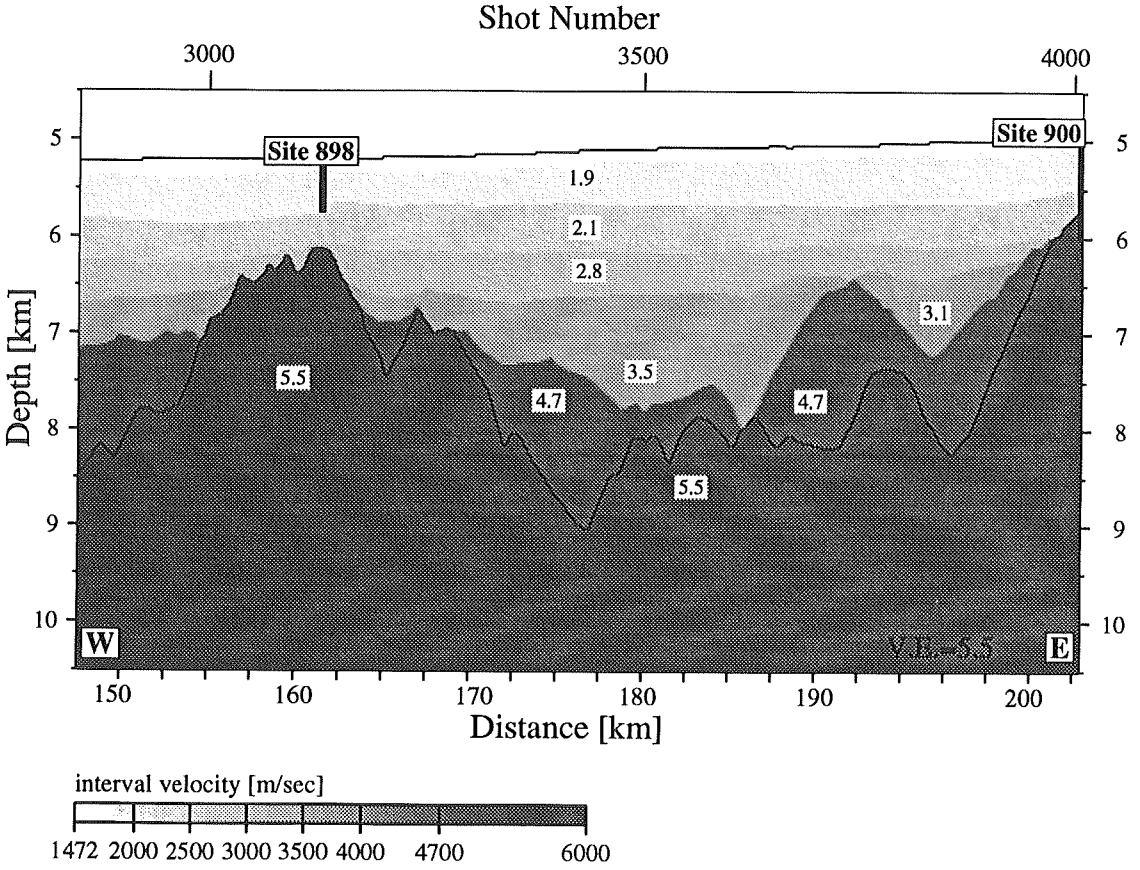

Figure 5.11: Velocity model of profile Lusigal 12 between Sites 898 and 900 after prestack depth migration: sediment velocities are below 4.7 km/sec, velocities higher than 5.5 km/sec characterise basement. Basement topography exhibits small highs and lows, covered by thick packages with a velocity of 4.7 km/sec extending over a range of 40 km on top the basement .

Three basement reflections with eastward dip direction are imaged approximately 2-10 km east of Site 898 (shotpoints 3150-3300, 3250-3350 and 3300-3500), extending landward from the top of the basement down to 10 km depth (Figure 5.8). These may be extensional structures accomodating top-to-the-east shear, and perhaps postdate structure H.

Drilling Site 898 did not reach basement so that this location is mainly described by geophysical investigations. The seismic image here shows an irregular surface and a series of small, oceanward dipping fault structures cutting into the upper 750 m of this basement high (Figure 5.8). From here to

the western end of the investigated seismic section of profile LG12, the basement deepens in three steps further oceanward to 9 km depth, and again, the velocity function runs from 1.9 to 3.5 km/sec within the sediment sequences to 4.7 and 5.5 km/sec within the basement (Figure 5.11).

5.4.3 Nature of the H Reflector

Estimation of the reflection coefficient R and analysis of the waveform of the bright crustal structure H (Figures 5.3, 5.9) provides additional information about the nature of the investigated structure shown to subcrop close to Site 900 (Figure 5.10). With the calibration method adapted from Warner (1990), the reflection coefficient of the seafloor is c. 0.22 (±0.03), which lies within the range for a soft waterbottom in deep water.

As this calibration (see section 2.3 for explanation) assumes reflections from simple interfaces and not from series of thin layers or other more complex structures, the reflection from the seabed was compared to that of its first multiple. The detailed image (Figure 5.12) reveals the waveform of the seabed for 16 CMPs, a distance of 200 m. The traces show a wavelet of 100 msec length, which consists of a small positive event (black), followed by a larger negative (gray) amplitude; the maximum amplitude (positive) is reached at 6.725 s TWT, again followed by a negative and a small positive amplitude. Flipping the waveform of the first multiple of the seafloor (by multiplying it by -1) provides a remarkably similar succession of positive and negative amplitudes (Figure 5.12). Thus, the waveforms of both the seafloor reflection and its first multiple are almost identical, pointing to an origin from a single interface.

Having calibrated the system, the ratio of the maximum amplitude of the H reflector and the seafloor, both determined after correction for geometrical spreading and picked from the envelope functions, gives the first estimate of the reflection coefficient of H of approximately 0.12. Allowing for anelastic attenuation and transmission losses, this value would increase to c. 0.15. This should be considered only as a very rough estimate, because this calculation assumes the Q factors determined by Boillot and others (1995b) in the area of the Galicia Bank margin. These authors define in the upper post-rift sediments a value of 10, increasing to 600 down towards the basement. Although this value may not be exactly correct for this area, it is used to provide a first estimate and the order of the reflection coefficient from H. With

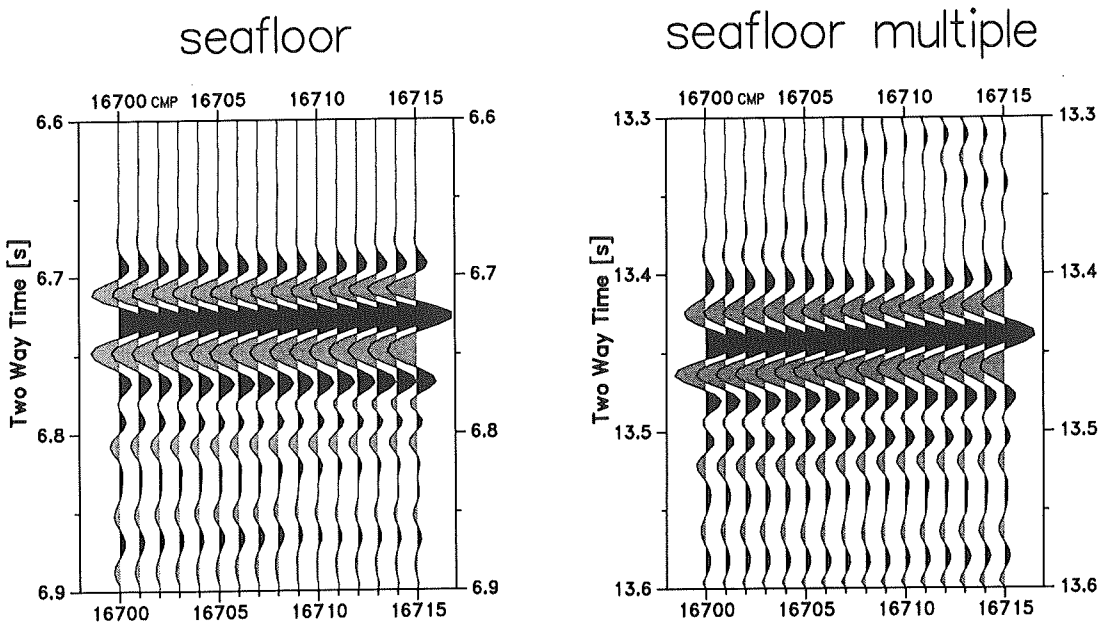

Figure 5.12: Waveform of the seafloor reflection in comparison with that of its first multiple (flipped) from profile LG12 showing that the waveforms are almost identical. Thus, the seafloor reflection represents a reflection from a single interface.

a value of about 0.15, H represents a strong intra-crustal reflection with a sharp increase in acoustic impedance.

The nature of H is further revealed by the comparison of its waveform with that of the seafloor (Figure 5.13), analysed for the same portion of data as for the analyses shown in Figure 5.12. The waveform of H exhibits almost the same succession of amplitudes as that of the seabed: a small positive and a larger negative preceed the maximum positive amplitude, followed again by a smaller negative and finally a positive amplitude. Although H is characterised by a gentle dip, its waveform is correlatable along all traces, and the small amplitudes are clearly distinguishable from the surrounding noise (Figure 5.13). Furthermore, each wavelet begins with a positive amplitude, even though on the first three traces inflections are present just prior to the onset of

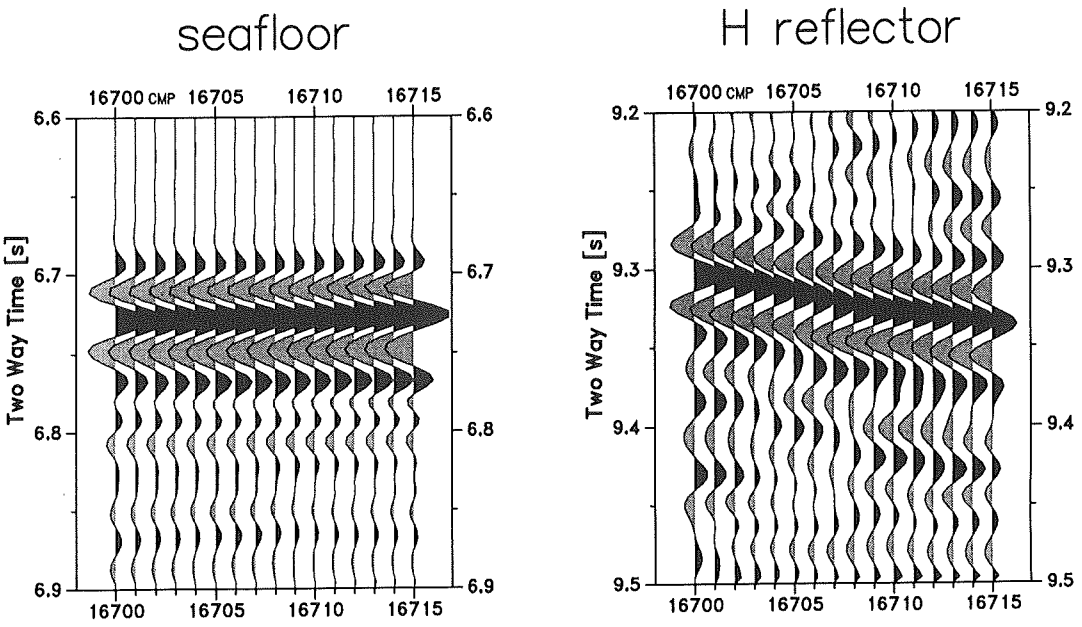

Figure 5.13: Comparison of H and seafloor reflection. Again, the waveforms are almost identical, in other words: H has the same polarity as the seafloor (it is positive), and probably represents a reflection from a single interface. H is perhaps the tectonic contact between tilted upper crustal blocks in the upper plate and a lower plate with higher velocity and density.

the wavelet of reflection H. This demonstrates that H has a consistent waveform, and that it is a positive polarity event like the seafloor. Furthermore, as it is known from the comparison of the seabed and its multiple that the seafloor marks a first order discontinuity, and the waveforms of the seabed and H are virtually the same (Figure 5.13), H is almost certainly a reflection from a single interface and not a thin layer or a series of thin layers.

It seems thus likely, that H marks a tectonic boundary, which separates an upper plate (with tilted blocks of upper crustal rocks - Figure 5.9) from a lower plate of higher velocity and density (the lower plate may be lower continental crust or mantle). Hence, the interpretation of H is consistent with a sharp boundary of some form and not with that of a transition zone. This constraint

coupled with the observation that the faults bounding the wedge-shaped blocks appear to detach onto H (Figure 5.9) implies that H is a detachment fault, separating a faulted upper plate from a higher velocity and density lower plate.

5.4.4 Synthetic Modeling

To test the velocity model generated by prestack depth migration, a synthetic section was calculated in the part of profile LG12, where the structure H had been identified within the basement (Figure 5.3). The basement high at shotpoint 4000 represents the drilled Site 900, and H appears to approach the basement surface close to the site. Further to the east, H is overlain by tilted blocks (Figure 5.9), identified by their velocities as basement (Figure 5.4).

The synthetic time section (Figure 5.14), created with the steps described in section 2.4, exhibits large diffraction hyperbolas of various dips from top of the basement and from interfaces within the basement. The sediment boundaries show regular and subparallel reflections, which can be correlated with reflections imaged on the near offset stack (Figure 5.15).

Whereas two large hyperbolas dominate the synthetic section between shotpoints 4100-4300 and 4200-4473, the corresponding segment of the near trace stack shows only few if any diffractions. The bright hyperbolas interfere on the synthetic so much that structure H, already only weakly imaged on the near trace stack, is covered here completely, except between shots 4050-4175. In this area, both stack and synthetics exhibit the H reflector. From shotpoint 4175 towards the east, H is traced more tentatively and gets covered again.

Good correlation is possible for the hyperbolas cutting down from the basement high at Site 900 at shotpoint 4000. The near offset stack reveals steeply dipping branches down to almost 12 sec TWT (Figure 5.15), also generated by the velocity model (Figure 5.14). Even the structures representing H close to the top of the basement coincide, but get less pronounced or disappear further to the east. The steeply dipping velocity interface on the east flank of Site 900, separating sediment from basement (compare Figure 5.4), correlates on both seismic sections.

This comparison reveals that the velocity interfaces produced by iterative prestack depth migration generate in the synthetic model much larger effects than imaged in the observed data. This is the case in especially in places, where an interface separates sequences with strong velocity contrasts, such as top

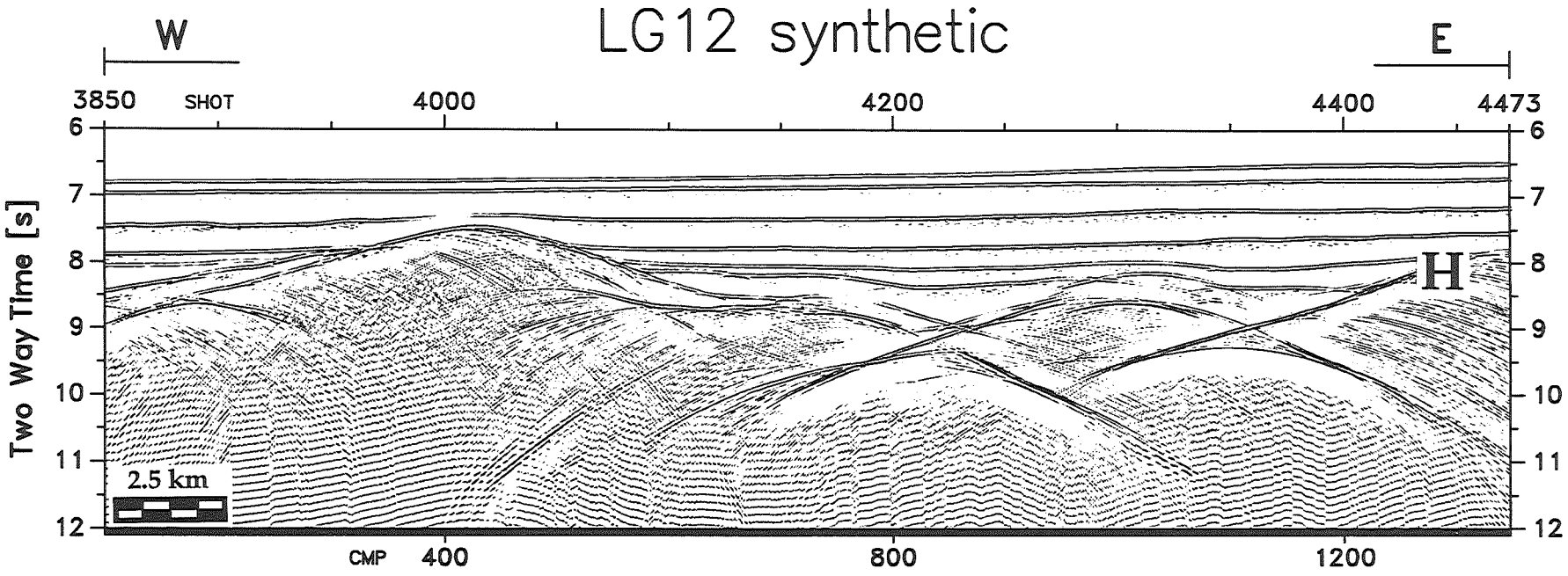

Figure 5.14: Synthetic time section of profile LG12 in the area of reflector H east of Site 900, derived from the velocity model shown in Figure 5.13. The seabed reflection and those from the sedimentary horizons appear as strong, undisturbed reflections. The top of the basement and inner basement velocity interfaces produce large diffraction hyperbolas of various dips.

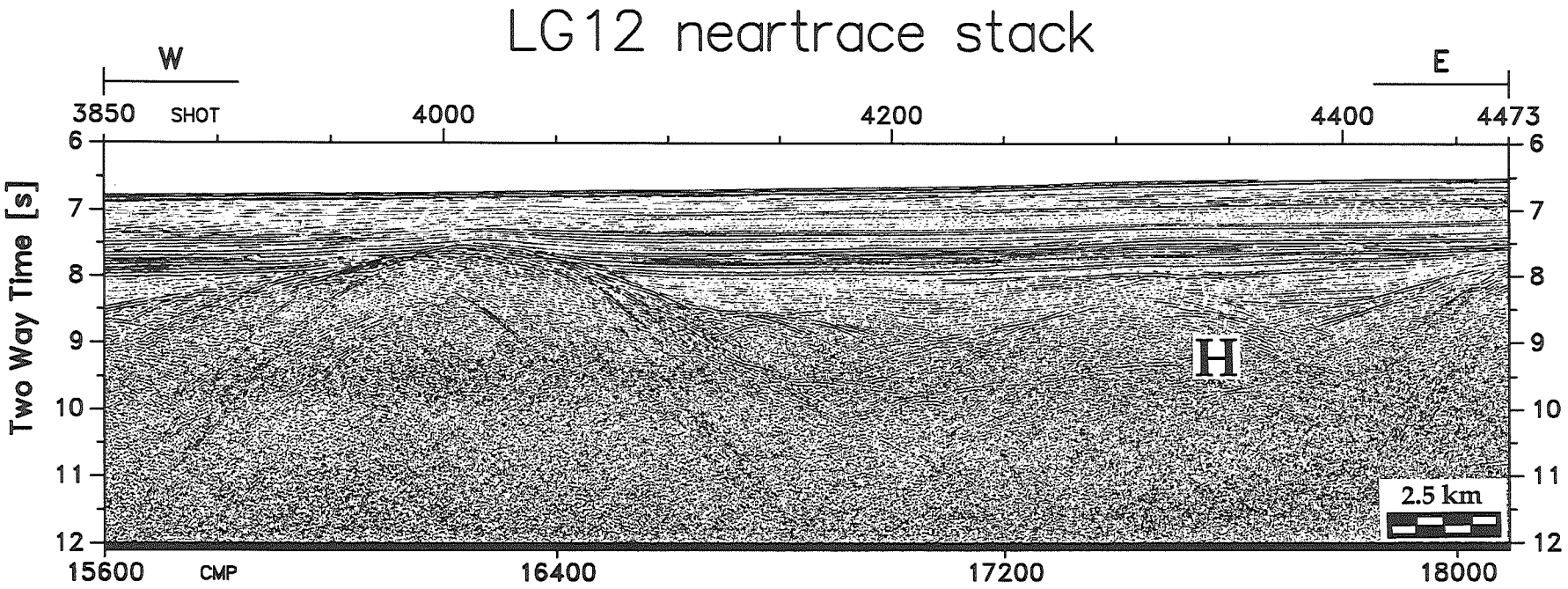

Figure 5.15: Near-trace stack of profile LG12 covering the same area as the synthetic seismogramm in Figure 5.14. The sediment interfaces are clearly correlatable to those in the synthetics. The diffraction hyperbolas at the basement reflections are pronounced in the western part of this section, the eastern half is more dominated by noise.

basement and within sediments. Such boundaries may be more gradational than implied by the velocity analyses. This difference between synthetic and observed data hence implies that the model applied is too simple. Nevertheless, this will not affect the results as long as the model is roughly correct (Versteeg, 1993). The seismic section images bright subsurface structures, but without doubt not all existing ones, as nature is far more complex than is possible to describe within a single model. Because the top of basement underwent metamorphosis and diagenetic processes duing rifting and faulting, there the differences and uncertainties may be more obvious than in the sedimentary layers.

5.5 Interpretation

The complexity of the basement reflections allows several interpretations. Here, one interpretation is presented that is consistent with all the observations (geological and geophysical); other possible interpretations will be discussed in the following section.

From the seismic data, at least two phases of rifting can be inferred (Figure 5.16). First a detachment fault (H) accommodated top-to-the-west motion, accompanied by the development of the small oceanward-thickening, landward-tilted, wedge-shaped fault blocks riding on H: the wedge-shaped blocks between Site 900 and basement high FB (shots 4025-4425). These wedge-shaped blocks are bound by westward-dipping normal-fault structures that are synthetic to and detach onto H (Figure 5.9). During progressive extension and exhumation of the lower plate to H, the unloading of the lower plate to H caused this to bow up, as inferred for detachment faults in the western United States (Lister & Davis, 1989). This may have rendered at least part of H inactive.

The change of dip direction of structure H from west to east is however remarkable and hard to explain within a single phase of faulting. Instead it is inferred that this, and the overlying wedge-shaped blocks, were rotated during a later phase of faulting and extension. The most pronounced structure interpreted to have been active during this later phase is the bright L reflection, which cuts down from the easternmost tilted block (Site 901) and probably marks the lowermost boundary of the middle basement high (FB). On the depth migrated section (Figure 5.8), L appears approximately planar down to 12 km depth, where it appears to flatten into a deeper detachment level along

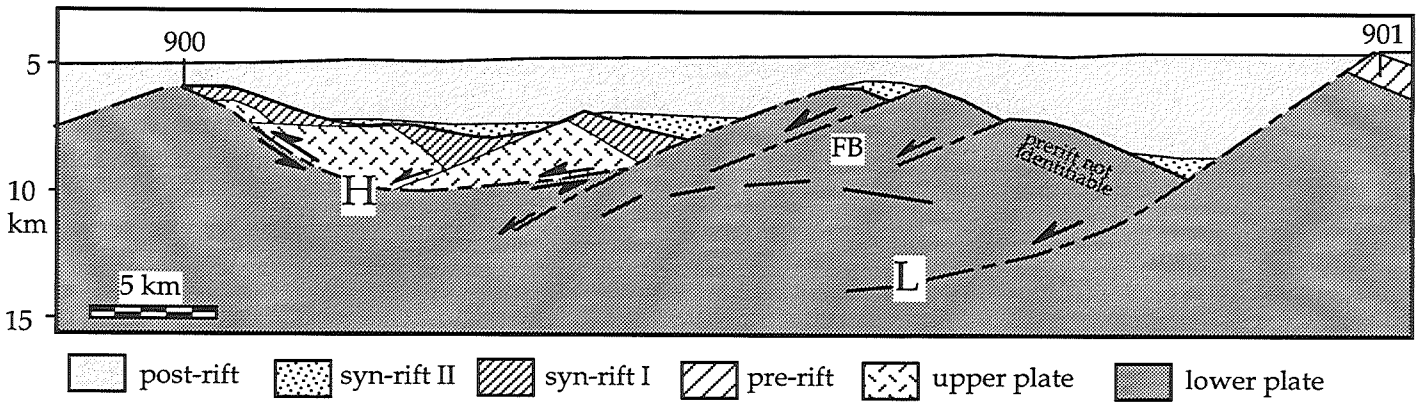

Figure 5.16: Interpretation of the depth section of profile LG12 between ODP Leg 149 Sites 900 and 901. The eastern basement high is capped by a seismic transparent layer of pre-rift/pre-tilting sediments. Further to the west, different tilted blocks are imaged. They are bound by fault structures (e.g. the listric strucure L) and a detachment (named here H), which developed during different phases of rifting: H developed during the syn-rift I stage accomodating top-to-the-west motion, and was subsequently cut and rotated by L during the syn-rift II stage. Backrotation of H first during syn-rift I and subsequently during syn-rift II explains its current orientation. H terminates at the top of the basement high 500 m east of the drilled Site 900 (see also Figures 5.9, 5.10). Wedge-shaped sedimentary sequences are either of early syn-rift/pre-rift or of syn-rift II age. Other interpretations possible are discussed later (see Figure 5.19).

which the continental block east of Site 900 moved to the west while tilting landwards (Figure 5.3). Other structures active at this time may include approximately planar faults bounding the western flanks of basement highs FB and 900, although these structures are less clearly imaged. Together, these faults would have formed an array of oceanward dipping faults, dissecting the original detachment system (H), and rotating the segments of that system landward.

Thus, one may identify a detachment fault, H, accommodating top-to-the-west motion, overlain by two wedge-shaped "horses" (Gibbs, 1984), and itself back-rotated both during the unloading of the footwall that accompanied extension, and also by later steeper faulting. This would require various phases of faulting during continental break-up in the IAP region.

Such an interpretation is supported by the results of ODP Leg 149 (Sawyer, Whitmarsh, Klaus et al., 1994 - see Figure 5.2). Site 897 confirmed a Peridotite Ridge between oceanic crust and the western end of the transition to continental crust. At Site 901, pre-rift or pre-tilting sediment of Tithonian age, capping conformably the westward most tilted crustal fault block, was drilled. This block is interpreted as thinned continental crust, because the overlying sediment is approximately 15 Ma older than the onset of seafloor spreading in this area (Whitmarsh & Miles, 1994) and is terrigeneous in nature (Shipboard Scientific Party, 1994c). Furthermore, as it is tilted within a fault block it must predate the movement along L and hence be either earlier syn-rift or even pre-rift sediment. This would also imply that the underlying basement is upper continental crust.

The third drilling location where basement was reached, Site 900, sampled amphibolite facies metamorphosed gabbro deformed at depths of 12-20 km (M.-O. Beslier, pers. comm.). Thus going from east to west, the basement appears to consist of upper crust, lower crust and upper mantle. Therefore it is conjectured that a cross-section through the upper lithosphere was exposed during the rifting process, probably by top-to-the-west motion along detachment H, and was subsequently dismembered by steeper normal faults.

A simple reconstruction based on the depth section presented in Figure 5.8 illustrates this interpretation further (Figure 5.17 - Reston et al., 1994). Assuming simple rigid block rotation for the restoration of the top of the fault blocks to the horizontal plane, the original geometry of the detachment can be reconstructed (Figure 5.17b). After restoration, H shows before block rotation a westerly dip in the eastern part of the section, flattens further to the west and

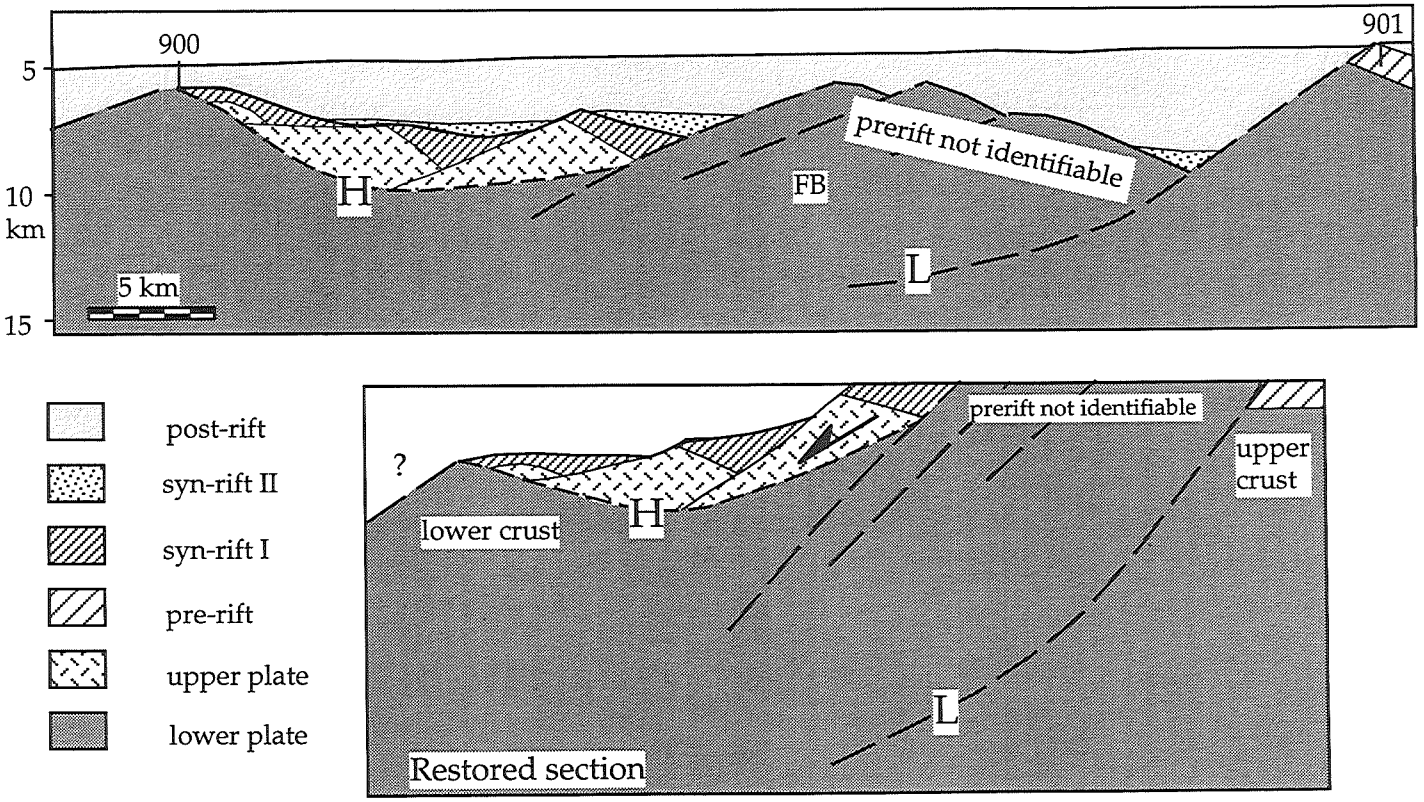

Figure 5.17: a) Interpreted depth section derived from prestack depth migration (Figure 5.16). Two phases of extension are identified: one related to detachment faulting along H, one related to subsequent block-faulting. b) Restoration of the section to its geometry when extension along the detachment H ceased. Detachment faulting probably brought lower crust closer to the surface at Site 900.

bows slightly up, perhaps because of unloading. The geometrical relationships reveal that detachment faulting may have exhumed lower continental crust at Site 900: the minimum distance to the possible detachment breakaway is c. 20 km, and the original fault dip may have a typical value of 45° (e.g. Wernicke & Axen, 1988). This results in a depth of approximately 15 km of the lower plate to the detachment before detachment faulting started, and hence Site 900 may have sampled lower crust.

The complex seismic image of the area west of Site 900 may also be differently interpreted (Figure 5.18). Between lower crust (Site 900) and serpentinised mantle material (found at Site 897, 27 km west of Site 898), the major and controlling structure may be a westward dipping low-angle normal fault corresponding to reflection F. It cuts down from 6 km at Site 900 to 9 km depth below the basement high IAP7, and extends over at least 15 km along the profile. F may represent on the west flank of Site 900 the same structure as H does on the east flank. If so, the basement high at IAP7 would be an upper-plate fault block to this master detachment, which accomodated extension by top-to-the-west motion.

As block-faulting or detachment structures are less pronounced, F may also have been later than H, perhaps coeval to L, in which case IAP7 would be part of the footwall to H. Within this scope, the Moho may lie nearby, and mantle material could be found at shallow levels. Finally, this basement high could represent a volcanic structure formed by magmatism accompanying break-up on the Iberian continental margin. Nevertheless this hypothesis seems rather unlikely because of the general absence of volcanism on this passive rifted margin and the local extent of this layer.

5.6 Discussion

It is generally accepted that north of the IAP, on the Galicia Bank margin, detachment faulting controlled continental break-up (e.g. Hoffmann & Reston, 1992). To focus on this interpretation, the discussion here concerns the differences and similarities between the structures of the IAP margin and those of the west Galicia rifted margin (see Chapters 3 and 4).

Reflection seismic profiles across the Galicia Bank passive margin image a series of fault-bound blocks tilted towards the continent. These have been shown by drill samples (Boillot, Winterer, Meyer et al., 1988) and subsequent sampling from diving (Boillot et al., 1988b) to consist of basement covered by

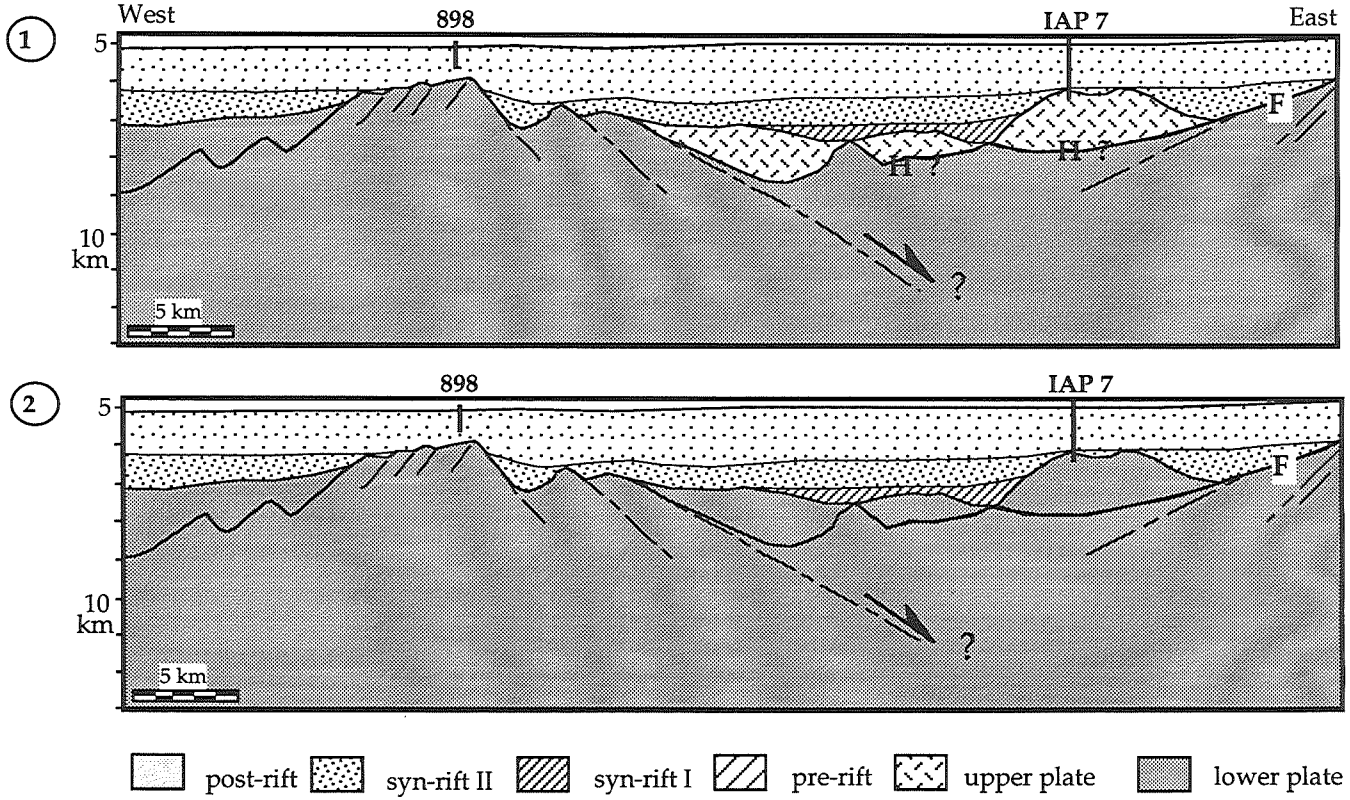

Figure 5.18: West of Site 900 basement topography is characterised by alternating, small-scale highs and basins between Sites 900 and 898, where the basement high is cut by a series of oceanward dipping normal faults. Thick lens-shaped sequences extend over a range of 40 km on top the basement with a velocity of 4.7 km/sec. Reflection F, cutting towards the west below the basement high IAP7 may be a low-angle normal-fault. F may either represent on the west flank of Site 900 the same structure as H east of it, or it may be a separated feature different to H. Therefore, the crustal block at IAP7 may either be an upper-plate or a lower-plate fault block to the master detachment H.

early syn-rift and pre-rift sediment. These fault blocks are underlain by the S reflector, a strong intra-crustal reflection interpreted as detachment fault (Wernicke & Burchfiel, 1982; Hoffmann & Reston, 1992). The block-bounding normal faults do not cut and offset S but instead appear to detach onto S, which is therefore probably a detachment fault, active at least in the late phase of rifting and continental break-up (Krawczyk & Reston, 1995).

The similarities between the IAP and Galicia Bank areas are obvious: both are characterised by extreme crustal thinning accomodated by block faulting above a detachment fault. In the Galicia Bank area the normal faults stop at the S reflector, which is therefore interpreted as a detachment fault. Parts of profile LG12 image similar fault blocks, bound by reflections that appear to detach onto a bright reflection (H). Thus the two margins appear similar in some respects.

This similarity led Boillot (pers. comm.; cf Krawczyk et al., subm.) to suggest another interpretation between Sites 900 and 901, based on analogy with the structures and timing on the Galicia Bank margin to the north (Boillot et al., 1994). In this region, the S reflector, and hence the controlling detachment fault, has been interpreted by other authors to reach the surface at the Peridotite Ridge (in contrast to the new results discussed in Chapter 3), which bounds the western end of the OCT (Boillot, Winterer, Meyer et al., 1987; 1988; Beslier et al., 1993). In the Iberia Abyssal Plain, it is possible that the eastward dipping portion of structure H continues beneath the westward dipping part (shotpoints 4250 - 4500; Figure 5.3) to cut across the oceanward dipping reflection L at depth. This model (Figure 5.19, A1) resembles that applied by Boillot et al. (1994) to the Galicia Bank margin, as H surfaces at Site 900, where highly sheared and deformed gabbros were sampled. However, such a continuation of the east-dipping reflection is not imaged.

The oceanward dipping, block-bounding normal faults stop likewise in interpretation A1 at the combined H-L reflector, therefore interpreted as a large detachment structure, which accomodated extension by top-to-the-east motion of the tilted blocks imaged between Sites 900 and 901. Additionally, the east flank of the fault block FB may be cut by continentalward dipping normal faults detaching onto L, further dissecting FB during that rifting episode. In contrast to the model suggested in the interpretation advanced here (Figure 5.16), motion along H is top-to-the-east. Furthermore, L represents a normal-fault structure detaching onto H, so causing the bow up of the most westward tilted fault block along H close to Site 900. As this interpretation assumes that

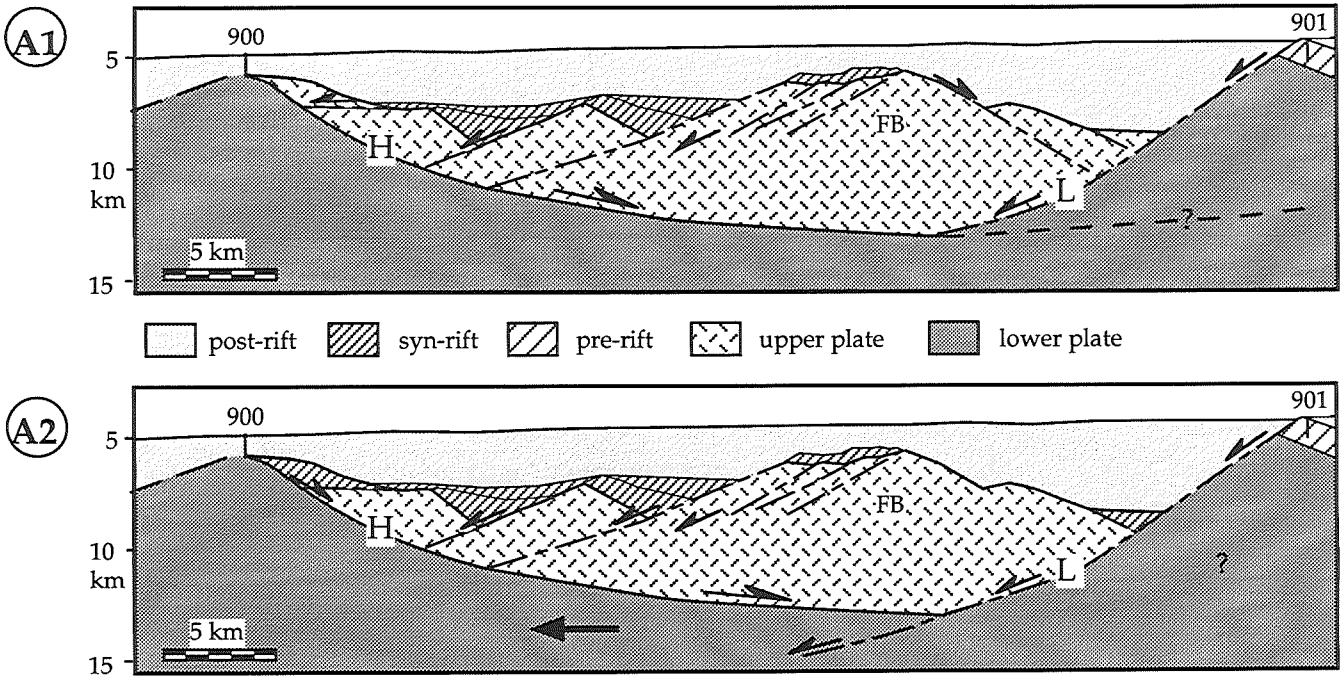

Figure 5.19: Alternative interpretations of the depth section of profile LG12 between ODP Leg 149 Sites 900 and 901 (compare Figure 5.16). A1) This interpretation assumes the eastward dipping part of H cutting across L at about 12 km depth by analogy to the Galicia Margin (e.g. Boillot et al, 1994). In this interpretation, extension may have been accomodated by top-to-the-east motion along detachment H, accompanied by subsequent block faulting. A2) A third possible interpretation involves an antithetic relationship between H and L: simultaneous activity accomodated top-to-the-east motion along H, whereas motion was top-to-the-west at L, cutting below H.

the H reflector links with structure L, but the new images and analyses reveal instead that H and L represent different structures, this interpretation is not convincingly supported by the seismic data.

A third possibility explaining the observed structures between shotpoints 4000-4900 is an antithetic relationship between reflectors H and L (Figure 5.19, A2). The tilted blocks could have slid along H to the east, while L was also active with a motion directed westwards, and cutting into deeper levels below H. In summary, this interpretation would require a top-to-the-east accomodation of extensional motion by the widespread detachment structure H, and the normal faults subsequently separating the overlying tilted blocks. Again, there is no clear evidence that H and L are connected.

Although the drilling results cannot shed more light onto the different interpretations, the first interpretation may explain best the observed structures, as it is best evidenced using various methods of analyses. These include iterative depth migration before stack, producing detailed velocity models, amplitude and waveform analyses, and reflection coefficient estimations. The results shown here support the interpretation, that different phases of detachment faulting developed this part of the Iberia Abyssal Plain, with westward motion of the overlying crustal blocks first along H, subsequently dissected further by westward dipping normal faults at the same time as motion occured along L (Figure 5.16).

A major difference between the Galicia Bank and the Iberia Abyssal Plain rifted margins is the width between the OCT and the first upper continental crust; on the IAP margin it lies approximately four times further landward from the OCT than on the west Galicia margin (Beslier et al., 1993). This difference may arise because on the IAP margin, the lower plate to the detachment fault has been exposed by extreme extension and later faulting, whereas on the Galicia margin, the S reflector and the lower plate are always overlain by upper plate fault blocks, consisting of the slices of upper crust. This in turn reflects the different timing of detachment fault activity on the two margins: detachment fault S was active right up to continental break-up, whereas to the south, detachment fault H was active during earlier rifting, and was dismembered by faulting occuring closer to break-up.

In conclusion, the analysis of the seismic reflection profile LG12 demonstrates that detachment tectonics controlled the extensional history along the drilled transect across the OCT in the Iberia Abyssal Plain. Extensional tectonics may have exposed a crustal cross-section of upper crust, lower crust

and mantle material. Top-to-the-west motion of crustal blocks along the underlying detachment structures and later block-faulting accomodated extension in different phases of rifting.

5.7 Model

The results are consistent with a simple model for the evolution of the IAP (Figure 5.20). Although an over-simplification, this model is advanced as a basis for further work and investigations of this margin. Depicted here as a Wernicke-type model, one more akin to the results of Harry and Sawyer (see Chapter 1 - Figure 1.8) may be more appropriate as such models include the variation of rheology with depth.

In this model, as lithospheric extension started, Newfoundland and Iberia moved apart along a large detachment, accomodating top-to-the-west simple-shear motion in the upper lithosphere. Asthenospheric upwelling followed and consequently decompression melting led to intrusion of melt into the lower crust. Because such melting occured beneath highly thinned lithosphere, it may be indistinguishable from that occuring at mid ocean ridges.

Extension of the upper lithosphere along a top-to-the-west detachment would have brought lower crustal and mantle rocks close to the surface to the west (Wernicke, 1981). After the detachment had become inactive, block-faulting may have accomodated continued extension. This faulting would have dissected the lower plate and the detachment itself, and rotation of the blocks would have tilted this back towards the continent. Finally, this model predicts a significant amount of mantle material between oceanic and continental crust, locally exposed at the seafloor during the last rift stage prior to continental break-up.

This model is consistent with the drilling results (Sawyer, Whitmarsh, Klaus et al., 1994). The transect of Sites 901-900-898 represents a transition from upper continental crust to lower crust (perhaps syn-rift intrusion) to mantle, as predicted by the model: Site 901 sampled continental material, Site 900 drilled a lower crustal tilted block, identified by its lithology (amphibolite facies gabbro, probably syn-rift), and finally, Sites 897 and 899 sampled upper mantle rocks at the western edge of the drilling transect (Site 897 lies just landward of oceanic crust).

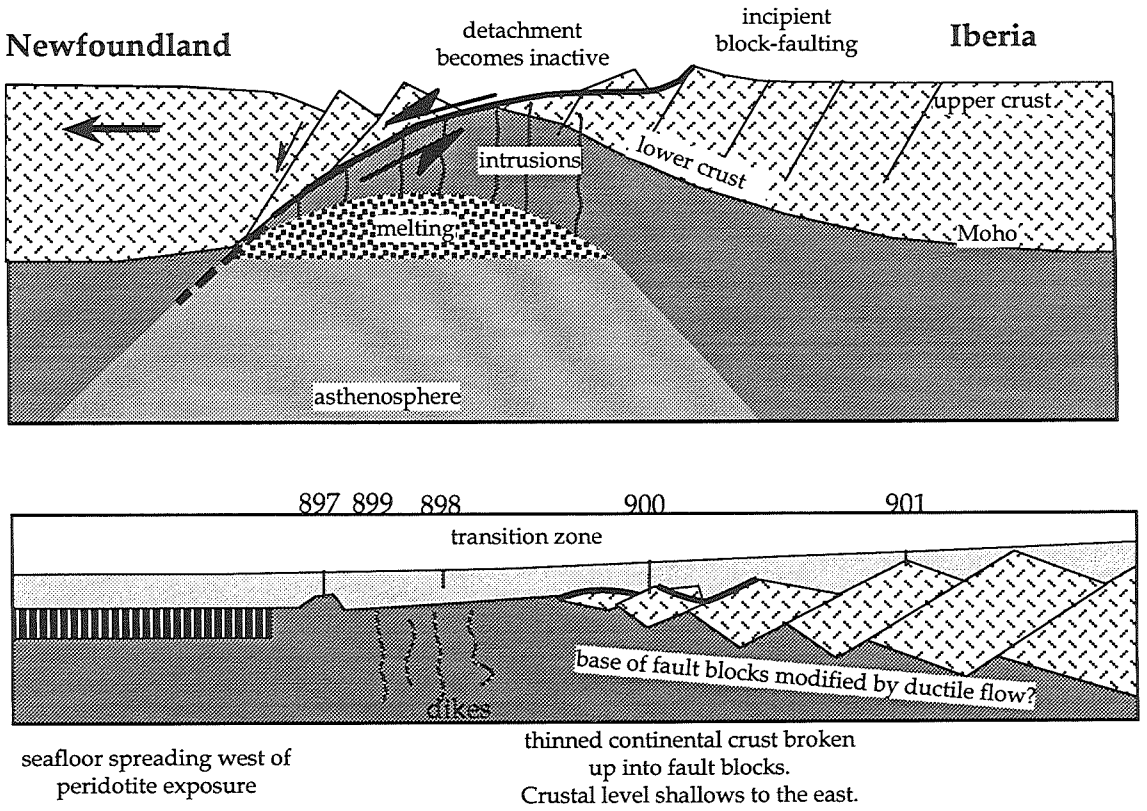

Figure 5.20: Model for the extension of the lithosphere controlled by detachment faulting during rifting on the IAP margin. During syn-rift I, lithospheric extension may have been accomodated by detachment faulting and accompanied by consequent upwelling, melting and intrusion of asthenospheric material in the lower crust. Subsequently, during syn-rift II, block-faulting cuts the upper plate into single tilted blocks, dismembering the detachment system and the lower plate. The resulting crustal cross section shows an oceanward deepening of lithospheric level, consistent with the results of ODP Leg 149.

5.8 Conclusions and Outlook

The evidence for detachment faulting during continental break-up in the IAP provides a major advance towards the understanding of the mechanisms of lithospheric extension on this segment of the Iberian passive continental margin.

The results of the new processing and prestack depth migration analyses of this reflection seismic profile across the IAP margin show deep reflections within the basement, which are associated with block faulting. Furthermore, the overlying sediments, deposited during different phases of rifting, are discernible by their interval velocities. Combined with the present knowledge of the mechanism of lithospheric extension in the area of the Galicia Bank, this profile supports the idea that in the IAP continental extension leading to break-up may also have been controlled by detachment fault systems active during different phases of rifting. As a consequence of exhumation during repeated extension, a cross-section through the upper lithosphere may be exposed, as one can identify upper crust, lower crust and finally mantle material from east to west along this transect across the OCT.

However, at this stage some uncertainties still remain. For instance, efforts from other disciplines are required to shed more light on the nature of the drilled transect, such as the age of the Site 900 gabbros: it is not known if they represent syn-rift or pre-rift or lower crust. Nevertheless, this model can only be tested by further drilling, and particularly the characterisation of reflector H, interpreted here as a master detachment fault with a strong reflection coefficient of c. 0.15. Although Site 900 drilled close to this reflector, sampling probably reached the lower plate to H. By drilling further just to the east, the upper plate, the detachment itself and the lower plate could all be sampled, so determining the nature of H, the sense of shear, and thus testing this model. More light will be also shed on this margin by the results of the IAM project (Banda et al., 1994) and by proposed drilling (Reston et al., 1994).

6 Conclusions and Outlook

The Galicia Bank and Iberia Abyssal Plain (IAP) segments of the western Iberian Atlantic margin are characterised by highly extended and thinned continental crust bounded westwards by a ridge of serpentinised peridotite within the transition zone between continental and oceanic crust (OCT). To better understand the evolution of these two parts of the margin, a dense grid of MCS profiles (Figure 2.1) was analysed by conventional processing including time and depth migrations, prestack depth migration and amplitude and waveform analyses (Figure 2.2). After optimum processing, the seismic sections image strong reflections below the break-up unconformity in both segments of the Iberian non-volcanic margin (see results of Chapters 3, 4, 5), suggesting detachment tectonics as controlling mechanism of the continental rifting and break-up off the West Iberia passive margin. While detachment faulting is generally accepted on the Galicia Bank margin, this study is the first time that such a model has been applied to the IAP segment of the Iberian margin. To focus on this interpretation, the similarities and differences of both the Galicia Bank and IAP areas are summarised here (compare also Chapters 3, 4, and 5).

The seismic images of the IAP and Galicia Bank areas show similarities in the structural setting as follows:

- the continental margins are characterised by extreme crustal thinning, although no clear Moho reflection is imaged.
- the OCT is bound to the west by a ridge of mantle material, proved by drilling ODP Legs 103 (Boillot, Winterer, Meyer et al., 1987), 149 (Sawyer, Whitmarsh, Klaus et al., 1994), and diving (Boillot et al., 1988b).
- continentalward tilted crustal blocks are bound by oceanward-dipping normal faults.
- velocities identify wedge-shaped sediment sequences within the tilted blocks.
- the oceanward-dipping normal faults stop at underlying bright reflections (S, H), which are therefore interpreted as detachment faults.
- both detachments may have accomodated extension by a top-to-the-west movement.
- the breakaway of S and H may be located to the east.

Furthermore, amplitude and waveform analyses revealed the internal structures of the S and H detachments, showing also similar characteristics:

- the waveforms of both S and H resemble strongly that of the seafloor on the respective datasets, which is shown by comparison with its first multiple to represent a reflection from a first order interface.
- both detachments have a strong reflection coefficient, with a value of c. 0.2 deduced for S, and a value of c. 0.15 estimated for H.
- S and H show positive polarity.
- S and H represent reflections from first order interfaces characterised by a stepwise increase in acoustic impedance, leading to the interpretation of S and H as sharp boundaries separating upper crustal upper plates from higher velocity and density lower plates.

Thus, the Galicia Bank and IAP segments of the Iberian continental margin are similar in a variety of aspects, all supporting the advanced interpretations of the key structures representing detachment faults, which controlled rifting and continental break-up. The analogy with the similar seismic image of the S reflector in the Galicia Bank area (see Chapters 3, 4) led further to suggest that continental break-up in the IAP could have been also controlled by detachment faults (Chapter 5), but as discussed below, the models differ in some respects.

A major difference between the Galicia Bank and the Iberia Abyssal Plain rifted margins is the width between the OCT and the first upper continental crust. On the IAP margin it lies approximately four times further landward from the OCT than on the west Galicia margin (Figure 5.1). This difference may arise because on the IAP margin, the lower plate to the detachment fault has been exposed by extreme extension and later faulting, whereas on the Galicia margin, the S reflector and the lower plate are always overlain by upper plate fault blocks, consisting of the slices of upper crust. This in turn may reflect the different timing of detachment fault activity relative to break-up on the two margins, the second major difference of the suggested detachment models. The results of the IAP data support the interpretation that different phases of detachment faulting developed this part of the Iberia Abyssal Plain, with westward motion of the overlying crustal blocks first along H, subsequently dissected further by westward dipping normal faults at the same time as motion occured along L (Figure 5.16). In contrast, detachment faulting along S may have been active just prior to continental break-up in the Galicia

Bank area (Figure 3.12).

The obvious similarity of the IAP area with the structures on the Galicia Bank margin to the north led Boillot and others (1994) to suggest another interpretation between Sites 900 and 901. This is based on analogy with their interpretation of the S reflector supposed to reach the surface at the Peridotite Ridge (in contrast to the new results discussed in Chapter 4), which bounds the western end of the OCT (Boillot, Winterer, Meyer et al., 1987; 1988; Beslier et al., 1993). The authors assume a connection between the eastward dipping portion of reflection H with the oceanward dipping reflection L, so that the image in the IAP is then almost the same as that on the Galicia Bank (Figure 5.19). As such a continuation of the east-dipping reflection is not imaged, this interpretation is not constrained by the data, and hence not further followed. Furthermore, the deepening of the lithospheric level towards the ocean is predicted for the lower plate to a west-dipping detachment but not for the Boillot model. The results of drilling on Leg 149 (which sampled upper crustal sediment, lower crust and mantle rocks going from east to west) also favour the top-to-the-west interpretation presented here.

Thus, the results of the IAP data support the interpretation that different phases of detachment faulting developed this part of the Iberia Abyssal Plain. Although the mechanism and sense of movement along H are not as much constrained as in the Galicia Bank area by a profile grid for the S reflector, this preliminary model may prove relevant, as it is supported by drilling results.

In conclusion, the Galicia Bank and IAP segments of the Iberian margin were formed by detachment tectonics, although some questions still remain. Among those are the timing and conditions of movement along the detachment structures, the temporal relationship between the eastward dipping shear structures cutting down from the Peridotite Ridge and S, and the complete analysis of the basement samples collected during ODP Leg 149. Besides further drilling, efforts will be made also by additional geophysical investigations, including refraction and wide-angle reflection experiments, to better reveal the deep structure of the margin and provide more information about crustal nature.

References

Austin, J.A., Tucholke, B.E. & Uchupi, E., 1989, Upper Triassic-Lower Jurassic salt basin southeast of the Grand Banks. - Earth and Planetary Science Letters, 92: 357-370.

Axen, G.J., 1992, Pore pressure, stress increase, and fault weakening in low-angle normal faulting. - JGR, 97, B6: 9879-8991.

Banda, E., Torné, M., Long, R., Mendes Victor, L., Senos, L. & Watts, A.B., 1994, The deep structure of the Iberian Atlantic margins investigated by the IAM project. - Annales Geophysicae, 12, Suppl. 1: 37.

Barnes, A. & Reston, T.J., 1992, A study of two mid-crustal bright spots from southeast Georgia (USA). - Geophysical Journal International, 108: 683-691.

Berndt, C., 1994, Auswirkungen des S-Reflektors auf die momentane Frequenz seismischer Signale. - Unpubl. Diploma thesis, Kiel University, 75 p.

Beslier, M.-O. & Brun, J.P., 1991, Boudinage de la lithosphère et formation des marges passives. - C.R. Acad. Sci. Paris, 313: 951-958.

Beslier, M.-O., Ask, M. & Boillot, G., 1993. Ocean-continent boundary in the Iberia Abyssal Plain from multichannel seismic data. - Tectonophysics, 218: 383-393.

Beslier, M.-O., Girardeau, J. & Boillot, G., 1990, Kinematics of peridotite emplacement during North Atlantic continental rifting, Galicia, NW Spain. - Tectonophysics, 184: 321-343.

Boillot, G., Recq, M. et al., 1987, Tectonic denudation of the upper mantle along passive margins: a model based on drilling results (ODP Leg 103, Western Galicia Margin, Spain). - Tectonophysics, 132: 335-342.

Boillot, G., Beslier, M.-O. & Girardeau, J., 1995, Nature, Structure and Evolution of the Ocean-Continent Boundary: The Lesson of the West Iberia Margin. - In E. Banda, M. Talwani & M. Torne, eds, Rifted Ocean-Continent Boundaries, NATO-workshop 1994, Mallorca, Kluwer, in press.

Boillot, G., Girardeau, J. & Kornprobst, J., 1988a, The rifting of the Galicia margin: crustal thinning and emplacement of mantle rocks on the seafloor. - In G. Boillot, E.L. Winterer, A.W.Mayer et al., eds, Proc. ODP, Sci. Results, 103: 741-756, College Station, TX (Ocean Drilling Program).

Boillot, G., Winterer, E.L., Meyer, A.W. et al., 1987, Proc. ODP, Initial Reports, 103. - Ocean Drilling Program, College Station, TX, 663 p.

Boillot, G., Winterer, E.L., Meyer, A.W. et al., 1988, Proc. ODP, Sci. Results, 103. - Ocean Drilling Program, College Station, TX, 858 p.

Boillot, G., Féraud, G., Recq, M. & Girardeau, J., 1989, "Undercrusting" by serpentinite beneath rifted margins: the example of the west Galicia margin (Spain). - Nature, 341: 523-525.

Boillot, G., Beslier, M.-O., Krawczyk, C.M., Rappin, D. & Reston, T.J., 1995b, The formation of passive margins: constraints from the crustal structure and segmentation of the deep Galicia margin (Spain). - In R.A. Scrutton et al., eds, Tectonics, Sedimentation and Palaeoceanography of the North Atlantic Margin. Geol. Soc. of London Spec. Publ, in press.

Boillot, G., Beslier, M.-O., Rappin, D., Banda, E. & Comas, M., 1993, Galicia Margin S´ Reflector. - ODP drilling proposal, 334 (Rev 3), 18 p.

Boillot, G., Comas, M.C., Girardeau, J., Kornprobst, J., Loreau, J.P., Malod, J., Mougenot, D. & Moullade, M., 1988b, Preliminary results of the Galinaute cruise: dives of the submersible Nautile on the western Galicia margin, Spain. - In G. Boillot, E.L. Winterer, A.W. Meyer et al., eds, Proc. ODP, Sci. Results, 103: 37-51, College Station, TX.

Bott, M.H.P., 1971, Evolution of young continental margins and formation of shelf basins. - Tectonophysics, 11: 319-327.

Buck, W. R., 1988, Flexural rotation of normal faults. - Tectonics, 7: 959-973.

Coward, M., 1986, Heterogeneous stretching, simple shear and basin development. - Earth and Planetary Science Letters, 80: 325-336.

de Charpal, O., Guennoc, P., Montadert, L. & Roberts, D.G., 1978, Rifting, crustal attenuation and subsidence in the Bay of Biscay. - Nature, 275: 706-711.

Denelle, E., Dezard, Y. & Raoult, J., 1986, 2-D prestack depth migration in the (S-G-W) domain, ext. abstract. - 56th SEG Meeting, Houston, TX, 37 p.

Emery, K.O. & Uchupi, E., 1984, The Geology of the Atlantic Ocean. - Springer Verlag, New York, 1050 p.

Falvey, D.A. & Mutter, J.C., 1981, Regional plate tectonics and the evolution of Australia passive continental margin: Buried mineral sources. - Journ. Austr. Petr. Expl. Assoc., 6: 1-29.

Gibbs, A., 1987, Development of extension and mixed-mode sediment basins. - In M.P. Coward, J.F. Dewey & P.L. Hancock, eds, Continental Extension Tectonics, Geol. Soc. London Spec. Publication no. 28: 19-33.

Girardeau, J, Evans, C.A. & Beslier, M.-O., 1988, Structural analysis of plagioclase-bearing peridotites emplaced at the end of continental rifting: hole 637A, ODP Leg 103 on the Galicia Margin. - In G. Boillot, E.L. Winterer, A.W. Meyer et al., eds, Proc. ODP, Sci. Results, 103: 209-223,

College Station, TX.

Goodwin, E., Thompson, G., and Okaya, D., 1989, Seismic identification of basement reflectors: the Bagdad Reflection Sequence in the Basin and Range Province-Colorado Transition Zone, Arizona. - Tectonics, 8: 821-831.

Grimaud, S., Boillot, G., Collette, B., Mauffret, A., Miles, P.R. & Roberts, D.G., 1982, Western extension of the Iberian-European plate boundary during early Cenozoic (Pyrenean) convergence: a new model. - Marine Geology, 45: 63-77.

Harry, D. & Sawyer, D., 1992, A dynamic model of extension in the Baltimore Canyon Trough region. - Tectonics, 11, 2: 420-436.

Hatton, L., Worthington, M.H. & Makin, J., 1986, Seismic Data Processing, Theory and Practice. - Blackwell Scientific Publications, Oxford, 177 p.

Hinz, K., 1972, Der Krustenaufbau des Norwegischen Kontinentalrandes und der Norwegischen See zwischen 66° und 68° N nach seismischen Untersuchungen. - Meteor Forschungsergebnisse, Reihe C, 10: 1-16.

Hoffmann, H.J. & Reston, T.J., 1992, The nature of the S reflector beneath the Galicia Bank rifted margin. Preliminary results from pre-stack depth migration. - Geology, 20: 1091-1094.

Horsefield, S., 1992, Crustal Structure across the Ocean-Continent Boundary. - Unpubl. PhD thesis, Cambridge University, 215 p.

Jackson, J., 1987, Active normal faulting and crustal extension. - In M.P. Coward, J.F. Dewey & P.L. Hancock, eds, Continental Extension Tectonics, Geol. Soc. London Spec. Publication no. 28: 3-17.

Judson, D., Lin, J., Schultz, P. & Sherwood, J., 1980, Depth migration after stack. - Geophysics, 45: 376-393.

Juhlin, C., 1990, Interpretation of the reflections in the Siljan Ring area based on results from Gravberg-1 borehole. - Tectonophysics, 173: 345-360.

Keen, C.E. & Dehler, S., 1993, Stretching and subsidence: Rifting of conjugate margins in the North Atlantic region. - Tectonics, 12, 5: 1209-1229.

Keen, C.E. & de Voogd, B., 1988, The Ocean-Continent Boundary at the rifted margin off Eastern Canada: new results from deep seismic reflection studies. - Tectonics, 7: 107-124.

Keener, C., Serpa, L. & Pavlis, T.L., 1993, Faulting at Mormon Point, Death Valley, California: A low-angle normal fault cut by high-angle faults. - Geology, 21: 327-330.

Klitgord, K.D. & Schouten, H., 1986, Plate kinematics of the Central Atlantic. -

In P.R. Vogt & B.E. Tucholke, eds, The Geology of North America (Vol. M): The western North Atlantic region, Geol. Soc. Am.: 351-378.

Krawczyk, C.M. & Reston, T.J., 1995, Detachment Faulting and Continental Breakup: the S Reflector offshore Galicia. - In E. Banda, M. Talwani & M. Torné, eds, Rifted Ocean-Continent Boundaries, NATO-workshop 1994, Mallorca, Kluwer, in press.

Krawczyk, C.M., Reston, T.J., Beslier, M.-O. & Boillot, G., submitted, Evidence for Detachment Tectonics on the Iberia Abyssal Plain rifted margin. - In D. Sawyer, R. Whitmarsh, A. Klaus et al., eds, Proc. ODP, Sci. Results, 149, College Station, TX.

Krawczyk, C.M., Reston, T.J., Beslier, M.-O., Boillot, G. & Leg149 scientific party, 1994, Analyses of reflection seismic data in the Iberia Abyssal Plain near Leg149 drill sites. - Annales Geophysicae, 12, Suppl. 1: 39.

Kusznir, N.J. & Park, R.G., 1987, The extensional strength of th continental lithosphere: its dependence on geothermal gradient, crustal composition and thickness. - In M.P. Coward, J.F. Dewey & P.L. Hancock, eds, Continental Extension Tectonics, Geol. Soc. London Spec. Publication no. 28: 35-52.

LePichon, X. & F. Barbier, 1987, Passive margin formation by low angle faulting within the upper crust: the northern Bay of Biscay margin. - Tectonics, 6: 133-150.

LePichon, X., Sibuet, J.C. & Francheteau, J., 1977, The fit of the continents around the North Atlantic Ocean. - Tectonophysics, 38: 169-209.

Lister, G.S. & Davis, G.A., 1989, The origin of metamorphic core complexes and detachment faults formed during Tertiary continental extension in the northern Colorado river region, U.S.A. - J. Struct. Geology, 11 : 65-94.

Lister, G.S., Etheridge, M.A. & Symonds, P.A., 1986, Detachment faulting and the evolution of passive continental margins. - Geology, 14 : 246-250.

Litak, R. and Hauser, E., 1992, The Bagdad Reflection Sequence as tabular mafic intrusions: Evidence from seismic modelling of mapped exposures. - GSA Bull, 104: 1315-1325.

Malod, J.A. & Mauffret, A., 1990, Iberian plate motions during the Mesozoic. - Tectonophysics, 184: 261-278.

Malod, J.A., Murillas, J., Kornprobst, J. & Boillot, G., 1993, Oceanic lithosphere at the edge of a Cenozoic active continental margin (northwestern slope of Galicia Bank, Spain). - Tectonophysics, 221: 195-206.

Mamet, B., Comas, M.C. & Boillot, G., 1991, Late Paleozioc Basin on the West

Galicia Atlantic margin. - Geology, 19: 738-741.

Masson, D.G. & Miles, P.R., 1984, Mesozoic sea floor spreading between Iberia, Europe and North America. - Marine Geology, 56: 279-287.

Masson, D.G., Cartwright, J.A., Pinheiro, L.M., Whitmarsh, R.B. Beslier, M-O. & Roeser, H., 1995, Localized deformation at the ocean-continent transition in the NE Atlantic. - Journal of Geol. Soc. London, in press.

Mauffret, A. & Montadert, L., 1987, Rift tectonics on the passive continental margin off Galicia (Spain). - Mar. Petr. Geol., 40: 49-70.

Mauffret, A., Mougenot, D., Miles, P.R. & Malod, J.A., 1989, Cenozoic deformation and Mesozoic abandoned spreading centre in the Tagus Abyssal Plain (west of Portugal): results of a multichannel seismic survey. - Canad. J. Earth Sci., 26: 1101-1123.

McKenzie, 1978, Some remarks on the development of sedimentary basins. - Earth and Planetary Science Letters, 40: 25-42.

Meissner, R., 1986, The Continental Crust, A Geophysical Approach. - Intern. Geophys. Series, 34, Academic Press Inc., 426 p.

Meissner, R. & Stegena, L., 1977, Praxis der seismischen Feldmessung und Auswertung. - Gebr. Bornträger, Berlin, 275 p.

Meissner, R. & Strehlau, J., 1982, Limits of stresses in the continental crust and their relation to the depth-frequency distribution of shallow earthquakes. - Tectonics, 1: 73-89.

Montadert, L., de Charpal, O., Robert, D., Guennoc, P. & Sibuet, J.C., 1979, Northeast Atlantic passive continental margin: rifting and subsidence processes. - In M.Talwani & W.B.F. Ryan, eds, Deep drilling results in the Atlantic ocean: Continental margin and palaeoenvironment, M. Ewing Series 3: 154-186, AGU, Washington.

Montenat, C., Guery, F., Jamet, M. & Berthou, J.Y., 1988, Mesozoic evolution of the Lusitania basin: comparison with the adjacent margin. - In G. Boillot, E.L. Winterer, A.W. Meyer et al., eds, Proc. ODP, Sci. Results, 103: 757-775, College Station, TX.

Mougenot, D., 1988, Geologie de la marge portugaise. - Memoire Science de la Terre Universite P. & M. Curie Paris, v. 88, 275p.

Mougenot, D., Kidd, R.B., Mauffret, A., Regnauld, H., Rothwell, R.G. & Vanney, J.R., 1984, Geological interpretation of combined Sea-Beam, Gloria and seismic data from Porto and Vigo seamounts, Iberian continental margin. - Mar. Geophys. Res., 6: 329-363.

Moullade, M., Brunet, M.-F. & Boillot, G., 1988, Subsidence and deepening of

the Galicia Margin: the palaeoenvironmental control. - In G. Boillot, E.L. Winterer, A.W. Meyer et al., eds, Proc. ODP, Sci. Results, 103: 733-740, College Station, TX.

Murillas, J., Mougenot, D., Boillot, G., Comas, M.C., Banda, E. & Mauffret, A., 1990, Structure and Evolution of the Galicia Interior Basin (Atlantic western Iberian continental margin). - Tectonophysics, 184: 297-319.

Mutter, J., Larson, R. & Northwest Australia Study Group, 1989, Extension of the Exmouth Plateau offshore northwestern Australia: Deep seismic reflection/refraction evidence for simple and pure shear mechanisms. - Geology, 17: 15-18.

Parsons, T. & Thompson, G.A., 1993, Does magmatism influence low-angle normal faulting? - Geology, 21: 247-250.

Peddy, C., Brown, L. & Klemperer, S., 1986, Interpreting the deep structure of rifts with synthetic seismograms. - AGU Geodyn. Series, 13: 301-310.

Pinheiro, L.M., Whitmarsh, R.B. & Miles, P.R., 1992, The Ocean-Continent Boundary off the western continental margin of Iberia, II.-Crustal Structure in the Tagus Abyssal Plain. - Geophys. Journal, 109: 106-124.

Pratt, T., Hauser, E., Hearn, T. & Reston, T.J., 1991, Reflection Polarity of the Midcrustal Surrency Bright Spot beneath southeastern Georgia: Testing the Fluid Hypothesis. - JGR, 96B: 10145-10158.

Raynaud, B., 1988, Diffraction modelling of 3-D lower crustal reflections. - Geophys. Journal, 93: 149-161.

Reid, I., 1994, Crustal structure of a nonvolcanic rifted margin. - JGR, 99, B8: 15161-15180.

Reston, T.J., 1990, The lower crust and the extension of the lithosphere: kinematic analysis of BIRPS deep seismic data. - Tectonics, 9: 1235-1247.

Reston, T.J., Krawczyk, C.M. & Hoffmann, H.J., 1995, Detachment tectonics during Atlantic rifting: analysis and interpretation of the S reflector, west Galicia margin. - In R.A. Scrutton et al., eds, Tectonics, Sedimentation and Palaeoceanography of the North Atlantic Margin. Geol. Soc. of London Spec. Publ., in press.

Reston, T.J., Beslier, M.O., Boillot, G., Krawczyk, C.M. & Sibuet, J.C., 1993, A Deep Hole off Galicia to study the Mechanism of Continental Breakup: Sedimentary and Subsidence history and the Nature of the S Reflector. - Drilling proposal subm. to the Ocean Drilling Program, 43 p.

Reston, T.J., Beslier, M.O., Boillot, G., Sawyer, D. & Whitmarsh, R., 1994, Rift-to-Drift processes within the Ocean-Continent Transition west of Iberia

(sequel to Leg 149 studies of a non-volcanic rifted margin). - Drilling proposal subm. to the Ocean Drilling Program, 45 p.

Royden, A., Sclater, J.G. & vonHerzen, R.P., 1980, Continental subsidence and heat flow: important parameters in formation of petroleum hydrocarbons. - Am. Assoc. Petr. Geol. Bull., 64: 173-187.

Sawyer, D.S., Whitmarsh, R.B. & ODP Leg 149 Scientific Party, 1993, ODP drills the West Iberia Rifted Margin. - EOS, 74, 40: 454-455.

Sawyer, D.S., Whitmarsh, R.B., Klaus, A. et al., 1994, Proc. ODP, Initial Reports, 149. - Ocean Drilling Program, College Station (TX), 719 p.

Scott, R.J & Lister, G.S., 1992, Detachment faults: Evidence for a low-angle origin. - Geology, 20: 833-836.

Sheridan, R.E., 1969, Subsidence of continental margins. - Tectonophysics, 7: 219-229.

Sherwood, J., 1989, Depth sections and interval velocities from surface seismic data. - Leading Edge, 8, 9: 44-49.

Shipboard Scientific Party, 1994a, Site 898. - In D.S. Sawyer, R.B. Whitmarsh, A. Klaus et al., eds, Proc. ODP, Initial Reports, 149: 115-146, College Station (TX).

Shipboard Scientific Party, 1994b, Site 900. - In D.S. Sawyer, R.B. Whitmarsh, A. Klaus et al., eds, Proc. ODP, Initial Reports, 149: 211-262, College Station (TX).

Shipboard Scientific Party, 1994c, Site 901. - In D.S. Sawyer, R.B. Whitmarsh, A. Klaus et al., eds, Proc. ODP, Initial Reports, 149: 263-268, College Station (TX).

Sleep, N.H., 1971, Thermal effects of the formation of the atlantic continental margin by continental breakup. - R. Astr. Soc. Geophys. Journal, 24: 325-350.

Sibuet, J.C., 1992, New constraints on the formation of the non-volcanic continental Galicia - Flemish Cap conjugate margins. - J. Geol. Soc. London, 149: 829-840.

Srivastava, S.P., Roest, W.R., Kovacs, L.C., Oakey, G., Levesque, S., Verhoef, J. & Macnab, R., 1990, Motion of Iberia since the Late Jurassic: results from detailed aeromagnetic measurements in the Newfoudland Basin. - Tectonophysics, 184: 229-260.

Talwani, M. & Eldholm, O., 1977, Evolution of the Norwegian-Greenland Sea. - Geol. Soc. Am. Bull., 88: 969-999.

Tankard, A.J. & Welsink, H.J., 1987, Mesozoic extension and styles of basin

formation in Atlantic Canada. - Am. Assoc. Petrol. Geol. Bull., 71: 1210-1232.

Thommeret, M., Boillot, G. and Sibuet, J., 1988, Structural map of the Galicia margin. - In G. Boillot, E.L. Winterer, A.W. Meyer et al., eds, Proc. ODP, Sci. Results, 103: 31-36, College Station, TX.

Tucholke, B.E., Austin, J.A. & Uchupi, E., 1989, Crustal structure and rift-drift evolution of the Newfoundland Basin. - In A.J. Tankard & H.R. Balkwill, eds, Extensional Tectonics and Stratigraphy of the North Atlantic Margins, AAPG Memoir, 46: 247-264, Tulsa (OK).

Versteeg, R.V., 1993, Sensitivity of prestack depth migration to the velocity model. - Geophysics, 58, 6: 873-882.

Warner, M., 1990, Absolute reflection coefficients from deep seismic reflections. - Tectonophysics, 173: 15-24.

Wernicke, B., 1981, Low-angle normal faults in the Basin and Range: Nappe tectonics in an extending orogen. - Nature, 291: 645-648.

Wernicke, B., 1985, Uniform-sense normal simple shear of the continental lithosphere. - Can. J. Earth Sci., 22: 108-125.

Wernicke, B., and Axen, G., 1988, On the role of isostasy in the evolution of normal fault systems. - Geology, 16: 848-851.

Wernicke, B. & Burchfiel, B.C., 1982, Modes of extensional tectonics. - J. Struct. Geol., 4 : 105-115.

White, R.S., Westbrook, G.K., Fowler, S.R., Spence, G.D., Barton, P.J., Joppen, M., Bowen, A.N., Prestcott, C. & Bott, M.H.P., 1987, Hatton Bank (northwest U.K.) continental margin structure. - In D. Matthews & C. Smith, eds, Deep Seismic Reflection Profiling of the Continental Lithosphere, Geophys. J. R. Astr. Soc. Spec. Issue 89, 1: 265-271.

Whitmarsh, R.B. & Miles, P.R., 1994, Models of the development of the west Iberia rifted continental margin at 40° 30´N deduced from surface and deep-towed magnetic anomalies. - Submitted to JGR.

Whitmarsh, R.B., Miles, P.R. & Mauffret, A., 1990a, The ocean-continent boundary off the western continental margin of Iberia, I.-Crustal structure at 40°30´N. - Geophys. Journ. Intern., 103: 509-531.

Whitmarsh, R.B., Miles, P.R. & Pinheiro, L.M., 1990b, The seismic velocity structure of some NE Atlantic continental rise sediments: a lithification index? - Geophys. Journal Int., 101: 367-378.

Whitmarsh, R.B., Pinheiro, L.M., Miles, P.R. Recq, M. & Sibuet, J.C., 1993, Thin crust at the western Iberia ocean-continent transition and ophiolites. - Tectonics, 12, 5: 1230-1239.

Wilson, R.C.L., Hiscott, R.N., Willis, M.G. & Gradstein, F.M., 1989, The Lusitanian Basin of west-central Portugal-Mesozoic and Tertiary tectonic, stratigraphic and subsidence history. - In A.J. Tankard & H.R. Balkwill, eds, Extensional tectonics and Stratigraphy of the North Atlantic margins, AAPG Memoir 46: 341-361, Tulsa (OK).

Winterer, E.L., Gee, J.S. & Van Waasbergen, R.J., 1988, The source area for lower Cretaceous clastic sediments of the Galicia margin: geology and tectonic and erosional history. - In G. Boillot, E.L. Winterer, A.W. Meyer et al., eds, Proc. ODP, Sci. Results, 103: 697-732, College Station, TX.

Yilmaz, Ö., 1987, Seismic Data Processing, Investigations in Geophysics Vol. 2. - SEG, Tulsa (OK), 526 p.

List of Figures

GEOMAR REPORTS

1 GEOMAR FORSCHUNGSZENTRUM FÜR MARINE GEOWISSENSCHAFTEN DER CHRISTIAN-ALBRECHTS-UNIVERSITÄT ZU KIEL
BERICHT FÜR DIE JAHRE 1987 UND 1988. 1989. 71 + 6 pp.
In German

2 GEOMAR FORSCHUNGSZENTRUM FÜR MARINE GEOWISSENSCHAFTEN DER CHRISTIAN-ALBRECHTS-UNIVERSITÄT ZU KIEL
JAHRESBERICHT / ANNUAL REPORT 1989. 1990. 96 pp.
In German and English

3 GEOMAR FORSCHUNGSZENTRUM FÜR MARINE GEOWISSENSCHAFTEN DER CHRISTIAN-ALBRECHTS-UNIVERSITÄT ZU KIEL
JAHRESBERICHT / ANNUAL REPORT 1990. 1991. 212 pp.
In German and English

4 ROBERT F. SPIELHAGEN
DIE EISDRIFT IN DER FRAMSTRASSE WÄHREND DER LETZTEN 200.000 JAHRE. 1991. 133 pp.
In German with English summary

5 THOMAS C. W. WOLF
PALÄO-OZEANOGRAPHISCH-KLIMATISCHE ENTWICKLUNG DES NÖRDLICHEN NORDATLANTIKS SEIT DEM SPÄTEN NEOGEN
(ODP LEGS 105 UND 104, DSDP LEG 81). 1991. 92 pp.
In German with English summary

6 SEISMIC STUDIES OF LATERALLY HETEROGENOUS STRUCTURES - INTERPRETATION AND MODELLING OF SEISMIC DATA.
Edited by ERNST R. FLUEH
Commission on Controlled Source Seismology (CCSS), Proceedings of the 8th Workshop Meeting, held at
Kiel - Fellhorst (Germany), August 27-31, 1990. 1991. 359 pp.
In English

7 JENS MATTHIESSEN
DINOFLAGELLATEN-ZYSTEN IM SPÄTQUARTÄR DES EUROPÄISCHEN NORDMEERES: PALÖKOLOGIE UND PALÄO-OZEANOGRAPHIE. 1991. 104 pp.
In German with English summary

8 DIRK NÜRNBERG
HAUPT- UND SPURENELEMENTE IN FORAMINIFERENGEHÄUSEN - HINWEISE AUF KLIMATISCHE UND OZEANOGRAPHISCHE ÄNDERUNGEN
IM NÖRDLICHEN NORDATLANTIK WÄHREND DES SPÄTQUARTÄRS. 1991. 117 pp.
In German with English summary

9 KLAS S. LACKSCHEWITZ
SEDIMENTATIONSPROZESSE AM AKTIVEN MITTELOZEANISCHEN KOLBEINSEY RÜCKEN (NÖRDLICH VON ISLAND). 1991. 133 pp.
In German with English summary

10 UWE PAGELS
SEDIMENTOLOGISCHE UNTERSUCHUNGEN UND BESTIMMUNG DER KARBONATLÖSUNG IN SPÄTQUARTÄREN SEDIMENTEN DES ÖSTLICHEN
ARKTISCHEN OZEANS. 1991. 106 pp.
In German with English summary

11 FS POSEIDON - EXPEDITION 175 (9.10.-1.11.1990)
175/1: OSTGRÖNLÄNDISCHER KONTINENTALRAND (65° N)
175/2: SEDIMENTATION AM KOLBEINSEYRÜCKEN (NÖRDLICH VON ISLAND)
Hrsg. von J. MIENERT und H.-J. WALLRABE-ADAMS. 1992. 56 pp. + app.
In German with some English chapters

12 GEOMAR FORSCHUNGSZENTRUM FÜR MARINE GEOWISSENSCHAFTEN DER CHRISTIAN-ALBRECHTS-UNIVERSITÄT ZU KIEL
JAHRESBERICHT / ANNUAL REPORT 1991. 1992. 152 pp.
In German and English

13 SABINE E. I. KÖHLER
SPÄTQUARTÄRE PALÄO-OZEANOGRAPHISCHE ENTWICKLUNG DES NORDPOLARMEERES UND EUROPÄISCHEN NORDMEERES ANHAND VON
SAUERSTOFF- UND KOHLENSTOFF- ISOTOTPENVERHÄLTNISSEN DER PLANKTISCHEN FORAMINIFERE
Neogloboquadrina pachyderma (sin.). 1992. 104 pp.
In German with English summary

14 FS SONNE - FAHRTBERICHT SO 78 PERUVENT: BALBOA, PANAMA - BALBOA, PANAMA, 28.2.1992-16.4.1992
Hrsg. von ERWIN SUESS. 1992. 120 pp.
In German with some English chapters

15 FOURTH INTERNATIONAL CONFERENCE ON PALEOCEANOGRAPHY (ICP IV): SHORT- AND LONG-TERM GLOBAL CHANGE:
RECORDS AND MODELLING 21-25 SEPTEMBER 1992, KIEL/GERMANY
PROGRAM & ABSTRACTS. 1992. 351 pp.
In English

16 MICHAELA KUBISCH
DIE EISDRIFT IM ARKTISCHEN OZEAN WÄHREND DER LETZTEN 250.000 JAHRE. 1992. 100 pp.
In German with English summary

17 PERSISCHER GOLF: UMWELTGEFÄHRDUNG, SCHADENSERKENNUNG, SCHADENSBEWERTUNG AM BEISPIEL DES MEERESBODENS; ERKENNEN
EINER ÖKOSYSTEMVERÄNDERUNG NACH ÖLEINTRÄGEN. Schlußbericht zu den beiden BMFT-Forschungsvorhaben 03F0055 A+B. 1993. 108 pp.
In German with English summary

18 TEKTONISCHE ENTWÄSSERUNG AN KONVERGENTEN PLATTENRÄNDERN / DEWATERING AT CONTINENTAL MARGINS.
Hrsg. von / ed. by ERWIN SUESS. 1993. 106+32+68+16+22+38+4+19 pp.
Some chapters in English, some in German

19 THOMAS DICKMANN
DAS KONZEPT DER POLARISATIONSMETHODE UND SEINE ANWENDUNGEN AUF DAS SEIMISCHE VEKTORWELLENFELD IM WEITWINKELBEREICH. 1993. 121 pp.
In German with English summary

20 GEOMAR FORSCHUNGSZENTRUM FÜR MARINE GEOWISSENSCHAFTEN DER CHRISTIAN-ALBRECHTS-UNIVERSITÄT ZU KIEL
JAHRESBERICHT / ANNUAL REPORT 1992. 1993. 139 pp.
In German and English

21 KAI UWE SCHMIDT
PALYNOMORPHE IM NEOGENEN NORDATLANTIK - HINWEISE ZUR PALÄO-OZEANOGRAPHIE UND PALÄOKLIMATOLOGIE. 1993. 104+7+41 pp.
In German with English summary

22 UWE JÜRGEN GRÜTZMACHER
DIE VERÄNDERUNGEN DER PALÄOGEOGRAPHISCHEN VERBREITUNG VON *BOLBOFORMA* - EIN BEITRAG ZUR REKONSTRUKTION UND DEFINITION VON WASSERMASSEN IM TERTIÄR.1993. 104 pp.
In German with English summary

23 RV PROFESSOR LOGACHEV - Research Cruise 09 (August 30 - September 17, 1993): SEDIMENT DISTRIBUTION ON THE REYKJANES RIDGE NEAR 59°N
Edited by H.-J. WALLRABE-ADAMS & K.S. LACKSCHEWITZ. 1993. 66+30 pp.
In English

24 ANDREAS DETTMER
DIATOMEEN-TAPHOZÖNOSEN ALS ANZEIGER PALÄO-OZEANOGRAPHISCHER ENTWICKLUNGEN IM PLIOZÄNEN UND QUARTÄREN NORDATLANTIK. 1993. 113+10+25 pp.
In German with English summary

25 GEOMAR FORSCHUNGSZENTRUM FÜR MARINE GEOWISSENSCHAFTEN DER CHRISTIAN-ALBRECHTS-UNIVERSITÄT ZU KIEL
JAHRESBERICHT / ANNUAL REPORT 1993. 1994.
In German and English

26 JÖRG BIALAS
SEISMISCHE MESSUNGEN UND WEITERE GEOPHYSIKALISCHE UNTERSUCHUNGEN AM SÜD-SHETLAND TRENCH UND IN DER BRANSFIELD STRASSE - ANTARKTISCHE HALBINSEL. 1994. 113 pp.
In German with English summary

27 JANET MARGARET SUMNER
THE TRANSPORT AND DEPOSITIONAL MECHANISM OF HIGH GRADE MIXED-MAGMA IGNIMBRITE TL, GRAN CANARIA: THE MORPHOLOGY OF A LAVA-LIKE FLOW. 1994. 224 pp.
In English with German summary

28 GEOMAR LITHOTHEK. Edited by JÜRGEN MIENERT. 1994. 12 pp + app.
In English

29 FS SONNE - FAHRTBERICHT SO 97 KODIAK-VENT: KODIAK - DUTCH HARBOR - TOKYO - SINGAPUR, 27.7. - 19.9.1994
Hrsg. von ERWIN SUESS. 1994.
Some chapters in German, some in English

30 CRUISE REPORTS:
RV LIVONIA CRUISE 92, KIEL-KIEL, 21.8.-17.9.1992: GLORIA STUDIES OF THE EAST GREENLAND CONTINENTAL MARGIN BETWEEN 70° AND 80°N
RV POSEIDON P 200/10, LISBON-BREST-BREMERHAVEN, 7.-23.8.1993: EUROPEAN NORTH ATLANTIC MARGIN: SEDIMENT PATHWAYS, PROCESSES AND FLUXES
RV AKADEMIK ALEKSANDR KARPINSKIY, KIEL-TROMSØ, 5.-25.7.1994: GAS HYDRATES ON THE NORTHERN EUROPEAN CONTINENTAL MARGIN
Edited by JÜRGEN MIENERT. 1994.
In English; report of RV AKADEMIK ALEKSANDR KARPINSKIY cruise in English and Russian

31 MARTIN WEINELT
BECKENENTWICKLUNG DES NÖRDLICHEN WIKING-GRABENS IM KÄNOZOIKUM - VERSENKUNGSGESCHICHTE, SEQUENZSTRATIGRAPHIE, SEDIMENTZUSAMMENSETZUNG. 1994. 85 pp.
In German with English summary

32 GEORG A. HEISS
CORAL REEFS IN THE RED SEA: GROWTH, PRODUCTION AND STABLE ISOTOPES. 1994. 141 pp.
In English with German summary

33 JENS A.HÖLEMANN
AKKUMULATION VON AUTOCHTHONEM UND ALLOCHTHONEM ORGANISCHEM MATERIAL IN DEN KÄNOZOISCHEN SEDIMENTEN DER NORWEGISCHEN SEE (ODP LEG 104). 1994. 78 pp.
In German with English summary

34 CHRISTIAN HASS
SEDIMENTOLOGISCHE UND MIKROPALÄONTOLOGISCHE UNTERSUCHUNGEN ZUR ENTWICKLUNG DES SKAGERRAKS (NE NORDSEE) IM SPÄTHOLOZÄN. 1994.
In German with English summary

35 BRITTA JÜNGER
TIEFENWASSERERNEUERUNG IN DER GRÖNLANDSEE WÄHREND DER LETZTEN 340.000 JAHRE.
DEEP WATER RENEWAL IN THE GREENLAND SEA DURING THE PAST 340,000 YEARS.1994. 6+109 pp.
In German with English summary

36 JÖRG KUNERT
UNTERSUCHUNGEN ZU MASSEN- UND FLUIDTRANSPORT ANHAND DER BEARBEITUNG REFLEXIONSSEISMISCHER DATEN AUS DER KODIAK-SUBDUKTIONSZONE, ALASKA. 1995. 129 pp.
In German with English summary

37 CHARLOTTE M. KRAWCZYK
DETACHMENT TECTONICS DURING CONTINENTAL RIFTING OFF THE WEST IBERIA MARGIN: SEISMIC REFLECTION AND DRILLING CONSTRAINTS. 1995. 133 pp.
In English with German summary